DISSERTATION

HIGH THROUGHPUT CHARACTERIZATION OF BUNYAVIRUS DIVERSITY, ECOLOGY, AND REASSORTMENT POTENTIAL

Submitted by

Marylee Kapuscinski

Department of Microbiology, Immunology, & Pathology

In partial fulfillment of the requirements

For the Degree of Doctor of Philosophy

Colorado State University

Fort Collins, Colorado

Summer 2023

Doctoral Committee:

Advisor: Mark Stenglein

Rebekah Kading
Jeff Wilusz
Greg Ebel
Punya Nachappa

ABSTRACT

HIGH THROUGHPUT CHARACTERIZATION OF BUNYAVIRUS DIVERSITY, ECOLOGY, AND REASSORTMENT POTENTIAL

Bunyavirales is an important group of viral pathogens with significant economic impacts. The Bunyavirales order contains the largest number of RNA viruses and can cause disease in plants, animals, and humans [1]. Notable plant pathogens include Tomato Spotted Wilt virus [2] which results in significant agricultural losses. Notable animal pathogens include Rift Valley fever virus [3] and Schmallenberg [4] virus resulting in significant livestock loss. Notable human pathogens include Crimean-Congo hemorrhagic fever virus [5], hantavirus [6], and La Crosse virus [7]. The effects of bunyavirus infections are felt worldwide because bunyaviruses are distributed globally. The emergence of novel bunyaviruses continues to threaten agricultural and livestock industries as well as human health.

Where or when a novel bunyavirus might emerge is unknown. Predicting emergence is difficult for three reasons. First, because bunyaviruses are RNA viruses [8], the high error-rate of the RNA-dependent RNA polymerase results in a large genetic diversity within a population of viruses [9]. Secondly, many important bunyaviruses are arthropod-borne [10], resulting in an intricate lifecycle between an invertebrate and vertebrate host. This results in constantly changing genetic diversity due to different selective pressures from different host types [11]. It also results in an ever-expanding

geographic range as vector range expands due to climate change and vertebrate host range changes due to urbanization, industrialization, and deforestation [12–16]. Third, bunyaviruses have segmented genomes which allows them to reassort and produce viral progeny with an altered vector-host range, pathogenesis, and virulence [1,17,18].

Therefore, this body of work aims to increase our ability to understand bunyavirus emergence and reassortment potential as a way to aid in outbreak preparedness and early response systems. To do this, we've combined traditional surveillance data with modern bioinformatics to expand our knowledge of bunyavirus genetic diversity, ecology, and reassortment potential.

Using whole-genome sequencing, we've characterized the genomes of 99 bunyaviruses, some of which have never been sequenced before. This aids in our understanding of the genetic diversity, co-infection dynamics, and reassortment potential. Next, we used existing metadata from orthobunyavirus sequences to determine reassortment potential given a shared geographic and vector-host range. Finally, we've developed a novel molecular assay to evaluate reassortment potential based on replication and transcription compatibility. Together, we've combined the strengths of viral surveillance and modern bioinformatics to demonstrate the benefit of combining both. We've developed systems that will help to delineate the mechanisms that either promote or inhibit reassortment potential, ultimately aiding in early response systems for outbreak preparedness.

ACKNOWLEDGEMENTS

This body of work would not be possible without the unending support of so many people. First, I'd like to thank Dr. Mark Stenglein for the continual guidance and support, but most of all for the variety of valuable skills you've instilled in me. It's been a long journey and I'm grateful for the time you invested into my future. I'd like to thank my committee members Dr. Rebekah Kading, Dr. Greg Ebel, Dr. Jeff Wilusz, and Dr. Punya Nachappa. I couldn't have imagined a stronger group of individuals; thank you for the encouragement, support, and guidance along the way. I'd like to thank Dr. Rebekah Kading for being an incredible role model of a successful scientist and mother. You've always been available to provide feedback, encouragement, and advice, thank you. I'd like to thank Dr. Jeff Wilusz for instilling in me a love for RNA, your enthusiasm is contagious. You've also been an incredible guide as I navigated my career, thank you. I'd like to thank Dr. Justin Lee who trained me to run the sequencing facility. I miss our daily discussions about life and science. You've been an incredible example and inspiration to me. A special thank you to Dr. Grace Borlee for being a mentor – unbeknownst to her. Before I even began the PhD program, you were teaching me how to streak bacteria and providing wisdom for life's struggles. Your mentorship only continued into my PhD and I am indebted to you. A special thank you to Dr. Carol Blair for serving on my committee during my preliminary exam, but mostly for the incredible contributions you've made to the field. I'm honored that you served on my committee. Thanks for being an incredible role model of a successful woman in science. To past

and present members of the Stenglein Lab: Joey, Case Rodgers, Shaun Cross, Tillie Dunham, Lexi Keene, Ali Brehm, Landon Basner, and Audrey Bankes. A special thank you to Landon Basner and Audrey Bankes who have contributed substantially to this body of work. A special thank you to Dr. Nicole Sexton, Dr. Emma Harris, Dr. Adeline Williams, Dr. Phillida Charley, Dr. Chilinh Nguyen, Dr. Taru Dutt, and Dr. Charlotte Avanzi for being incredible friends and peers – from encouragement, to brainstorming, to reading my R21 grant for prelims, you've all been an incredible support system and I'm forever grateful for you. Thank you to Dr. Christie Mayo for recognizing potential in me and always encouraging me – thanks for being my cheerleader. To Kirsten Reed and Dr. Molly Carpenter, you've both been such sweet friends and peers – thank you for the encouragement, comradery, and friendship. To Darby Gilfilan, for years of encouragement and contribution to this body of work – your kindness will forever be remembered.

A special thank you to my personal support system, without which this would not be possible. They've seen me through the highs and lows and I'm forever grateful. My deepest and most sincere thank you goes to Mark and Barb Ouradnik for watching my son, Peter, so that I could continue pursuing this PhD. Words will never describe the peace I was able to have, knowing that he was protected and loved by you. To my friends Rachel Maas, Emmalie Pfankuch, Kate Frisch, and Kaitlin Kunze for your never-ending prayers and support, thank you! To my step-dad, Timothy Couch Jr., for more than I can possibly put into words: Watching you achieve success as a scientist and work in academia was my first exposure to this world and it clearly left an indelible mark.

You always pushed me to be my best and pursue my dreams, you are my greatest cheerleader. Thanks for being the best dad I could have asked for. To my brother, Bolton Couch, thanks for always bringing joy to my life – life wouldn't be complete without you.

Finally, I owe my deepest gratitude to my husband, Sean Kapuscinski, and my son, Peter Kapuscinski. Sean, without you there is absolutely no way I would have completed this. Thank you for being my confidant and true north. You've sacrificed so much for me to achieve this – thank you. Peter, thank you for being the biggest joy in my life. Thank you both for your never-ending patience and unconditional love.

TABLE OF CONTENTS

ABSTRACT ii

ACKNOWLEDGEMENTS iv

LIST OF TABLES xi

LIST OF FIGURES xii

Chapter 1: Introduction 1

1.1 The significance of bunyaviruses 1

1.2 Review of *Bunyavirales* 2

1.2.1 Bunyavirus genomics 3

1.2.2 Bunyavirus vector-host dynamics 5

1.2.3 Bunyavirus reassortment potential 6

1.3 A note on *Orthobunyavirus* classification 7

1.4 Research focus 8

Chapter 2: Genomic characterization of 99 viruses from the bunyavirus families *Nairoviridae*, *Peribunyaviridae*, and *Phenuiviridae*, including 35 previously unsequenced viruses 9

2.1 Introduction 9

2.2 Results 11

2.2.1 Samples and sequencing 11

2.2.2 Phylogenetic analyses 24

2.2.3 Reassortment 32

2.2.4 Co-infection 42
2.3 Discussion 44
2.3.1 Reassortment 46
2.3.2 Co-infection of viral stocks 47
2.3.3 Taxonomic implications 48
2.4 Conclusions 48
2.5 Materials and Methods 49
2.5.1 Sample collection 49
2.5.2 Library preparation and sequencing 49
2.5.3 Sequence analysis 50
2.5.4 Validation of assemblies by sanger sequencing 51
2.5.5 Sequence alignments and phylogenetic analyses 53
2.5.6 Co-infection analysis 54
Chapter 3: A scoping review of Orthobunyavirus sympatry and ecology: Barriers to reassortment 57
3.1 Introduction 57
3.2 Results 59
3.2.1 Overview of metadata 59
3.2.2 Orthobunyavirus geographic distribution 62
3.2.3 Orthobunyavirus vector and host range 76
3.2.4 Delineating reassortment potential 80
3.3 Discussion 92

3.4 Materials and Methods 95
3.4.1 Data curation 95
3.4.2 Data visualization 98
Chapter 4: Minigenome Melees: A novel high throughput method to evaluate reassortment potential between orthobunyaviruses 99
4.1 Introduction 99
4.2 Results 101
4.2.1 Overview of minigenome melees 101
4.2.2 Composition of the barcoded minigenome library 106
4.2.3 Barcoded minigenomes are functional 110
4.2.4 ss-RT-qPCR and NGS as readouts for barcoded minigenomes 111
4.3 Discussion 113
4.4 Materials and Methods 117
4.4.1 Cells 117
4.4.2 Plasmids 117
4.4.3 Barcoded minigenomes 117
4.4.4 Cell culture transfections 120
4.4.5 Harvesting cells 122
4.4.6 Nano-luciferase assays 123
4.4.7 RNA extraction 124
4.4.8 Amplicon library preparation and sequencing 124
4.4.9 Strand-specific reverse transcription quantitative PCR (ss-RT-qPCR) 126

4.4.10 Phylogenetic analysis of the M segment 128

4.4.11 Pairwise alignment of minigenome UTRs 129

Chapter 5: Discussion 129

APPENDICES 132

REFERENCES 148

LIST OF TABLES

Table 2.1. Sequenced genomes of 88 viruses belonging to *Peribunyaviridae* (*Orthobunyavirus* or *Pacuvirus*)

Table 2.2. Sequenced genomes of 6 viruses belonging to Phenuiviridae (Phlebovirus and Uukuvirus)

Table 2.3. Sequenced genomes of 5 viruses belonging to Nairoviridae (Orthonairovirus)

Table 3.1. List of viruses with shared vector ecology

Table 4.1. Scheme for differentiating plus and minus strand reads from NGS

Supplemental Table 2.1. Primers used in this study. (XLSX attached separately)

Supplemental Table 2.2. Pairwise nucleotide identities from a global alignments of the L, GPC, or N coding sequences. (XLSX attached separately)

Supplemental Table 3.1. List of virus detections by country

Supplemental Table 3.2. Number of serogroups detected at a country-level

Supplemental Table 4.1 Primers used in this study (XLSX attached separately)

LIST OF FIGURES

Figure 2.1. Characteristics of sequenced bunyavirus isolates

Figure 2.2. L segment phylogeny for viruses in Orthobunyavirus

Figure 2.3. M segment phylogeny for viruses in Orthobunyavirus

Figure 2.4. S segment phylogeny for viruses in Orthobunyavirus

Figure 2.5. Phylogenetic analysis of viruses in Nairoviridae

Figure 2.6. Phylogenetic analysis of viruses in Phenuiviridae

Figure 2.7. Co-phylogenies of Orthobunyavirus L and S segment trees

Figure 2.8. Co-phylogenies of Orthobunyavirus L and M segment trees

Figure 2.9. Co-phylogenies of Orthobunyavirus S and M segment trees

Figure 2.10. Co-phylogenies of Nairoviridae L, M, and S segment trees

Figure 2.11. Co-phylogenies of Phenuiviridae L, M, and S segment trees

Figure 3.1. Summation of metadata

Figure 3.2. Many orthobunyavirus serogroups occupy the same country

Figure 3.3. Geographic distribution of virus isolations within serogroups

Figure 3.4. Orthobunyavirus sympatry within serogroups

Figure 3.5. Isolation sources sans mosquito species

Figure 3.6. Orthobunyavirus ecology within mosquito species

Figure 4.1. Design of minigenome melee system

Figure 4.2. Strand-specific RT-qPCR and next-generation sequencing library prep design

Figure 4.3. M-segment minigenomes represent a wide range of genetic diversity within the orthobunyavirus genus

Figure 4.4. Nucleotide similarity between UTRs of viruses used

Figure 4.5. Barcoded minigenomes are functional.

Figure 4.6. Amplicon sequencing measures replication and transcription efficiency.

Figure 4.7. Strand-specific RT-qPCR measures replication and transcription efficiencies.

Supplemental Figure 2.1. Coverage depth across all genome segments for all sequenced viruses (PDF attached separately)

Supplemental Figure 2.2. Tree containing all available *Orthobunyavirus* sequences

Supplemental Figure 2.3. Tree containing all available *Phlebovirus* sequences

Supplemental Figure 2.4. Tree containing all available *Nairoviridae* sequences

Supplemental Figure 2.5. L segment phylogeny for viruses in *Peribunyaviridae: Pacuvirus*.

Supplemental Figure 4.1. Tapestation traces of *in vitro* transcribed minigenome RNA (PDF attached separately)

CHAPTER 1: Introduction

1.1 The significance of bunyaviruses

For centuries viruses have been a significant cause of economic and agricultural losses, but most importantly the cause of millions of lives lost [19]. Significant examples include Influenza viruses, SARS-CoV viruses, MERS viruses, and Ebola virus [19]. The recent SARS-CoV-2 pandemic has resulted in an all too personal reminder of the devastating impacts, many of which the world is still recovering from. While we've learned many lessons, this body of work will focus on two of them. First, emergence and re-emergence of viruses will continue to occur and impact humans [9,20–22]. Second, methods that allow for early detection of viral strains with pathogenic potential is imperative to decreasing the economic losses inherent in viral outbreaks [23,24].

A large number of pathogenic viruses are RNA viruses [24,25]. RNA viruses have an increased evolutionary rate because of the error-prone RNA-dependent RNA polymerase (RdRp) [20,24]. This unique feature increases the number of mutations present in a virus population, thereby increasing the rate of viral evolution and the genetic diversity in a population. Contributing to the importance of RNA viruses is the fact that many are zoonotic – transmitted from animal to human [24]. A rise in zoonotic diseases has coincided with an increased human population, urbanization, increased agricultural practices, deforestation, and increased trade which brings animals and humans into close contact [20,21,24–27]. Therefore, RNA viruses pose a significant threat to humans – significant lives lost (e.g. 1918 Spanish Flu, SARS-CoV-2) and

significant economic losses due to the loss of livestock (e.g. High Pathogenic Avian Influenza).

Arthropod-borne viruses present an added layer of complexity to public health [28]. Most arboviruses are RNA viruses [29], compounding the risk for emergence of novel strains due to ease of transmission between the vector and host. The geographic range of vectors continues to increase because of climate change, human travel, and urbanization [30]. Additionally, increased agricultural practices and deforestation continue to bring humans into closer contact with animals, thereby increasing the emergence of zoonotic arboviruses.

Bunyaviruses are a trifecta: they are RNA viruses with error prone polymerases that increase genetic diversity and mutation rates, some are arboviruses (*Peribunyaviridae*, *Phenuiviridae*, *Nairoviridae*) and therefore differential selective pressures from the host and vector influence virus evolution, and they are segmented which affords them the ability to reassort. Together, these factors increase the genetic diversity and rate of viral evolution within bunyaviruses, presenting a significant risk for the emergence and reemergence of pathogenic strains.

1.2 Review of *Bunyavirales*

Bunyaviruses (*Negarnaviricota*: *Bunyavirales*) are the largest order of RNA viruses [1]. Capable of causing disease in plants, animals, and humans, bunyaviruses are a significant group of pathogens. There are 12 different bunyavirus families: *Arenaviridae*, *Cruliviridae*, *Fimoviridae*, *Hantaviridae*, *Leishbuviridae*, *Mypoviridae*,

Nairoviridae, *Peribunyaviridae*, *Phasmaviridae*, *Phenuiviridae*, *Tospoviridae*, and *Wupedeviridae*. Families containing human pathogens include *Hantaviridae*, *Nairoviridae*, *Arenaviridae*, *Peribunyaviridae*, and *Phenuiviridae* [31,32]. Because viruses within this order can infect and cause disease in plants, animals, and humans the effects are widespread and have resulted in economic, agricultural, and health burdens. Notable examples include Crimean-Congo Hemorrhagic Fever (*Nairoviridae*) [5,33], Rift Valley Fever virus (*Phenuiviridae*) [34], Lassa fever virus (*Arenaviridae*), Hantavirus (*Hantaviridae*), and Schmallenberg virus (*Peribunyaviridae*) [4,35,36]. The World Health Organization's list of priority pathogens includes Crimean-Congo Hemorrhagic Fever virus, Rift Valley Fever virus, and Lassa Fever virus [37]. Additionally, the NIAID's pathogen priority list includes La Crosse virus (*Peribunyaviridae*) and California Encephalitis virus (*Peribunyaviridae*) [38]. *Bunyavirales* presents a significant global threat to plant, animal, and human health.

1.2.1 Bunyavirus genomics

The genomes of bunyaviruses are comprised of tri-segmented, single stranded, negative sense RNAs [1,8]. Each segment encodes 1-3 viral proteins. The S segment encodes the viral nucleoprotein which studs each viral genome segment, thereby protecting it from degradation by host cell machinery. An additional non-structural segment protein (NSs) is encoded by the S segment for some bunyaviruses. The NSs protein has been shown to downregulate the host interferon response, thereby aiding in the proliferation of the viral infection [39,40]. The L segment encodes the viral RNA-

dependent RNA polymerase which is responsible for replication and transcription of the viral genome segments. The M segment encodes the glycoproteins (Gp1 and Gp2) as one polyprotein which is post-translationally cleaved. The glycoproteins stud the virus envelope and are responsible for virus entry into the host cell. Some bunyaviruses encode an additional NSm protein, located on the M segment. The function of the NSm protein is not well understood, but is thought to aid in viral packaging and pathogenesis[41]. Encoding only a few viral proteins, bunyaviruses exhibit both simplicity and function in their genomes.

As RNA viruses, bunyaviruses have evolved fine-tuned mechanisms to replicate within the host undetected. Within the virus particle, each genome segment is part of a ribonucleoprotein complex (RNP) which provides protection to the genome and an efficient mechanism for replication and transcription of the genome segments upon entry into the host cell [1,8]. The RNP is comprised of one genome segment, heavily studded with nucleoprotein to protect it from degradation by host defenses, and pre-loaded with a RdRp protein for quick replication and transcription. Although the viral genomes appear to be circular using electron microscopy [42] the genomes do not form a true circle [43]. Rather, the terminal 11 nucleotides of the 5' and 3' ends of the genome are reverse complements of each other, resulting in the formation of a panhandle through base-pairing. The panhandle structure allows the viral RdRp to recognize and begin priming the viral genome for replication and transcription [1]. The terminal 11 nucleotides are highly conserved within each bunyavirus family, resulting in the co-evolution of RdRps within each bunyavirus family.

The RdRP is the workhorse of all bunyaviruses and performs both replication, transcription, and cap-snatching. The negative-sense genomes are replicated to produce anti-genomes which are then used to make more negative sense genomes for packaging into nascent virus particles. To make more viral protein, the RdRp transcribes mRNA from the negative sense genome. Because bunyavirus mRNAs are plus strand RNA, the RdRP performs cap-snatching to disguise their mRNAs as cellular mRNAs and avoid detection by host degradation machinery [44,45].

1.2.2 Bunyavirus vector-host dynamics

Bunyaviruses within the *Peribunyaviridae*, *Phenuiviridae*, and *Nairoviridae* families are arboviruses [10]. As arboviruses, they are sustained by a dual-host tropism [10,16,28]. Blood feeding arthropods, such as mosquitoes and ticks, transmit the virus to a vertebrate host. The virus must be amplified within the vertebrate to sufficient titer in order for the vector to become infected upon subsequent feeding. Therefore, the vector-host dynamic influences the transmission and spread of bunyaviruses as well as the genetic diversity and virus evolution.

There are a wide range of bunyavirus vectors. Typical bunyavirus vectors include mosquitos (*Peribunyaviridae* and *Phenuiviridae*), ticks (*Nairoviridae* and *Peribunyaviridae*), phlebotomine flies (*Peribunyaviridae*), and midges (*Peribunyaviridae*). The broad diversity of vectors complicates the ecology of bunyaviruses. The distribution of these vectors determines where the viruses are circulating. However, with increased climate change, deforestation, and urbanization

vector range is continually expanding [12,14,15,46–49]. This results in an expansion of bunyavirus distribution and the introduction of bunyaviruses to naïve populations.

1.2.3 Bunyavirus reassortment potential

Reassortment, a by-product of segmented genomes, aids in the genetic diversity of segmented virus populations [17,50]. Reassortment is the shuffling of genome segments during a viral co-infection. This can lead to the emergence of viral progeny with a different phenotype than either parental virus. Phenotypic changes can include increased disease pathogenicity, altered host range, and increased virulence. Reassortment has been shown to occur frequently within Bunyavirales [18,51].

Evidence for bunyavirus reassortment comes from natural isolations as well as laboratory research. Ngari virus (*Peribunyaviridae*: Bunyamwera serogroup) was isolated from humans during an outbreak in Kenya that caused hemorrhagic fever [18,52,53]. Genomic studies found the L and S segments to be closely related to Bunyamwera virus and the M segment related to an unidentified orthobunyavirus. Before the discovery of Ngari virus, viruses belonging to the bunyamwera serogroup were not known to cause significant human disease. This is an example of altered pathogenicity due to reassortment. Reassortment has been documented *in vitro* and *in vivo* between La Crosse virus and Jamestown Canyon virus (*Peribunyaviridae*: California serogroup) [54]. Many other notable examples include Iquitos virus (*Peribunyaviridae*) [18,55], Sin Nombre virus (*Hantaviridae*) [56], Rift Valley Fever virus (*Phenuiviridae*) [57], and Crimean-Congo Hemorrhagic Fever virus (*Nairoviridae*) [58].

General patterns have emerged from the research that has amassed on bunyavirus reassortants. First, reassortment is restricted to viruses belonging to the same family. Second, reassortment between closely related viruses occurs more frequently (intratypic) than distantly related viruses (intertypic). Third, the M-segment tends to reassort more often than the L or S segments. And finally, superinfection-resistance provides opportunity for more distantly related viruses to reassort by preventing dual-infections of closely related viruses within a certain time-frame [18,59,60].

1.3 A note on *Orthobunyavirus* classification

Historically, viruses belonging to the *Peribunyaviridae* family have been classified based on serology. Based on serology, orthobunyaviruses are grouped into one of 18 serogroups. Because of frequent reassortment among this family, this classification system is confusing. For example, the L and S segments of one virus may be closely related to that of one serogroup, but the M segment may be more closely related to viruses belonging to a different serogroup. In Chapter 2 we present tanglegrams which help to visualize the disparate phylogenetic relationships between the L, M, and S segments (**Figures 2.7-2.9**). While we recognize the discrepancies in the serogroup classification, we continue to use it for the sake of clarity in this dissertation. Additionally, some viruses discussed within this paper have not undergone serology and are classified based on genetic information alone.

1.4 Research focus

This body of research aims to characterize the genetic diversity, ecology, and reassortment potential of bunyaviruses. To accomplish this, we've sequenced the genomes of 99 bunyaviruses from three different families (*Phenuiviridae*, *Peribunyaviridae*, and *Nairoviridae*). This large-scale sequencing project genetically characterized a large portion of bunyavirus genomes and is discussed in Chapter 2. Next, we sought to determine which viruses within the *Peribunyaviridae* family have an increased risk for reassortment potential, discussed in Chapter 3. Finally, we aimed to improve molecular assays used to evaluate reassortment potential between bunyaviruses. The result is a novel molecular assay that increases throughput, discussed in Chapter 4. Finally, I discuss measures to bolster existing efforts to detect and respond to the emergence of viral pathogens.

CHAPTER 2: Genomic characterization of 99 viruses from the bunyavirus families Nairoviridae, Peribunyaviridae, and Phenuiviridae, including 35 previously unsequenced viruses[1]

2.1 Introduction

New pathogens continue to emerge and threaten human, animal, and plant health. For humans alone, an average of two new disease-causing agents are reported each year [61–63]. These pathogens have primarily been viruses, have usually been associated with animal reservoirs, and many are vector-borne [62]. Bunyaviruses (Riboviria: Negarnaviricota: Bunyavirales) rank among the most serious infectious threats to humans (e.g. Crimean Congo hemorrhagic fever virus [5]), animals (e.g. Rift Valley fever virus [64]), and plants (e.g. tomato spotted wilt virus [2]) [8,65]. Bunyaviruses accounted for approximately 20% of the 188 human pathogenic viruses identified between 1901 and 2005 [63], and new pathogenic bunyaviruses continue to emerge [55,66–69]. Traditionally bunyaviruses have been grouped according to their serological cross-reactivity (i.e. they have been binned into serogroups), but molecular data and the discovery of many new viruses has driven the reorganization of the order. The order *Bunyavirales* now includes 12 families: *Arenaviridae*, *Cruliviridae*, *Fimoviridae*, *Hantaviridae*, *Leishbuviridae*, *Mypoviridae*, *Nairoviridae*, *Peribunyaviridae*, *Phasmaviridae*, *Phenuiviridae*, *Tospoviridae*, and *Wupedeviridae* [32,70].

---

[1] Adapted from Kapuscinski ML, Bergren NA, Russell BJ, Lee JS, Borland EM, Hartman DA, et al. Genomic characterization of 99 viruses from the bunyavirus families Nairoviridae, Peribunyaviridae, and Phenuiviridae, including 35 previously unsequenced viruses. PLOS Pathogens. 2021;17: e1009315. doi:*10.1371/journal.ppat.1009315*

Bunyaviruses have segmented, negative-sense or ambisense RNA genomes. Many currently characterized bunyavirus genomes are composed of three segments: a large (L) segment encoding a protein that functions as an RNA-directed RNA polymerase (RdRp); a medium (M) segment encoding glycoproteins (Gn and Gc); and a small (S) segment encoding a nucleoprotein (NP) and, in some clades, a non-structural protein, NSs. Some bunyavirus lineages have different numbers of genome segments. For instance, the majority of viruses in the *Arenaviridae* family are bisegmented, and some plant-infecting emaraviruses (family *Fimoviridae*) have 8 segments [71].

Like all viruses with segmented genomes, bunyaviruses are capable of reassortment, which appears to have occurred commonly during bunyavirus evolution [18]. Reassortment has happened between relatively distantly related bunyaviruses (intertypic reassortment) and between closely-related co-circulating strains (intratypic reassortment) [18,59], and can have epidemiological significance. For example, Ngari virus is a reassortant bunyavirus associated with outbreaks of hemorrhagic fever [52]. Iquitos and Itaya viruses are emerging reassortant viruses (*Peribunyaviridae*: Orthobunyavirus) that have both been associated with human illness in Peru [55,69]; an intra-lineage reassortant strain of Rift Valley fever virus (*Phenuiviridae*: Phlebovirus) was recently isolated from an ill traveler returning home to China [72]; and severe fever with thrombocytopenia syndrome virus (SFTSV) is a newly-recognized, tick-borne phenuivirus that causes severe human disease and for which reassortment has been recognized in strains detected in human patients [73]. Given the emergence potential of bunyaviruses and the contribution of reassortment to the generation of new virus strains, having the

capability to recognize novel and reassortant viruses is paramount to public health preparedness.

The US Center for Disease Control and Prevention's (CDC) Division of Vector-borne Diseases (DVBD), Arboviral Diseases Branch (ADB), maintains an Arbovirus Reference Collection (ARC). The ARC contains viruses that were isolated from arthropod vectors and vertebrate hosts, as well as from human clinical specimens. Isolates have been collected and deposited into the ARC over a 90-year period. As one of the largest collections of arboviruses in the world, the ARC is an invaluable resource for scientists and public health workers. The ARC includes 2,766 unique isolates, of which 835 are bunyaviruses. Some of these viruses have been genetically characterized, but many have not. Genetic characterization of the viruses in the ARC would expand the value and impact of this collection even further as a scientific and public health resource and infuse a significant amount of novel and important molecular data into the public domain for actionable use. Therefore, the objective of this project was to generate additional and novel genome sequence and phylogenetic data for a large group of bunyaviruses lacking genetic characterization to facilitate the rapid identification and characterization of emerging bunyaviruses.

2.2 Results

2.2.1 Samples and sequencing

Coding-complete genomes were generated for 99 bunyaviruses [74]. We focused on viruses classified in the *Peribunyaviridae* (orthobunyaviruses), *Nairoviridae*

(orthonairoviruses), and *Phenuiviridae* (banyangviruses and phleboviruses). These viruses constituted a globally and phylogenetically diverse set. The isolates were originally collected from vertebrate and arthropod hosts from 27 countries on six continents over the span of seven decades, from 1940 to 2005; **Figure 2.1 and Tables 1.1–2.3**). Most samples were collected during the 1950s, 60s, and 70s, and 67% of samples originated from North and South America (**Figure 2.1B and 2.1C**). Isolates originated from a variety of invertebrate and vertebrate hosts, though *Aedes*, *Anopheles*, and *Culex* mosquitoes were the predominant source of samples (**Figure 2.1D**). We focused on viruses for which there was limited existing sequence information at the initiation of this project (**Figure 2.1E and Tables 2.1–2.3**). Viruses had diverse passage histories. Some viruses were passaged through grivet (*Chlorocebus aethiops*) Vero or hamster (*Mesocricetus auratus*) BHK-21 cell cultures, others were passaged in suckling laboratory mice. Passage histories have been noted in **Tables 2.1–2.3**. More information on these viruses can be accessed through the Arbovirus Catalog (*https://www.cdc.gov/arbocat*) or the ARC website (*https://www.cdc.gov/ncezid/dvbd/specimensub/ arc/index.html*), however taxonomy may vary between these sources and ICTV as taxonomic updates are instituted.

At the time of submission, 203 of the genome segment sequences we generated shared less than 97% pairwise nucleotide identity with existing sequences in the NCBI nucleotide database, as measured by BLASTn (**Figure 2.1E**). For 35 of the viruses, all 3 segments shared <85% nucleotide identity with existing sequences by B alignment. These 35 viruses represent previously unsequenced viruses (category 1 viruses in

Tables 2.1–2.3 and Figure 2.1E). For 37 of the viruses, different strains of the same viruses had been previously sequenced or existing sequences were not complete (e.g., only one segment had been sequenced; categories 2 and 3 in **Tables 2.1–2.3**). For 26 of the viruses, coding complete genomes already existed (category 4 in **Tables 2.1–2.3**). In almost all of these 26 cases, sequences had been deposited by other groups during the course of our study.

Table 2.1. Sequenced genomes of 88 viruses belonging to *Peribunyaviridae* (*Orthobunyavirus* or *Pacuvirus*).

Sequence Status	Virus	Abbreviation	Strain (Passage)	Serogroup	Collection Date	Collection Country	Isolation Source	Original Virus Description	GenBank Accession
4	Abras	ABRV	75V1183 (P4V1)	Patois	1974	Ecuador	*Culex* mosquito	[75]	MK896654 –MK896656
1	Acará	ACAV	BeAn 27639 (P2SM1)	Capim	1961	Brazil	Mouse	[76,77]	MK896651 –MK896653
2	Aino	AINOV	JaNAr 28 (P9SM1)	Simbu	1964	Japan	*Culex* mosquito	[78]	MH484276 –MH484278
4	Ananindeua	ANUV	BeAn 109303 (P36SM1)	Guama´	1966	Brazil	Opossum	[79]	MK896648 –MK896650
3	Anopheles B	ANBV	Original	Anopheles B	1940	Colombia	*Anopheles* mosquito	[80]	MK896642 –MK896644
1	Antequera	ANTV	AG80-226 (V2SM2V1)	Resistencia	1980	Argentina	*Culex* mosquito	[81,82]	MK896639 –MK896641
4	Babahoyo	BABV	75V2858 (P2SM2)	Patois	1975	Ecuador	*Culex* mosquito	[75]	MH484273 –MH484275
1	Bakau	BAKV	MM-2325 (P8SM1)	Bakau	1956	Malaysia	*Culex* mosquito	[83]	MK896633 –MK896635
1	Bangui	BGIV	DakHB 754 (P9SM1)	Ungrouped	1970	Central African Republic	Human	[84,85]	MK896630 –MK896632
1	Barranqueras	BQSV	AG80-381 (V1SM3)	Resistencia	1980	Argentina	*Culex* mosquito	[81,82]	MK896627 –MK896629
3	Batama	BMAV	DakAnB 1292 (P8SM2)	Tete	1970	Central African Republic	Bird	[86]	MK896624 –MK896626
1	Belem	BLMV	BeAn 141106 (P11SM1)	Ungrouped	1968	Brazil	Bird	[87]	MK896621 –MK896623

1	Benevides	BVSV = BENV	BeAr 153564 (P?SM2V1)	Capim	1968	Brazil	Mouse		MK896618 –MK896620
1	Benfica	BENV = BNFV	71U344 (P?SM6)	Capim	1971	Peru	Hamster	[88]	MK896615 –MK896617
1	Bertioga	BERV	76V25643 (P?SM3)	Guama´	1976	Brazil	*Culex* mosquito	[89,90]	MK896612 –MK896614
4	Birao	BIRV	DakArB 2198 (P?SM1)	Bunyamwera	1969	Central African Republic	*Anopheles* mosquito	[91]	MH484282 –MH484284
1	Bobaya	BOBV	DakAnB 2208 (P9SM1)	Simbu	1971	Central African Republic	Bird	[85,86]	MW415980-MW415982
3	Boracéia	BORV	SPAr 395 (P?SM2)	Anopheles B	1962	Brazil	*Anopheles* mosquito	[92]	MK896609 — MK896611
2	Boracéia	BORV	SPAr 4080 (P?)	Anopheles B	1965	Brazil	*Anopheles* mosquito	[93]	MK896606 –MK896608
4	Bozo	BOZOV	DakArB 7343 (P?SM2)	Bunyamwera	1975	Central African Republic	*Aedes* mosquito	[94]	MH484285 –MH484287
2	Bruconha	BRUV	77V14676 (P?V1SM5)	C	1976	Brazil	*Culex* mosquito	[79]	MK896603 –MK896605
2	Bunyamwera	BUNV	46A-122 (V3)	Bunyamwera	2006	Kenya	*Aedes* mosquito	[95]	MH484288 –MH484290
1	Bushbush	BSBV	TRVL 26668 (P?SM3)	Capim	1959	Trinidad & Tobago	*Culex* mosquito	[76,96]	MK896597 –MK896599
3	Buttonwillow	BUTV	A 7956 (P?SM3H1SM1)	Simbu	1961	USA	Rabbit	[97,98]	MH484291 –MH484293
4	Caimito	CAIV	VP 488A (P8V2SM1)	Ungrouped	1971	Panama	Sand fly	[99,100]	MK896592 –MK896594

1	Cananéia	CNAV	SPAn 64962 (SM4V1)	Guama´	1976	Brazil	Mouse	[79]	MK896589 –MK896591
4	Caraparú	CARV	BeAn 3994 (P?SM11)	C	1956	Brazil	Monkey	[101]	MK896586 –MK896588
2	Enseada	ENSV	78V213 (P?V1SM2)	Ungrouped	1976	Brazil	*Culex* mosquito	[79]	MK896583 –MK896585
4	Fort Sherman	FSV	86MSP18 (P2V1)	Bunyamwera	1985	Panama	Human	[102]	MH484294 –MH484296
2	Gamboa	GAMV	75V20086 (P?SM1V1)	Gamboa	1975	Ecuador	*Aedeomyia squami-pennis* mosquito	[103,104]	MK896574 –MK896576
2	Guajará	GJAV	18315 (P?SM4)	Capim	1975	Ecuador	Hamster	[75,89]	MK896571 –MK896573
1	Guaratuba	GTBV	76V25271 (P?SM3)	Guama´	1976	Brazil	*Culex* mosquito	[79]	MK896568 –MK896570
3	Gumbo Limbo	GLV	FE3-71H (P4V1)	C	1963	USA	*Culex* mosquito	[105]	MK896565 –MK896567
4	Itaquí	ITQV	BeAn 12797 (P?SM4V1SM2)	C	1959	Brazil	Mouse	[106,107]	MK896558 –MK896560
1	Itimirim	ITIV	SPAn 47817 (SM6)	Guama´	1976	Brazil	Rat	[79]	MK896555 –MK896557
1	Juan Díaz	JDV	MARU 8563 (P?SM5ppfV2SM1)	Capim	1962	Panama	Mouse	[103]	MK896552 –MK896554
3	Kaikalur	KAIV	VRC 713423–2 (P7SM1)	Simbu	1971	India	*Culex* mosquito	[108]	MH484297 –MH484299
4	Kairi	KRIV	TRVL 8900 (P13SM1)	Bunyamwera	1955	Trinidad & Tobago	*Aedes* mosquito	[109,110]	MH484300 –MH484302
1	Ketapang	KETV	MM 2549 (P5SM2)	Bakau	1956	Malaysia	*Culex* mosquito	[83,89]	MK896546 –MK896548

1	Las Maloyas	LMV	AG80-24 (P?V1SM4)	Anopheles A	1980	Argentina	*Anopheles* mosquito	[81,82]	MK896543 –MK896545
1	Lednice	LEDV	6118 (P3SM2)	Turlock	1980	Czechoslovakia	*Culex* mosquito	[111]	MK896540 –MK896542
2	Lokern	LOKV	A 10391 (P?SM5)	Bunyamwera	NA	NA	NA	[112]	MH484303 –MH484305
2	Lukuni	LUKV	ColAn 57389 (P?SM5)	Anopheles A	1976	Colombia	Vertebrate	[76,96]	MK896537 –MK896539
4	Madrid	MADV	BT 4075 (P13SM2)	C	1961	Panama	Human	[113,114]	MK896531 –MK896533
2	Main Drain	MDV	R4680 (SM3V1)	Bunyamwera	1974	USA	*Anopheles* mosquito	[115,116]	MH484309 –MH484311
2	Main Drain	MDV	72V2567 (V1SM1V2)	Bunyamwera	1972	USA	*Aedes* mosquito	[115,116]	MH484306 –MH484308
4	Marituba	MTBV	BeAn 15 (SM3SH1V1SM2)	C	1954	Brazil	Monkey	[101,117]	MK896528 –MK896530
1	Minatitlán	MNTV	M67U5 (P5SM1)	Minatitla´n	1967	Mexico	Hamster	[75]	MK896525 –MK896527
4	Mirim	MIRV	BeAn 7722 (SM1V1)	Guama´	1957	Brazil	Monkey	[118]	MK896522 –MK896524
1	Moriche	MORV	TRVL 57896 (P?SM2V1)	Capim	1964	Trinidad & Tobago	*Culex* mosquito	[89,119]	MK896519 –MK896521
2, 3	M'Poko	MPOV	BA 365 (P?AM1)	Turlock	1966	Central African Republic	*Culex* mosquito	[120]	MK896534 –MK896536
4	Murutucú	MURV	BeAn 974 (P14SM2)	C	1955	Brazil	Monkey	[101]	MK896516 –MK896518
2	Nepuyo	NEPV	HB7-451 (P?SM6)	C	1967	Honduras	Bat	[121,122]	MK896513 –MK896515
3	Nola	NOLAV	DakAr B 2882 (P10SM2)	Bakau	1970	Central African	*Culex* mosquito	[87]	MK896510 –MK896512

						Republic			
4	Northway	NORV	234 (P?SM1BHK(1) SM4)	Bunyamwera	1971	USA	*Aedes* mosquito	[123,124]	MH484312 –MH484314
1	Okola	OKOV	YM 50 (P9SM1)	Tanga	1964	Cameroon	*Eretmapodites* mosquito	[87]	MK896507 –MK896509
4	Oriboca	ORIV	BeAn 17 (P12V4ppf3V1SM1)	C	1954	Brazil	Monkey	[101,117]	MK896501 –MK896503
1	Pacora	PCAV	J19 (P31SM1)	Ungrouped	1958	Panama	*Culex* mosquito	[87]	MK896498 –MK896500
1	Pahayokee	PAHV	FE3-52F (P?BHK(1) SM1)	Patois	1963	USA	*Culex* mosquito	[125]	MK896495 –MK896497
2	Patois	PATV	BT 4971 (SM7V1)	Patois	1961	Panama	Rat	[126,127]	MK896489 –MK896491
4	Peaton	PEAV	CSIRO 110 (SM1)	Simbu	1976	Australia	*Culicoides* biting midge	[128]	MH484318 –MH484320
3	Potosi	POTV	89–3380 (V3SM2)	Bunyamwera	2005	USA	*Aedes* mosquito	[129]	MH484321 –MH484323
2	Pueblo Viejo	PVV	E4-816 (V2)	Gamboa	1974	Ecuador	*Aedeomyia squami-pennis* mosquito	[104]	MK896484 –MK896486
1	Resistencia	RTAV	AG80-504 (V1SM3V4SM3)	Resistencia	1980	Argentina	*Culex* mosquito	[81,82]	MK896478 –MK896480
3	Restan	RESV	TRVL 51144 (SM2SH1SM2)	C	1963	Trinidad & Tobago	*Culex* mosquito	[130]	MK896475 –MK896477
1	San Juan	SJV	75V2374 (P?SM3)	Gamboa	1975	Ecuador	*Aedeomyia squami-*	[104]	MK896472 –MK896474

							pennis mosquito		
1	Santa Rosa	SARV	M2-1493 (SM5)	Bunyamwera	1972	Mexico	*Aedes* mosquito	[76]	MH484324–MH484326
1	Santarém	STMV	BeAn 238758 (P6SM1)	Ungrouped	1973	Brazil	Rat	[87]	MK896469–MK896471
4	Sedlec	SEDV	Av 172 (P4SM1BHK2)	Simbu	1984	Czechoslovakia	Bird	[131]	MH484327—MH484329
3	Shokwe	SHOV	SAAr 4042 (P6SM2V1)	Bunyamwera	1962	South Africa	*Aedes* mosquito	[91,132,133]	MH484330–MH484332
2	Tacaiuma	TCMV	SpH 32580 (SM3)	Anopheles A	1975	Brazil	Human	[113]	MK896460–MK896462
1	Tanga	TANV	MP 1329 (P7SM1)	Tanga	1962	Tanzania	*Anopheles* mosquito	[134,135]	MK896457–MK896459
2	Tataguine	TATV	79V1463 (SM2)	Tanga	1979	Gambia	*Anopheles* mosquito	[136]	MK896454–MK896456
1	Telok Forest	TFV	MalP 72–4 (P?SM2)	Bakau	1972	Malaysia	Monkey	[87]	MK896451–MK896453
2	Tensaw	TENV	A9-171B (P?SM5)	Bunyamwera	1960	USA	*Anopheles* mosquito	[137]	MH484333–MH484335
1	Termeil	TERV	BP 8090 (P3SM2)	Ungrouped	1972	Australia	*Aedes* mosquito	[138]	MK896448–MK896450
2	Thimiri	THIV	VRC 66414 (P15SM1)	Simbu	1963	India	Bird	[139]	MH484336–MH484338
1	Timboteua	TBTV	BeAn 116382 (SM2V1)	Guama´	1967	Brazil	Mouse	[140]	MK896445–MK896447
4	Tinaroo	TINV	CSIRO 153 (P?BHK4SM2)	Simbu	1978	Australia	*Culicoides* midge	[141]	MH484339–MH484341
4	Tlacotalpan	TLAV	61D240 (P9V1)	Bunyamwera	2005	Mexico	*Mansonia titillans*	[142]	MH484342–MH484344

							mosquito		
2	Turlock	TURV	USA 847–32 (P4SM2V1)	Turlock	1954	USA	*Culex* mosquito	[143,144]	MK896442-MK896444
2, 3	Vinces	VINV	24188 (P?SM4)	C	1976	Ecuador	Hamster	[75]	MK896439–MK896441
2, 3	Weldona	WELV	77V5691 (P4V2)	Tete	1976	USA	midge (species unknown)	[145]	MK896433–MK896435
1	Wongal	WONV	MRM 168 (P6SM1)	Koongol	1960	Australia	*Culex* mosquito	[146,147]	MK896430–MK896432
1	Wyeomyia	WYOV	Original (P8SM1V1)	Wyeomia	1940	Colombia	*Wyeomyia melanocephala* mosquito	[80]	MH484345–MH484347
3	Yaba-7	Y7V	Yaba 7 (P5SM1)	Simbu	2005	Nigeria	*Mansonia 20ocktail* mosquito	[148]	MH484348–MH484350
4	Zegla	ZEGV	BT 5012 (P?SM7)	Patois	1961	Panama	Rat	[113,127]	MK896421–MK896423

Sequence status as of October 3, 2019

1= Completely new genome sequence

2= New strain sequence information

3= Addition of missing genome segments or coding complete segments

4= Sequence information already existed. In almost all of these cases, sequences were deposited by other authors during the course of this study.

* Passage number as defined in ARC metadata

** Currently recognized country names

*** Based on ARC metadata compiled by the CDC

Table 2.2. Sequenced genomes of 6 viruses belonging to *Phenuiviridae* (*Phlebovirus* and *Uukuvirus*).

Sequence Status	Virus	Abbreviation	Strain (Passage)	Serogroup	Collection Date	Collection Country	Isolation Source	Original Virus Description	GenBank Accession
4	Bujaru	BUJV	BeAn 47693 (P10SM2)	Sandfly fever	1962	Brazil	Rat	[76]	MK896442 – MK896444
2	Kaisodi	KASDV	G 14132 (P6SM1)	Sandfly fever	1957	India	Ixodid tick	[149,150]	MK896549 – MK896551
4	Palma	PLMV	PoTi 4.92 (P?SM3)	Sandfly fever	1992	Portugal	Ixodid tick	[151]	MK896492 – MK896494
2	Punta Toro	PTV	D-4021A (SM15)	Sandfly fever	1966	Panama	Human	[152]	MK896481 – MK896483
1	Sunday Canyon	SCAV	RML 52301–11 (SM5V1SM2)	Sandfly fever	1969	USA	Argasid tick	[153]	MK896463 – MK896465
2	Zaliv Terpeniya	ZTV	LEIV 21C (P7SM2)	Uukuniemi	1969	Russia	Ixodid tick	[154]	MK896424 – MK896426

Sequence status as of October 3, 2019

1= Completely new genome sequence

2= New strain sequence information

3= Addition of missing genome segments or coding complete segments

4= Sequence information already existed. In almost all of these cases, sequences were deposited by other authors during the course of this study.

* Passage number as defined in ARC metadata

** Currently recognized country names

*** Based on ARC metadata compiled by the CDC

Table 2.3. Sequenced genomes of 5 viruses belonging to *Nairoviridae* (*Orthonairovirus*).

Sequence status	Virus	Abbreviation	Strain (Passage)	Serogroup	Collection Date	Collection Country	Isolation Source	Original Virus Description	GenBank Accession
4	Estero Real	ERV	K 329 (P3SM1)	Ungrouped	1980	Cuba	Argasid tick	[155]	MK896577 – MK896579
2	Hughes	HUGV	Dry Tortugas (P15SM2)	Hughes	1962	USA	Argasid tick	[156]	MK896561 – MK896563
4	Sapphire II	SAPV	75V8196 (P4SM1)	Hughes	1975	USA	Argasid tick	[157]	MK896466 – MK896468
1	Wanowrie	WANV	Ig 700 (P7SM1)	Ungrouped	1954	India	Ixodid tick	[87,89]	MK896436 – MK896438
4	Yogue	YOGV	DakAnD 5634 (P7SM1)	Yogue	1968	Senegal	Bat	[87]	MK896427 – MK896429

Sequence status as of October 3, 2019

1= Completely new genome sequence

2= New strain sequence information

3= Addition of missing genome segments or coding complete segments

4= Sequence information already existed. In almost all of these cases, sequences were deposited by other authors during the course of this study.

* Passage number as defined in ARC metadata

** Currently recognized country names

*** Based on ARC metadata compiled by the CDC

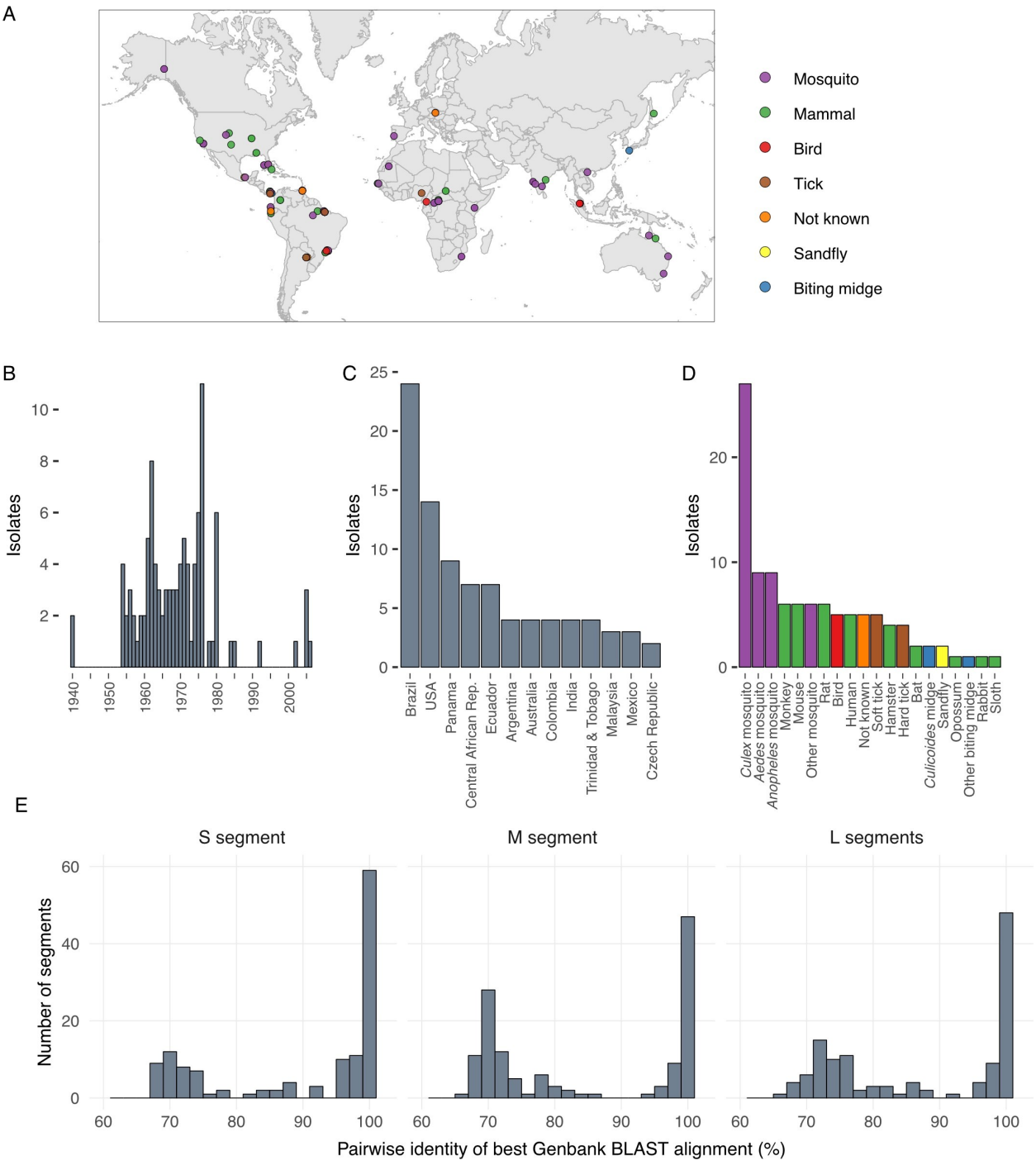

Figure 2.1. Characteristics of sequenced bunyavirus isolates.
Bunyavirus isolates were collected from around the world over the span of 7 decades from a variety of vertebrate and arthropod hosts. (A) Map showing original collection location of isolates, color-coded by host type, NK (not known); (B) histogram showing the number of isolates collected each year; (C) histogram showing the number of isolates from the indicated countries, for countries with 2 or more isolates; (D) histogram showing the number of isolates from the indicated host type. (E) histograms showing the pairwise percent nucleotide identity for the highest scoring BLASTn alignments to existing sequences in the NCBI nucleotide database for the sequenced S, M, and L segments.

Several viruses with nearly identical sequences had been given different names and, conversely, some viruses with the same name had quite different sequences. For instance, wongal virus had previously been classified with koongol virus in the species Koongol orthobunyavirus, but no sequence information for wongal virus was available [32]. Both viruses were isolated from *Culex annulirostris* mosquitoes several days apart from the same location in Australia [146]. We found that these viruses shared >99.7% pairwise nucleotide identity across all three segments. Thus, koongol and wongal viruses are the same virus. Similarly, all three segments of the Santa Rosa and Lokern (strain A 10391) viruses that we sequenced shared >98.5% identity.

In contrast, the Lukuni virus isolate that we sequenced (strain ColAn 57389) was unexpectedly different from the previously sequenced Lukuni virus (strain TRVL 10076) [158]. These two viruses shared <70% pairwise nucleotide identity across all three segments. Instead, the L and S segments of Lukuni virus strain ColAn 57389 were more similar to those of the Las Maloyas virus isolate that we sequenced (85% and 87% pairwise nucleotide identity). Likewise, the Guajara´ virus that we sequenced (strain 18315) and the previously sequenced Guajará virus
(strain BeAn 10615) shared less than 78% pairwise nucleotide identity over all three segments [158]. These unexpected differences highlight the utility of sequencing additional strains of already-sequenced viruses.

2.2.2 Phylogenetic analyses

We performed a coalescent phylogenetic analysis of the L, M, and S segments (**Figures 2.2–2.6**). Trees included all of the viruses that we sequenced and all of the

bunyavirus sequences from the genera in question in the NCBI RefSeq database as phylogenetic landmarks. We also created trees containing all available sequences annotated under the relevant taxa in the NCBI taxonomy database (**S2–S4 Figures**). New orthobunyavirus genome sequences fell throughout the Orthobunyavirus genus (**Figures 2.2-2.4 and S2–S4**). The numbers of genome sequences sequenced in this study from the orthobunyavirus serogroups included: Anopheles A (3), Anopheles B (3), Bakau (4), Bunyamwera (16), Capim (7), Wyeomyia (1), Turlock (3), Koongol (1), Gamboa (3), Guama (7), Minatitlán (1), Group C (11), Patois (5), Simbu (9). Additionally, 5 viruses sequenced fell within the family Nairoviridae, 7 in the family Phenuiviridae and 2 in the genus Pacuvirus (**Figures 2.5 and 2.6 and S5**).

Several virus genomes that were sequenced as part of this study had not been assigned to serogroups. We compared the phylogenetic placement of these viruses to that of viruses that had been categorized into established serogroups (**Tables 2.1–2.3**). Bangui virus was placed in L and S segment trees within an undesignated clade just prior to the divergence of the Anopheles A and B serogroup (**Figures 2.2–2.4**). The Belem, Pacora, and Brazoran viruses formed a monophyletic clade on all three orthobunyavirus trees (**Figures 2.2–2.4**), indicating a common ancestor between the three viruses. However, this clade was placed in different locations on the phylogenies for the different segments. On L and M segment trees, these three viruses branched basally to the Patois, Guama, Minatitlán, Group C, and Capim serogroups with strong posterior probability support (**Figures 2.2 and 2.3**). The S segment phylogeny showed this clade diverging from all other orthobunyaviruses with posterior probability support of 1.0 (**Figure 2.4**).

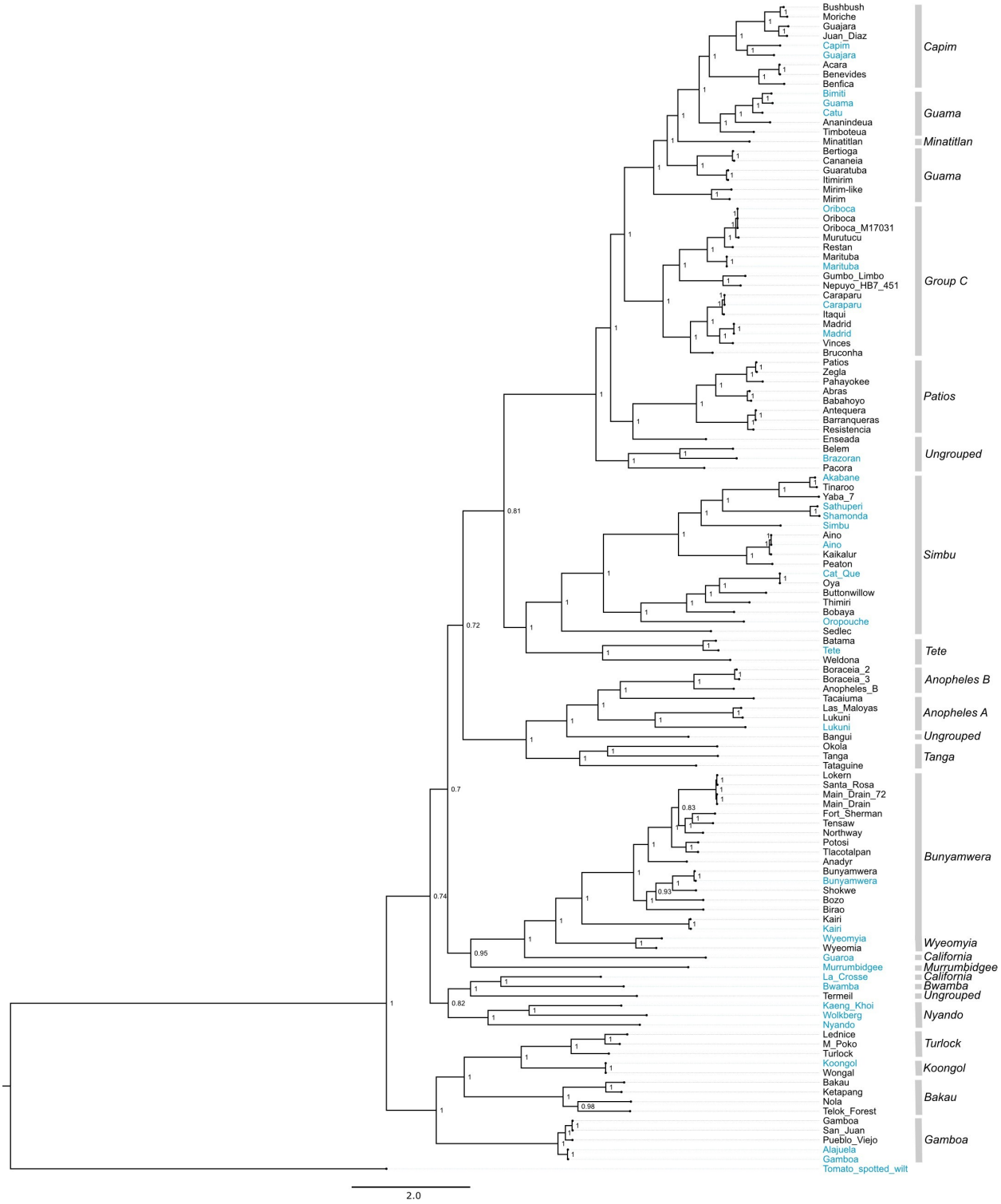

Figure 2.2. L segment phylogeny for viruses in *Orthobunyavirus*.
Bayesian phylogenetic tree using the ORF on the L segment. Numbers at nodes indicate posterior probability values. Reference sequences (sequences present in the NCBI RefSeq database) are included as phylogenetic landmarks and colored blue. Sequences from this study are colored black. Classical serogroup distinctions are indicated. Scale bars represent substitutions per site.

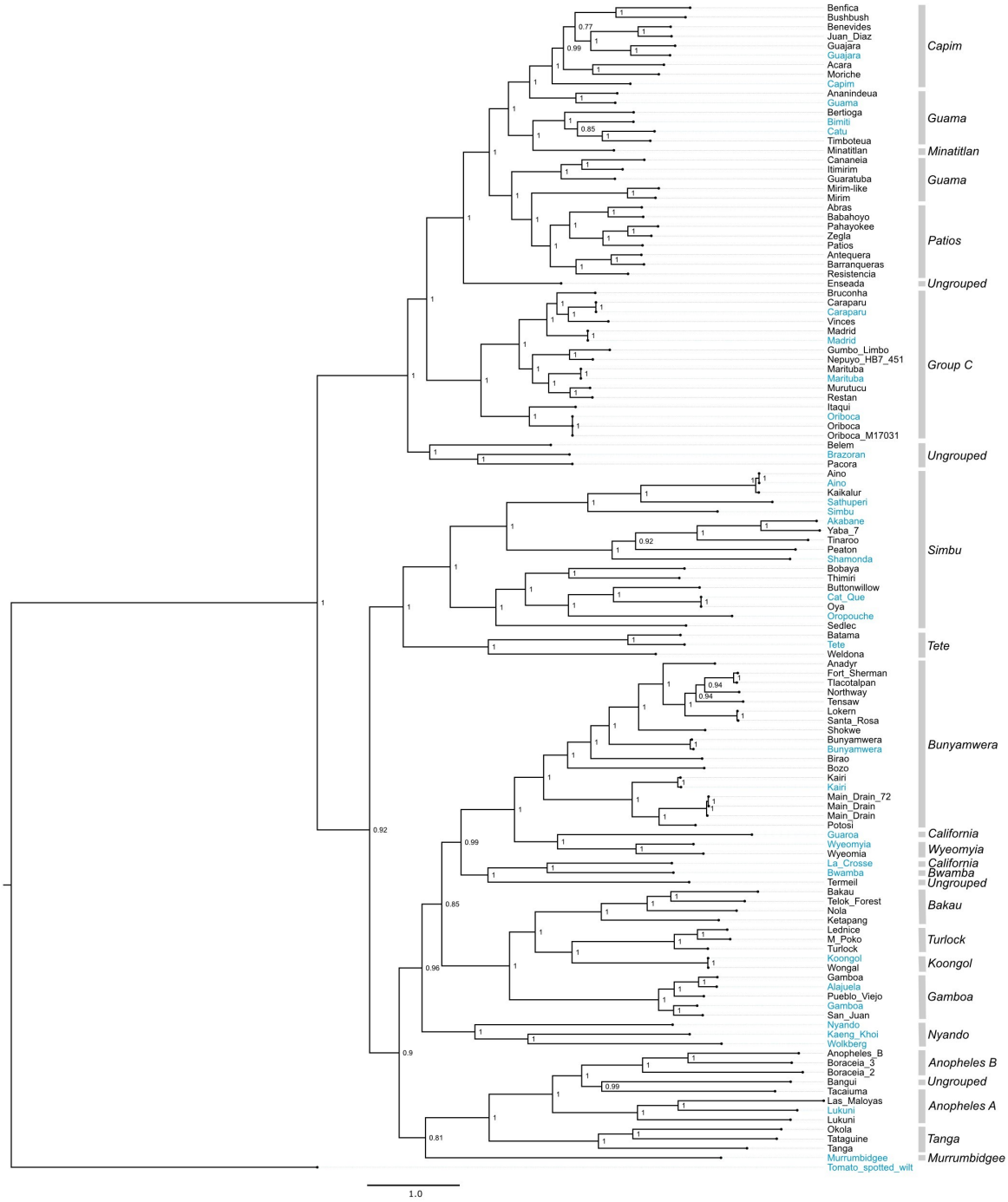

Figure 2.3. M segment phylogeny for viruses in *Orthobunyavirus*.
Bayesian phylogenetic tree using the ORF encoding Gn/Gc on the M segment. Numbers at nodes indicate posterior probability values. Reference sequences are colored blue and sequences generated in this project are colored black. Classical serogroup distinctions are indicated. Scale bars represent substitutions per site.

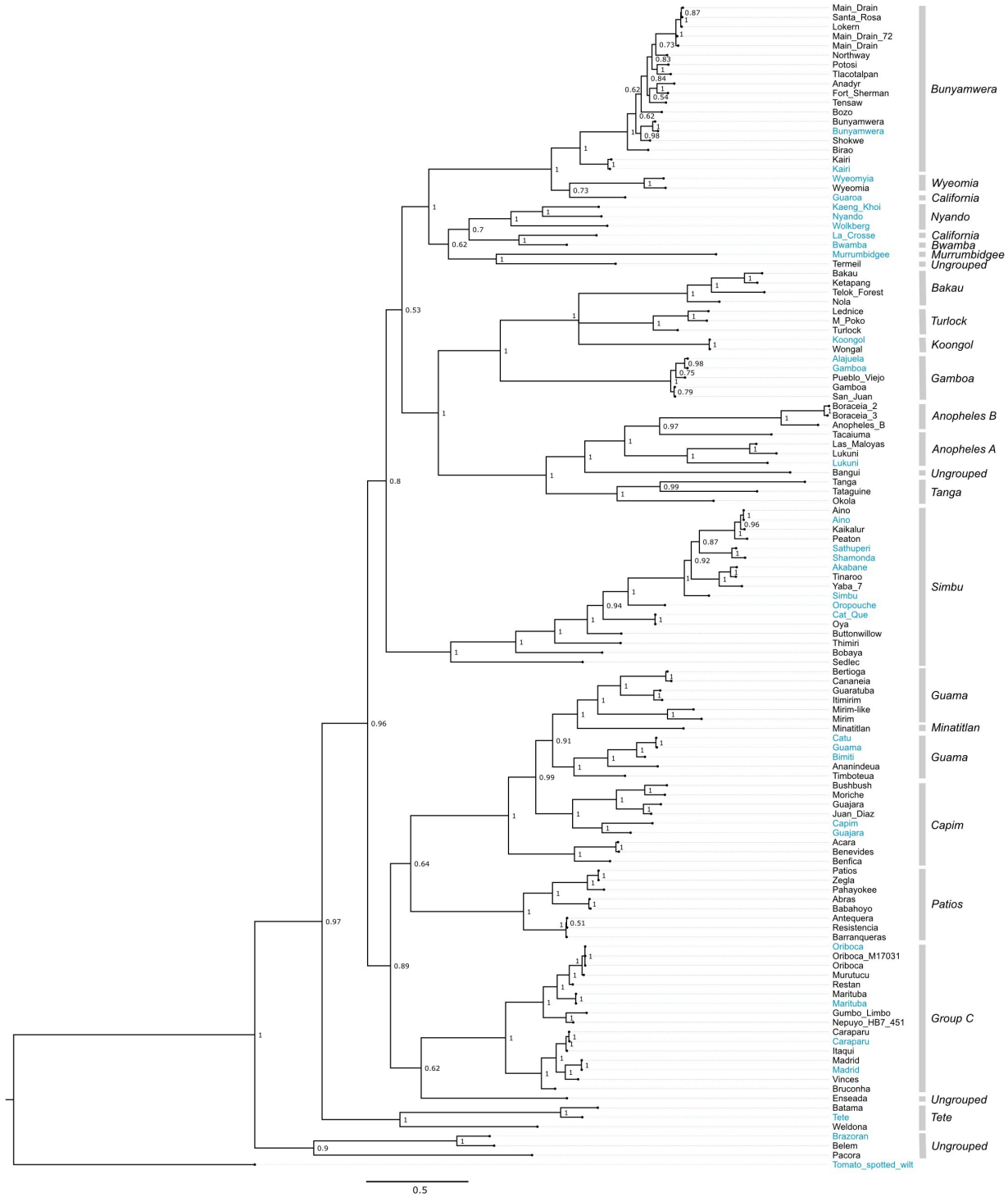

Figure 2.4. S segment phylogeny for viruses in *Orthobunyavirus*.
Bayesian phylogenetic tree using the ORF encoding NP on the S segment. Numbers at nodes indicate posterior probability values. Reference sequences are colored blue and sequences generated as part of this study are colored black. Classical serogroup distinctions are indicated. Scale bars represent substitutions per site.

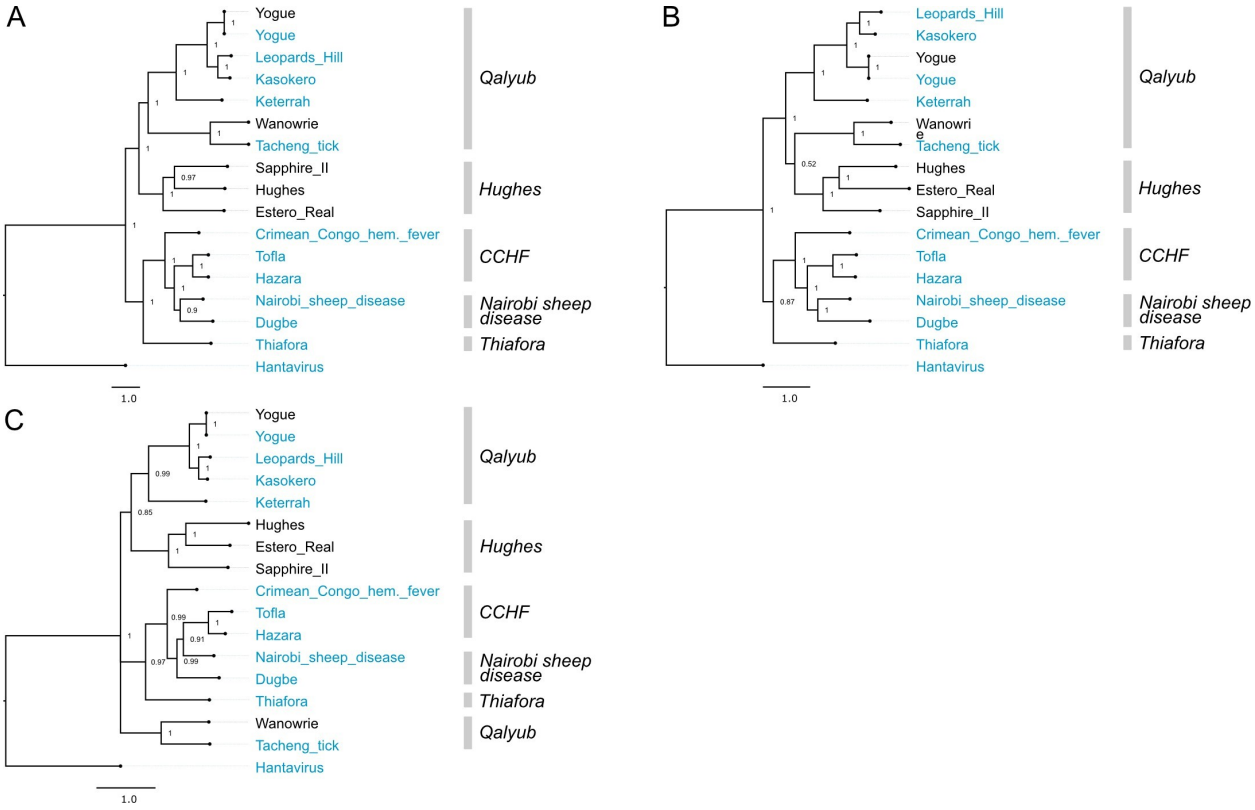

Figure 2.5. Phylogenetic analysis of viruses in *Nairoviridae*.
Bayesian phylogenetic tree using (A) the ORF encoding the RdRp on the L segment, (B) the ORF encoding Gn/NSm/Gc on the M segment, and (C) the ORF encoding NP on the S segment. Numbers at nodes indicate posterior probability values. Reference sequences are included as phylogenetic landmarks and colored blue. Sequences generated in this study are colored black. Classical serogroup distinctions are indicated. Scale bars represent substitutions per site.

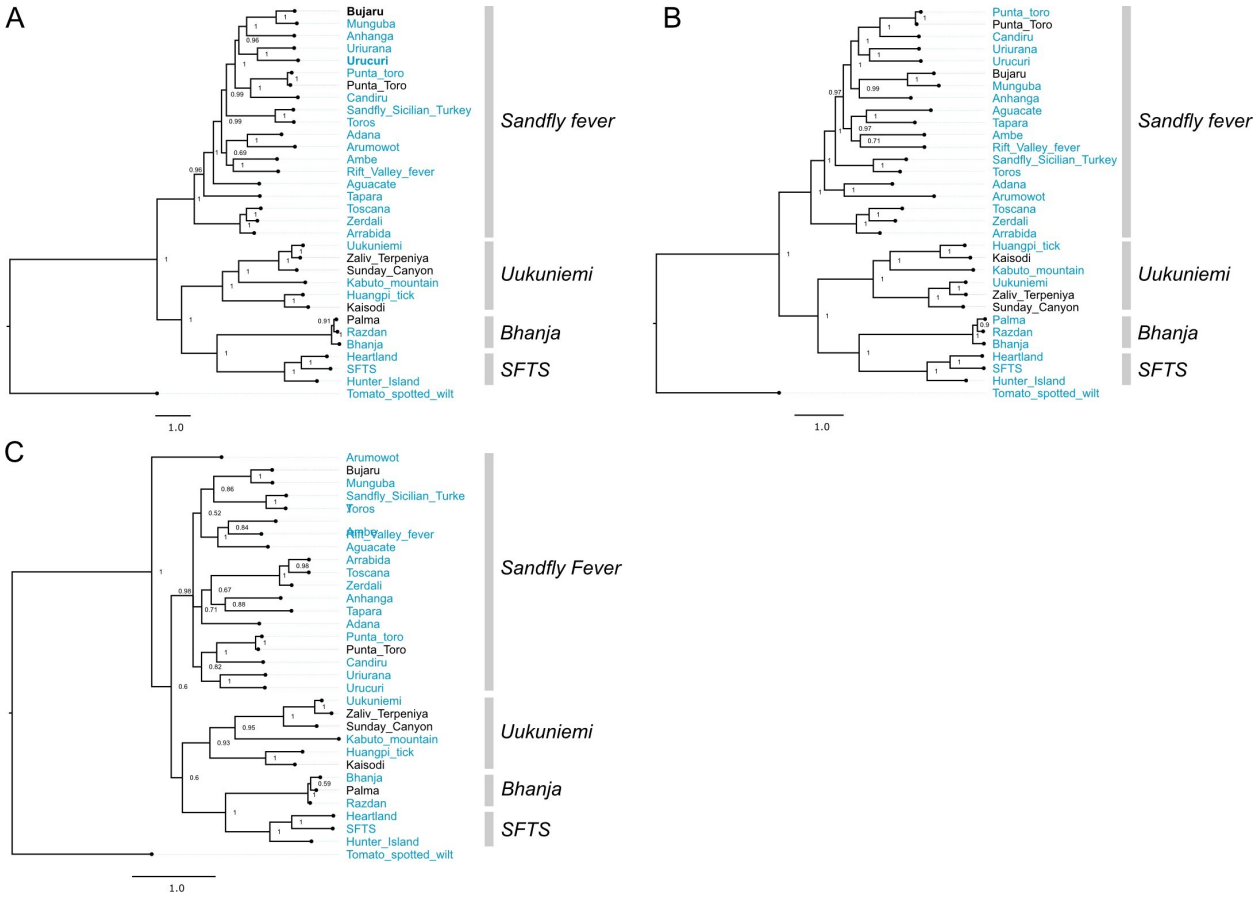

Figure 2.6. Phylogenetic analysis of viruses in *Phenuiviridae*.
Bayesian phylogenetic tree using (A) the ORF encoding the RdRp on the L segment, (B) the ORF encoding Gn/Gc on the M segment, and (C) the ORF encoding NP on the S segment. Numbers at nodes indicate posterior probability values. Reference sequences are included as phylogenetic landmarks and colored blue. Sequences generated in this study are colored black Classical serogroup distinctions are indicated. Scale bars represent substitutions per site.

Enseada virus exhibited a similar discrepant placement in the 3 orthobunyavirus trees. The L segment of Enseada virus diverged off of the Patios serogroup (**Figure 2.2**). The M segment of Enseada virus diverged prior to the bifurcation of the Guama, Capim, Patois, and Minatitlan serogroups (**Figure 2.3**). Finally, the S segment of Enseada diverged just prior to the Group C serogroup (**Figure 2.4**). All of these placements were well-supported, with posterior support of 1.

Across all segments, Termeil virus branched basal to the California encephalitis and Bwamba serogroups. On the S segment phylogeny, Termeil virus grouped with

Murrumbidgee virus (aka Trubanaman virus [159,160]), though posterior probability support was low (**Figure 2.4**).

The placement of two viruses in our trees diverged from their expected placements based on assigned serogroup classification. Tacaiuma virus has been assigned to the Anopheles A group. However, in the L, M, and S segment phylogenies, Tacaiuma virus instead clustered with high support with viruses in the Anopheles B serogroup (**Figures 2.2–2.4**). Guaroa virus has been assigned to the California serogroup, but did not cluster with La Crosse virus as this would suggest. Instead, across all segments, Guaroa virus branched basally to the Wyeomyia serogroup (**Figures 2.2–2.4**).

Caimito virus and Santarem virus grouped together with viruses in the genus Pacuvirus (**S2.5 Figure**). Our results coincide with the recent proposal to reclassify Caimito virus as belonging to the genus Pacuvirus (*Peribunyaviridae*) [161]. Our phylogenies consistently placed Santarem virus with Caimito virus. We propose Santarem be classified in the Pacuvirus genus along with Caimito virus.

Among the nairoviruses, Wanowrie consistently fell within the Qalyub serogroup of the Orthonairovirus genus, most closely related to Taˇchéng tick virus, though there was insufficient support in the S segment tree to group these two viruses with the rest of those in the Qalyub serogroup (**Figure 2.5**). Estero Real virus was consistently placed within the Hughes serogroup for all three segments with strong posterior probability support (**Figure 2.5**).

In phenuivirus trees, Bujaru and Punta Toro viruses consistently grouped within the Sandfly fever serogroup, as expected (**Figure 2.6**). Also, expectedly, Zaliv Terpeniya

and Sunday Canyon grouped within the Uukuniemi serogroup and Palma grouped with Bhanja serogroup across all segments (**Figure 2.6**). One deviation of note within the phenuivirus trees is the divergent placement of Arumowot virus S segment (**Figure 2.6**).

2.2.3 Reassortment

To further evaluate reassortment among the viruses we sequenced, we created co-phylogenies (tanglegrams) of L, M, and S segments (**Figures 2.7–2.11**). Prior to generation of these co-phylogenies, we collapsed interior nodes with support values < 0.95 so that poorly supported branching patterns would not produce false signals of reassortment. We also performed all possible pairwise global alignments of the coding regions of the segments to identify pairs of viruses with differential nucleotide identities between segments, for instance, pairs of viruses with closely related L and S segments but relatively divergent M segments (**S2.2 Table**). Numerous local topological incongruencies were apparent in the trees, but here we focus on the clearest examples of reassortment that were well supported by both phylogenetic discordance and large discrepancies in pairwise genetic distances.

These analyses identified evidence of widespread reassortment among the orthobunyaviruses (**Figures 2.7–2.9**). In some cases, these corresponded to reassortment events that had been previously identified, but in other cases these were newly described. Most, but not all, well supported instances of reassortment involved viruses with similar L and S segments but relatively different M segments. This was evident in the relatively similar topologies of the L and S segment trees and the increased degree of crossing-over in the L-M and M-S tanglegrams. This corresponds to reassortant

progeny that comprise the L and S segment of one co-infecting parent virus and the M segment of the second parent. In contrast, the differential placement of Brazoran, Belem and Pacora viruses on the L and M as opposed to the S segment phylogenies supports the hypothesis that this group of viruses resulted from an ancestral reassortment event involving the replacement of an S segment [68].

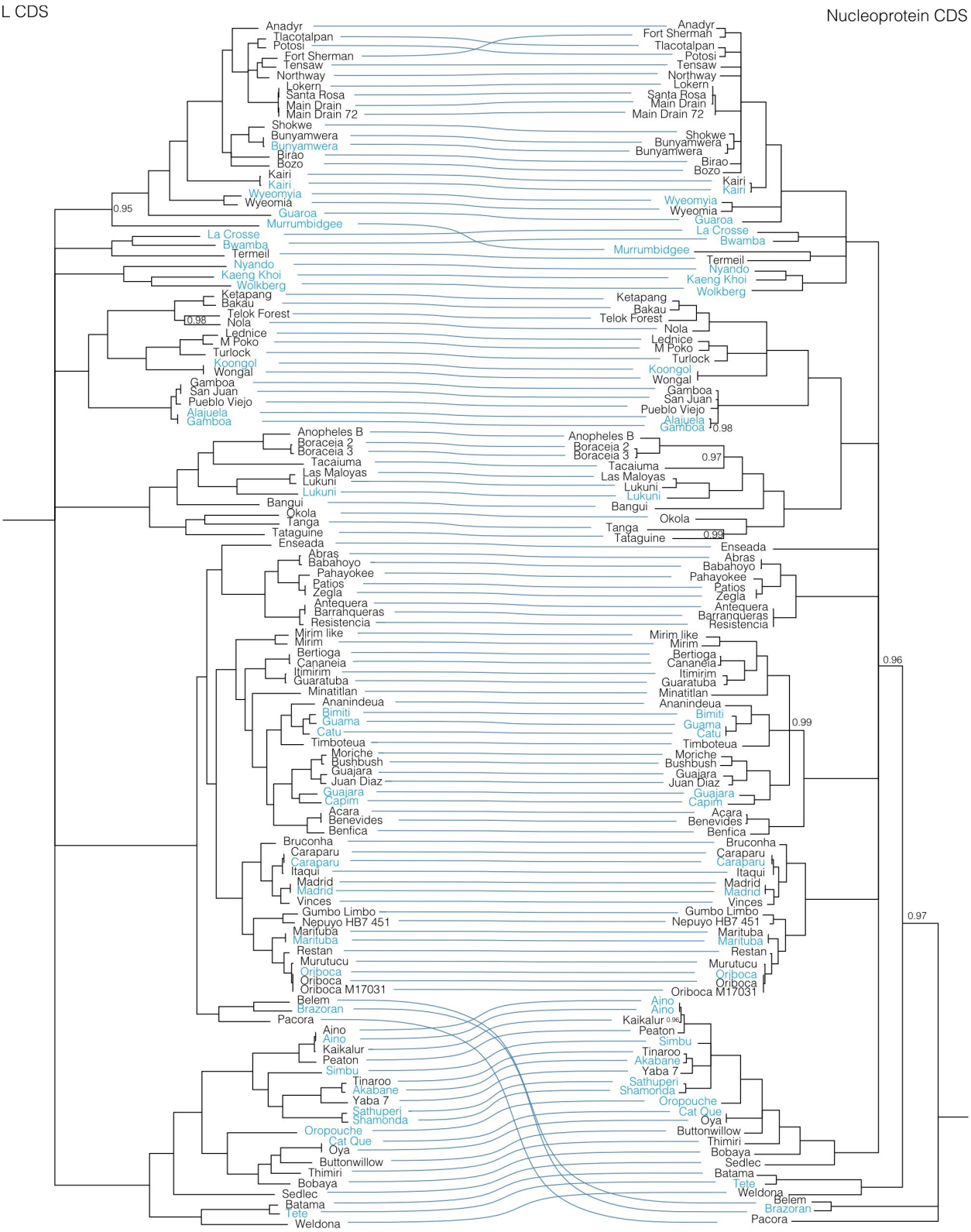

Figure 2.7. Co-phylogenies of *Orthobunyavirus* L and S segment trees.
Branches with support values < 0.95 were converted to polytomies. All other branch support values were 1 unless indicated. Trees were rooted with outgroups as in Figures 2.2–2.4.

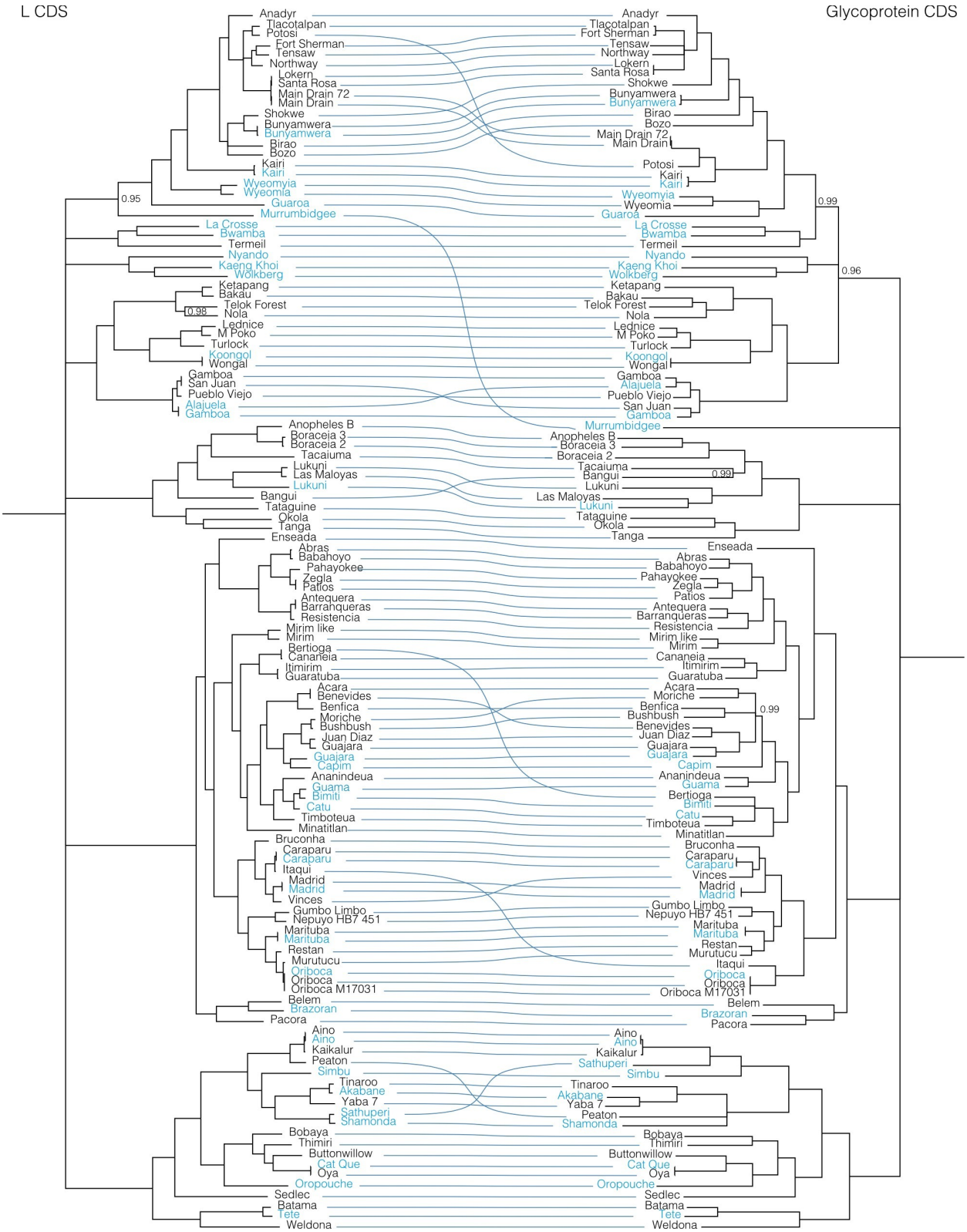

Figure 2.8. Co-phylogenies of *Orthobunyavirus* L and M segment trees.
Branches with support values < 0.95 were converted to polytomies. All other branch support values were 1 unless indicated. Trees were rooted with outgroups as in Figures 2..2–2.4.

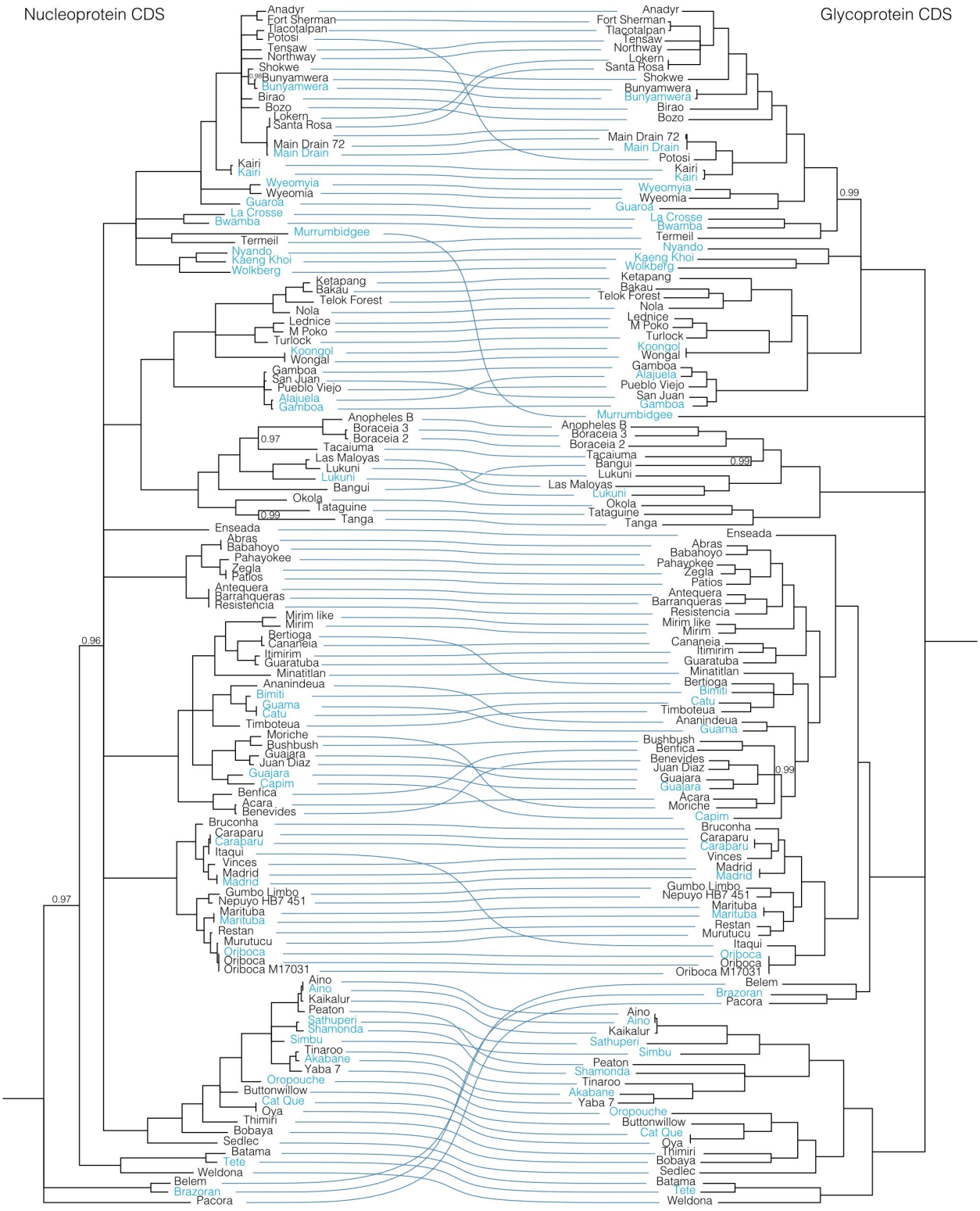

Figure 2.9. Co-phylogenies of *Orthobunyavirus* S and M segment trees.
Branches with support values < 0.95 were converted to polytomies. All other branch support values were 1 unless indicated. Trees were rooted with outgroups as in Figures 2.2–2.4.

Consistent with previous reports, there was evidence of extensive reassortment involving all 3 segments in the Bunyamwera serogroup [52,162,163]. The Fort Sherman and Anadyr virus isolates sequenced in this study have S segments with 90% pairwise nucleotide identity but relatively different L and M segments that shared <75% pairwise nucleotide identity. This is one of the few examples we identified of viruses with closely related S segments but relatively different L and M segments. The S and L segments of Potosi virus were most closely related to those of Tlacotalpan virus, but the M segment was more related to Kairi and Main Drain viruses (**Figures 2.2–2.4 and 2.7–2.9 and S2.2 Table**). Both Main Drain isolates that we sequenced had S and L segments that were >95% identical to those of Santa Rosa and Lokern viruses. But the Main Drain M segments clustered instead with those of Potosi and Kairi viruses. Shokwe and Bunyamwera viruses L and S segments grouped together, but their M segments did not form a monophyletic cluster.

In the Bakau serogroup, Ketapang and Bakau viruses had similar L and S segments (81 and 88% identical) but relatively different M segments (66% identical). The M segment of Bakau virus was instead more closely related to that of Telok Forest virus, with which it shared 70% pairwise nucleotide identity.

The two Boracéia virus strains that we sequenced (SPAr 395 and SPAr 4080) were isolated from Anopheles cruzii mosquitoes in São Paulo, Brazil in 1962 and 1965, respectively (**Table 2.1**). These isolates had closely related L and S segments with >91% pairwise nucleotide identity but M segments that shared only 63% identity (**Figure 2.7 and S2.2 Table**). The Bangui virus L and S segments branched basally to the viruses in

the Anopheles A and B groups in the L and S segment trees, but in the M segment tree, Bangu virus fell on a well-supported branch with Tacaiuma virus nested within these groups. Patois and Zegla viruses had nearly identical L and S segments with 97% and 99.7% pairwise nucleotide identity, but their M segments shared only 73% identity.

In the Simbu group viruses, Aino, Kaikalur and Peaton viruses formed a well-supported cluster on L and S segment trees, but the M segment of Peaton virus was at the end of a long, separately placed branch. The Tinaroo and Akabane virus L and S segments were 87 and 95% identical, but the M segments shared only 65% pairwise nucleotide identity. A similar pattern was evident for Athuperi and Shamonda viruses.

Antequera, Barrenqueras, and Resistencia viruses exhibited patterns of sequence relatedness indicative of multiple past reassortment events. The S segments of these three viruses were all 99% identical. The L segments of Antequera and Barrenqueras were also nearly identical (99%), but these were both only 90% identical to the L segment of Resistencia virus. The M segments of the three viruses all shared <71% pairwise nucleotide identity.

In the Guama and Capim group viruses, there were several examples of apparent M segment reassortment. Bertioga and Cananeia viruses had highly related L and S segments but M segments that were only 67% identical. The same pattern was evident for Itimirim and Guaratuba viruses, for Moriche and Bushbush viruses, for Acara and Benevides viruses, for Guajara and Juan Diaz viruses, and for the trio of Bimiti, Guama and Catu viruses.

Reassortment has also clearly shaped the evolution of the Group C orthobunyaviruses, as has been previously noted [18,164,165]. Caraparu and Itaqui viruses had nearly identical L and S segments but quite different M segments. The M segment of Itaqui virus was instead much more similar to that of Oriboca virus. The L and S segments of Vinces virus clustered with those of Madrid virus, but the Vinces virus M segment was more closely related to that of Caraparu virus. Restan, Murutucu, and Oriboca virus formed a well-supported cluster on L and S segment trees, but on the M segment tree, Restan amd Murutucu viruses remained clustered together while the Oriboca virus M segment was on a branch basal to the other Group C viruses with Itaqui virus.

There was little evidence for reassortment among the orthonairoviruses in our analysis. The only instance of possible reassortment was for Hughes virus. Despite similar pairwise nucleotide identities between the three segments of Hughes, Sapphire II, and Estero Real viruses, these three viruses had different branching patterns on the three segment trees, albeit with long branch lengths and support values <1 (**Figure 2.10 and S2.2 Table**). In phlebovirus tanglegrams, Aguacate and Tapara viruses showed evidence of reassortment, but there was no strong evidence for reassortment among the phleboviruses sequenced in this study (**Figure 2.11**).

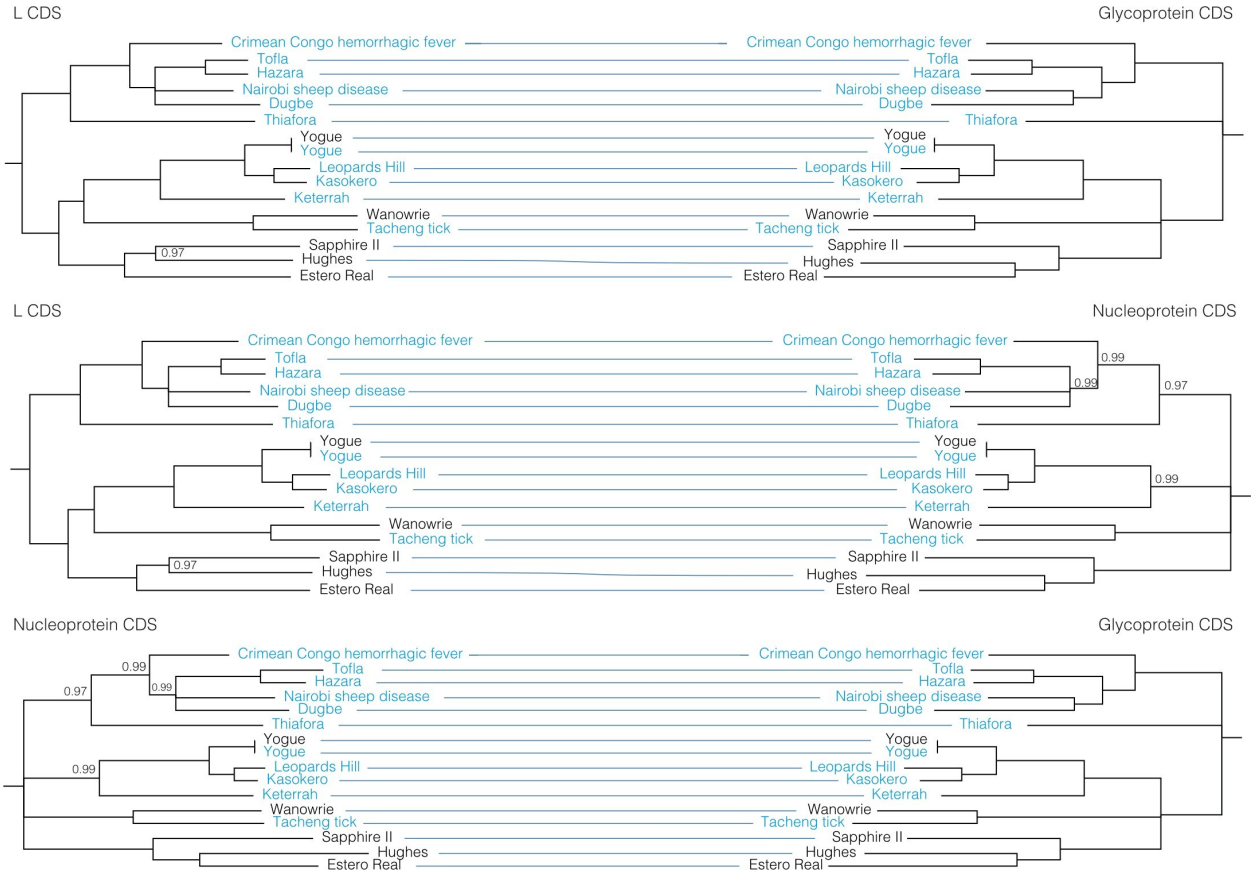

Figure 2.10. Co-phylogenies of *Nairoviridae* L, M, and S segment trees.
Branches with support values < 0.95 were converted to polytomies. All other branch support values were 1 unless indicated. Trees were rooted with outgroups as in Figure 2.5.

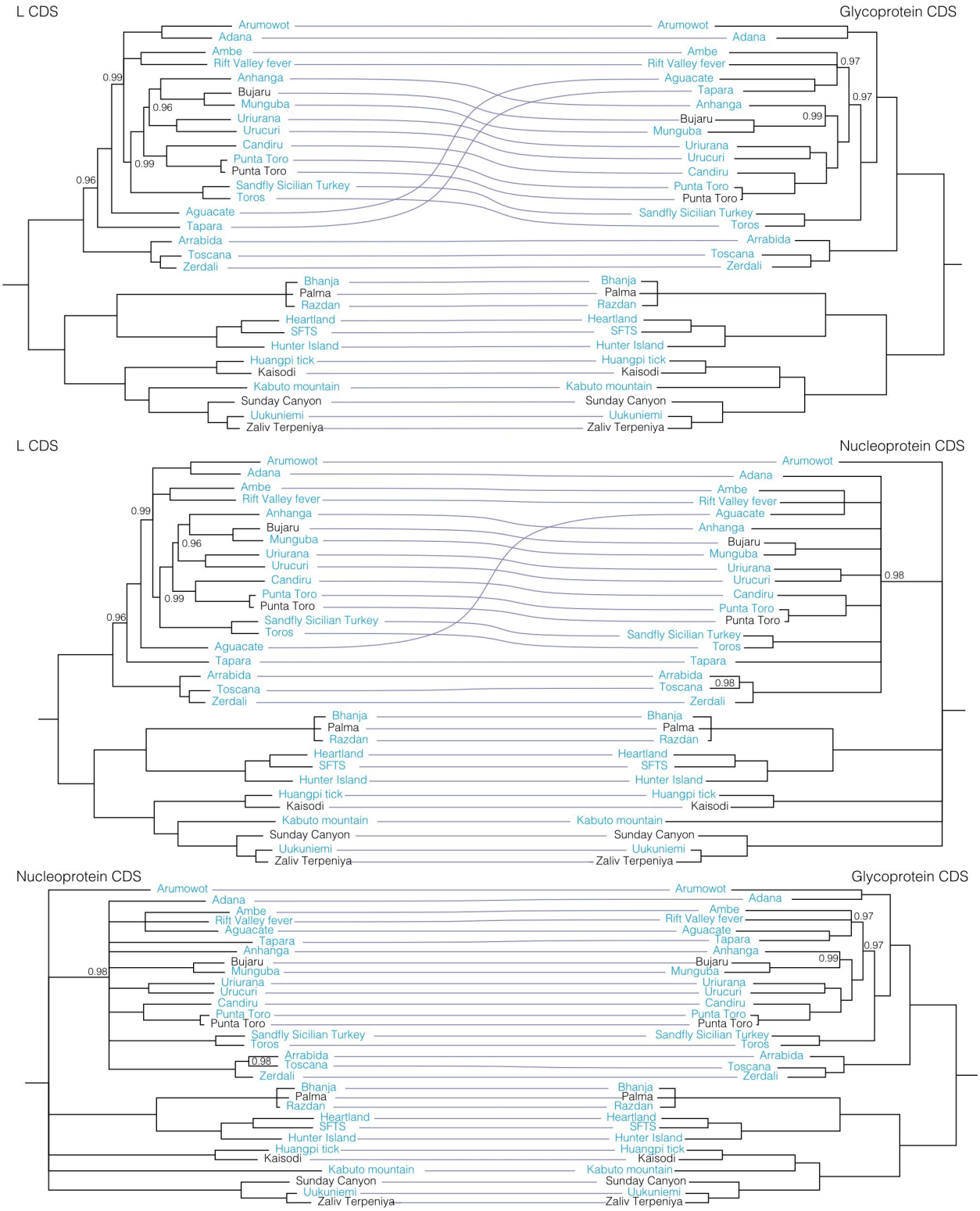

Figure 2.11. Co-phylogenies of *Phenuiviridae* L, M, and S segment trees.
Branches with support values < 0.95 were converted to polytomies. All other branch support values were 1 unless indicated. Trees were rooted with outgroups as in Figure 2.6.

2.2.4 Co-infection

We identified evidence of co-infection (i.e. RNA from more than one virus) in four virus stocks: Abras virus, Guaratuba virus, Hughes virus, and one of the two Main Drain virus isolates. The initial indication that there might be co-infection in these stocks was the assembly of more than the expected three bunyavirus contigs from the corresponding datasets and was followed up with additional computational and molecular tests to validate possible co-infections.

In the Abras virus dataset, six coding-complete sequences assembled, including 2 L, 2 M, and 2 S segments. Three of the segments matched the previously sequenced Abras virus isolate 75V1183 (the same isolate that we sequenced) with 99–100% nucleotide identity [166]. The other three segments belonged to a previously unsequenced bunyavirus in the Guama serogroup most closely related to Mirim virus, with which it shared 77–81% pairwise nucleotide identity. Abras virus was present at a much higher abundance: 33,462 reads mapped to the three Abras virus segments, whereas only 2,091 reads mapped to the Mirim-like segments. Using RT-PCR with segment-specific primers (**S2.1 Table**), and RNA re-extracted from another vial of the isolate, we successfully amplified all six segments to confirm the coinfection. Additionally, we attempted to plaque-purify both viruses from the original isolate by Vero cell plaque assay. However, among the 90 viral plaques screened, none purely represented the coinfecting Guama serogroup virus, and passage of the co-infecting virus on Vero cells in an attempt to isolate it repeatedly failed. Additional preparations of Abras virus in the ARC that had been passaged in suckling mouse brain did not contain this co-infecting

virus, leading us to suspect that the contaminant was introduced during original preparation of this particular virus stock that was sequenced during this study. Notably, Aguilar et al. (2018) did not report a co-infecting virus after also sequencing Abras isolate 75V1183 [166].

The Guaratuba virus dataset also produced 6 coding complete or partial bunyavirus segment sequences. Coding-complete sequences were assembled for all three segments of Guaratuba virus, as inferred based on their phylogenetic placement with other Guama serogroup viruses. An additional L, M, and S segment were assembled, but only the S segment was coding-complete. The additional partial L, M, and S sequences were 98% identical at the nucleotide level to strain 76V-25880 of Enseada virus [79,167]. The Guaratuba virus sequences had 7x more mapping reads (3,164) than the coinfecting Enseada-like virus (457). The Enseada virus-like sequences from the Guaratuba datasets were only 85–93% identical to the Enseada virus isolate strain 78V-213 genome that we sequenced for this project, indicating that these sequences were not attributable to cross-contamination during sample processing and library preparation. We used RT-qPCR to confirm the presence of all six segments in the original RNA from which the sequencing library was made. An independent RNA extract from Vero cells infected with Guaratuba virus from a second vial from the same lot was also positive for all 6 segments by RT-qPCR.

The Hughes virus dataset produced 4 bunyavirus contigs corresponding to a complete L, M, and S segment, and a partial M segment of about 1.2 kb. This partial M segment was nearly identical to a previously published Hughes virus M segment

sequence (99.4% identical to strain DT-1, accession KP792739.1) The full length M sequence was only 81% identical to Hughes virus strain DT-1 and 72% identical to Hughes virus strain G2126 (accession KU925471). The partial M sequence had a coverage level of 2.4% relative to the full-length M sequence.

For Main Drain virus strain 72V2567, we assembled coding complete sequences for the L, M, and S segments with 452,386 mapping reads. In addition, 90 reads mapped to Cache Valley virus strain 6V633. We were able to corroborate the detection of the Cache Valley virus-like sequences using RT-qPCR with discriminating primers (**S2.1 Table**). The L, M, and S partial sequences were 98.5%, 95.9%, and 99% identical to Cache Valley virus respectively (MH166879.1, MH166878.1, MH166877.1).

2.3 Discussion

Bunyaviruses comprise one of the largest viral orders, and some bunyaviruses pose substantial threats to humans, animals, and plants [63]. We generated complete genome sequences for 99 bunyaviruses belonging to the families *Nairoviridae*, *Peribunyaviridae*, and *Phenuiviridae*, and analyzed them phylogenetically. Our results were consistent with recently published phylogenies on the Patois serogroup viruses [166] and a diversity of orthobunyaviruses in the Anopheles A, Capim, Guamá, koongol, Mapputta, Tete, and Turlock serogroups [158], but difficult to compare entirely given the inclusion of different viruses in each published analysis. Given the large number of viruses sequenced in this study, we elected to limit additional sequences in our phylogenies to new sequences plus those in NCBI RefSeq.

The phylogenies recapitulated assigned serogroups relatively well, however there were several points of inconsistency between the two. It is not that surprising that the determined phylogenetic relationships did not completely recapitulate established serogroups. Serology is based on similarities/dissimilarities in the surface proteins of the virion particle (encoded exclusively by M segments), whereas phylogenetic analysis can assess the relationships between any genes of any viral genome segment. Although one might expect the M segment to recapitulate the classical serogroup distinctions, this was not the case (**Figures 2.3, 2.5B, and 2.6B**). The L segment is the most conserved segment among all three families and most closely recapitulates the classical serogroup distinctions (**Figures 2.2, 2.5A, and 2.6A**). However, we found that several serogroups were not monophyletic in L segment phylogenies. For example, the Guama serogroup consisted of polyphyletic clades on all segments (**Figures 2.2–2.4**). Capim and Patois serogroups were also polyphyletic in the S segment tree (**Figures 2.4, 2.5C, and 2.6C**). Additionally, we were unable to resolve several ancestral branches which resulted in several polytomies, particularly in orthobunyavirus trees (**Figure 2.4**).

Many human pathogenic viruses in the genus Orthobunyavirus are found within the California, Bunyamwera, Simbu, and Group C serogroups. To these serogroups we have collectively added 33 coding-complete genome sequences. Although the pathogenic potential remains to be determined for many of the viruses sequenced in this study, viruses falling within serogroups for which there were previously no genomic data available will facilitate the identification and prioritization of novel potentially pathogenic strains for further study.

2.3.1 Reassortment

These new sequences also contribute to a richer database with which to resolve the origins of reassortant viruses. Briese et al. [18] proposed that many, if not all, currently recognized bunyaviruses are the product of recent or ancient reassortants between known and/or possibly extinct viruses. High-level analysis for evidence of reassortment supported this hypothesis, and the conclusion that reassortment is a major factor driving bunyavirus genetic variability particularly in the Bunyamwera, Capim, and Group C serogroups (**Figures 2.7–2.9**). Reassortment among bunyaviruses has the potential to result in the emergence of novel human pathogens, as has been the case with Iquitos virus [55], Itaya virus [69], and Ngari virus [168].

L and S segment trees were largely concordant, and reassortment was, in almost all cases, evident as pairs or groups of viruses that had similar L and S segments but different M segments. Previous studies have reported that reassortant bunyaviruses tend to combine the S and L segments from one parent with the M segment from the other parent, making this a seemingly common phenomenon [52,168–170], although this is not always the case [18]. Linkage disequilibrium analysis of LACV isolates from field-collected mosquitoes showed evidence of frequent reassortment among strains in the field, and among all three genome segments [159]. Among the viruses we analyzed, there were several examples of pairs of viruses that had nearly identical S segments but relatively different L and M segments, suggesting recent reassortment events that may have involved the joining of the S segment of one parental virus with the L and M segment of the second parent. The reassortment that has happened frequently throughout

bunyavirus evolution has introduced phylogenetic scrambling that makes it difficult to tease apart exact relationships. Sequencing and analysis of larger numbers of bunyaviruses will continue to shed light on the reassortment that has driven and continues to shape bunyavirus evolution.

2.3.2 Co-infection of viral stocks

We also uncovered evidence of co-infections present in four virus stocks. It is possible that multiple viruses could be co-isolates from pools of mosquitoes containing multiple viruses. Overlapping ranges of the co-infecting viruses could provide support for this hypothesis. For instance, we detected Cache Valley virus reads in the Main Drain strain 72V2567 isolate. This Main Drain virus stock was derived from *Aedes vexans* mosquitoes collected in New Mexico, USA, in 1972, and Cache Valley virus is broadly distributed in Northern and Central America [171]. Similarly, there was evidence of an Enseada virus co-infection in the Guaratuba virus isolate that we sequenced. Guaratuba and Enseada virus have both been isolated from pools of *Culex* mosquitoes collected in 1976 in Brazil [79,167].

Ultimately, however, the true origins of these apparent co-infections are not knowable from our data alone. It is possible that cross-contamination may have occurred during isolation or passage. The failure to identify the co-infecting Mirim-like virus in an independent stock of Abras virus supports this alternative in that case. We can exclude cross-contamination during RNA extraction, library preparation, and sequencing because the co–infecting viruses were not identical to any of the other viruses we sequenced, and

we confirmed the presence of coinfecting RNAs in separate vials of a stock for the Abras, Hughes, and Guaratuba virus isolates. Testing of the original samples and resequencing earlier passages of a virus could resolve ambiguity about the origin of co-infections, but it is likely that the source material for most of these isolates is no longer available. Continuing surveillance and direct sequencing of virus genomes in field samples without virus passage in cell culture will provide additional insight into the extent to which individual vectors or vector populations harbor bunyavirus co-infections, and the extent to which this impacts reassortment potential.

2.3.3 Taxonomic implications

The recent expansion in sequenced bunyaviral genomes–and of RNA virus genomes in general–has led to a restructuring of bunyavirus taxonomy [32,65,70,172–174]. Some of the viruses sequenced in this study will undoubtedly lead to the establishment of new genera and species, particularly within the Orthobunyavirus genus. Our data highlight some unresolved issues with bunyavirus taxonomy that are attributable to pervasive reassortment. For instance, the question of how should pairs of viruses that are nearly identical in 2 of the 3 genome segments but highly divergent in the 3rd, like Bertioga and Cananéia viruses, or Santa Rosa and Main Drain viruses, be classified?

2.4 Conclusions

This study contributed 35 totally new bunyavirus genome sequences to the public domain. These sequences further enrich the reference data available for the identification

of emerging bunyaviruses, facilitate the resolution of phylogenetic relationships among known and newly-described viruses, and provide additional context towards the identification of reassortant strains. In addition, the generation of such a large dataset permitted expanded analyses of coinfection and reassortment. Each of these analyses provided foundational data which will support future investigations on the genetic diversity, reassortment, and virus-vector-host interactions in this important group of emerging human pathogens.

2.5 Materials and Methods

2.5.1 Sample collection

Viruses represented a subset of bunyaviruses catalogued within the ARC [175] (**Tables 2.1–2.3**) that spanned most serogroups as well as ungrouped viruses. RNA was extracted from archived tissue culture supernatants or suckling mouse brain preparations using the QIAamp Viral RNA mini kit according to manufacturer's instructions and eluted in 100µl AVE buffer (Qiagen). TURBO DNase was used to remove residual DNA (ThermoFisher), according to the manufacturer's protocol. RNA concentrations were measured fluorometrically using the Qubit RNA HS Assay kit and a Qubit 3 fluorometer (Life Technologies).

2.5.2 Library preparation and sequencing

The KAPA RNA HyperPrep Kit was used to prepare sequencing libraries from total RNA according to the manufacturer's protocol using half-scale reactions and the Kapa

Dual-indexed Adapter Kit (Kapa Biosystems). Pooled libraries were length-selected for 375–500-bp fragments using a BluePippin 2% cassette (Sage Biosciences). If the length-selected concentration was less than 0.5 nM, additional PCR cycles were performed using the KAPA Library Amplification Kit, until the fluorescence reached that of the kit's internal standard #1. Amplified libraries were cleaned using a 1:1.4 ratio of solid phase reversible immobilization (SPRI) beads (Kapa biosystems). Final length-selected and amplified libraries were diluted to 4 nM and the final concentration determined using the KAPA Library Quantification Kit. Paired-end 2x150bp sequencing was performed on an Illumina NextSeq, producing an average of 2.8 million read pairs per dataset.

2.5.3 Sequence analysis

Reads were demultiplexed and assessed for quality using FastQC [176]. Cutadapt was used to remove low quality and adapter-derived bases [177]. Read pairs with >96% pairwise nucleotide (nt) identity were collapsed using cd-hit-est to remove likely PCR duplicates [178,179]. Host sequences were filtered by mapping reads to the human (NCBI GCRh38) and/or the mouse (UCSC mm10) genomes using the Bowtie2 aligner with parameters,—local—sensitive—scoremin C,60,0 using paired reads [180]. Host-filtered reads were assembled into contigs using SPAdes genome assembler [181]. BLASTn was used to taxonomically assign contigs by nucleotide similarity to the highest scoring sequence in the NCBI nt database with an expect (E) value less than 1e-8 [182,183]. Contigs not taxonomically assigned using BLASTn were assigned by protein-level similarity using DIAMOND aligner to query the NCBI protein database with an expect

value of 1e-3 [184]. Viral contigs were validated by inspecting alignment of mapped reads to draft assemblies in Geneious v11.0.2 [185].

Draft bunyavirus genome assemblies were manually validated by aligning host-filtered reads to contigs using Bowtie2 as described above and alignments were independently validated by two people. Bases at the ends of genomes with less than 4x coverage of the same base were trimmed. After removing low quality data and duplicate and host reads, an average of 3.1% of read pairs remained. We performed de novo assembly to generate draft viral genome segment sequences, which were validated manually by remapping reads to draft assemblies and by Sanger sequencing. Viral reads accounted for an average of 88% of host filtered unique reads, which produced 748-fold mean coverage depth across virus genomes (**S2.1 Figure**). In all cases, sequences validated by Sanger sequencing matched NGS-generated sequences, confirming assemblies and ruling out sample mix-ups.

All genome sequences have been deposited into GenBank under accessions MH484273– MH484350, MK896421–MK896656, MK965544, and MW415980-MW415982. All sequences deposited in GenBank are coding-complete. Quality-filtered sequence reads have been deposited in the sequence read archive (SRA) under Bioproject ID PRJNA543521.

2.5.4 Validation of assemblies by sanger sequencing

Independent Sanger sequence confirmation from re-extracted RNA was obtained from at least one genome segment for 71 of 99 viruses (197 segments). This validation

was performed to ensure that the sequencing data were derived from the intended virus stocks, especially when working with such a large sample set. For 54 viruses, sequences from all three genome segments were independently confirmed. Primers for each segment of each virus were designed from multiple sequence alignments of Illumina-generated sequences for viruses in each serogroup, using Geneious v11.0.2 [185]. Previously-published consensus primers were used when available, such as for viruses in the genus Orthonairovirus and in the genus Orthobunyavirus, phlebotomus fever serogroup [186], Bunyamwera serogroup, and Simbu serogroup [187] (**S2.1 Table**). Viral RNA was re-extracted from a separate vial of the same lot as the original isolate in a 96-well plate format using a Qiagen Biorobot 9604 (Qiagen, Valencia, CA, USA) according to manufacturer's instructions. Nucleic acids were eluted in 100 µl AVE elution buffer supplied with the extraction kit, and stored at -20˚C. Amplification of viral RNA was performed in both forward and reverse directions using the Qiagen OneStep RT- PCR kit (Qiagen, Valencia, CA, USA) according to manufacturer's instructions and using the appropriate primer pair listed in **S2.1 Table**. Amplicons were purified using either the column-based QIAquick PCR Purification Kit (Qiagen) for individual samples or in a 96-well plate format using the Mag-Bind Viral DNA/RNA 96 Kit (Omega Bio-tek, Norcross, GA) on a KingFisher Flex System (ThermoFisher Scientific, Waltham, MA) according to the manufacturer's instructions. Sanger sequencing services were provided by GeneWiz (South Plainfield, NJ, USA). Sequence files were imported into Geneious v11.0.2 for end-trimming and generation of consensus sequences and aligned to the Illumina-generated sequences in either Geneious v11.0.2 or MultiAlign (Corpet 1988) software.

2.5.5 Sequence alignments and phylogenetic analyses

To optimally align sequences, different strategies were used specific to the segment and bunyaviral genus. The open reading frame (ORF) encoding the RdRp protein on the L segment was used for all genera. The ORF of the M segment encoding the Gn/Gc glycoproteins was also used for all genera. The NSm ORF was removed from the alignment because outgroups contained a different genomic organization. Additionally, coding regions for the mucin and GP38 domains were removed from the orthonairovirus sequence alignment. S segments were aligned using the ORF encoding the nucleoprotein. Outgroups were used to root and provide polarity characteristics to the phylogenetic trees. Outgroups were chosen so as to not provide excessive gaps and disturbances in the alignments. Orthotospovirus sequences were used as the outgroups for orthobunyavirus and phlebovirus analyses. Orthohantavirus sequences were used as the outgroup for orthonairovirus analyses. All available reference sequences for each genus were pulled from GenBank's RefSeq database and included in phylogenetic analyses. Alignments were performed on amino acid sequences using the Muscle algorithm and manually inspected afterwards using Seaview v4.1[188,189]. After alignment, sequences were then converted back to their original nucleotide sequences for phylogenetic analysis. Poorly aligned, divergent positions characterized by excessive gaps in the alignment were removed using the Gblocks server under less strict conditions [190]. A coalescent phylogenetic analysis of the L, M, and S segments was conducted for orthonairoviruses, orthobunyaviruses, and phleboviruses: the L segment of pacuviruses was also executed. The analysis was conducted in MrBayes run once for 10 million steps,

sampling every 5,000 steps and discarding the first 10% as burn-in [191,192]. The general time-reversible substitution model (GTR+I+Γ4) was used after determining this model to be optimal using ModelTest [193]. Convergence was assessed by examining the stationary ln-likelihood and effective sample size (ESS, >200) parameters using Tracer v1.4 (http://tree.bio.ed.ac.uk/software/tracer). All phylogenies were executed on the phylo.org server [194]. Output tree files were analyzed using FigureTree v.1.3.1 (http://tree.bio.ed.ac.uk/ software/Figuretree/).

Co-phylogenies were generated using these trees and a co-phylogeny visualization tool, available at https://github.com/stenglein-lab/TreeTangler, and were rooted using the outgroups described above. Prior to generation of co-phylogenies, nodes with support values lower than 0.95 were collapsed to polytomies using TreeGraph2 software [195].

To place the sequences in the context of all available related sequences, we downloaded all full-length L protein sequences annotated under the genera Orthobunyavirus (NCBI taxonomic ID [taxid] 11572) and Phlebovirus (taxid 11584), and the family Nairoviridae (taxid 1980415). We aligned these sequences using the MAFFT aligner, and, because of the large number of sequences, inferred maximum likelihood trees using FastTree software using model parameters -lg -gamma [196,197].

2.5.6 Co-infection analysis

To search for evidence of possible co-infections, we determined the ratio of the number of reads in each dataset that aligned to a given virus (virus self-mapping reads)

to the number of reads that mapped to any bunyavirus protein sequence in the NCBI nr database, including bunyaviruses sequenced in this study. Self-mapping reads were quantified by aligning host-filtered reads to the corresponding assembled genomes using Bowtie2 as described above. Total bunyavirus reads were quantified by aligning host-filtered reads to a database composed of all the protein sequences for bunyavirus-annotated sequences in the NCBI database and from newly assembled genomes in this report, using DIAMOND as above. When the ratio of these two values was less than 0.95, we manually inspected contigs from the dataset to identify sequences of possible co-infecting viruses.

Candidate coinfections were validated using PCR and independent cell cultures. Specifically, PCR primers were designed that would discriminate between putative co-infecting viruses and the primary virus in each isolate. The originally sequenced stock virus from the ARC was also inoculated onto grivet (*Chlorocebus aethiops*) Vero cell (ATCC CCL-81) cultures for virus isolation, and supernatant was collected when cultures exhibited cytopathic effects (CPE). Approximately 1x106 cells were pelleted by centrifugation at 23 x g for 10 min at room temperature and then frozen at -80˚C. RNA was extracted from cell pellets by adding 1 ml of TRIzol (ThermoFisher) to pellets, pipetting to lyse, and incubating at room temperature for 5 minutes, following the TRIzol protocol. cDNA was made using our standard reverse transcription protocol. Specifically, 500 ng of RNA or 5.5 µl of RNA was incubated at 65˚C for 5 minutes and immediately placed on ice. Random 15-mer at 25 µM, 2 µl of 1X Superscript III buffer, 5 mM dithiothreitol, 1 mM each dNTPs (ThermoFisher), and 100 U Superscript III Reverse

Transcriptase (Invitrogen) was added to this solution. Reaction mixtures were then incubated at 25˚C for 5 minutes then at 42˚C for 45 minutes, and finally at 70˚C for 15 minutes with a 4˚C hold. The resulting cDNA was then diluted 1:10 in water. Using segment-specific primers (**S2.1 Table**), qPCR was performed using LUNA Universal qPCR Master Mix (NEB M3003L) according to the manufacturer's protocol.

In an attempt to separate and isolate the individual co-infecting viruses (see results), the original Abras isolate was plaqued on Vero cells. Ninety individual plaques were picked for RNA extraction and PCR-confirmation using segment-specific primers (**S2.1 Table**). Single virus stocks were cultured from plaques that were Sanger sequence-confirmed to have only one of the infecting genotypes present.

Chapter 3: A scoping review of Orthobunyavirus sympatry and ecology: Barriers to reassortment

3.1 Introduction

Orthobunyaviruses, are a large group of segmented RNA viruses[8], and include significant emerging viruses [36,198,199]. Orthobunyaviruses are mainly vectored by mosquitoes or midges [1,10] and can infect animals and humans [1,8,10] . An emerging orthobunyavirus, Schmallenberg virus infects ruminants and can cause teratogenic effects including fetal mutations and abortions [35,36]. Endemic to the United States, La crosse virus causes pediatric encephalitis [7,198,200]. The ability of orthobunyaviruses to reassort compounds the risk for emergent and newly emergent orthobunyavirus strains with significant economic and health impacts.

Reassortment, the shuffling of genome segments during a co-infection, is a major driver of orthobunyavirus evolution [17,18]. Although viral reassortment typically leads to less fit progeny viruses [17], frequent reassortment has been documented within the orthobunyavirus genus [18,51]. Reassortants can have a significant change in phenotype such as altered pathogenesis, altered host or vector range, and an increase in virulence [1,17,18]. Ngari virus is a prime example of a novel virus with a gain of function as a result of reassortment. Ngari virus is a reassortant with the L and S segments of Bunyamwera virus and the M segment of Batai virus [17,52,168]. Bunyamwera virus and Batai virus cause febrile illness in humans, but Ngari virus causes hemorrhagic fever. While reassortment is an important mechanism for the

evolution of orthobunyaviruses, it can pose a significant risk to animal and human health.

Reassortment potential is dependent on several factors. First, two parental viruses must be circulating in the same geographic region, known as sympatry. Second, the two viruses must have a shared vector-host range in order for a co-infection to be possible. Reassortment is only possible if the two viruses infect the same cell at the same time. Lastly, the two viruses must have molecular compatibility between their genome segments and viral proteins. While much research has focused on delineating the factors that might predict reassortment potential, these factors are still poorly understood.

Closely related orthobunyaviruses reassort more frequently – intratypic reassortment [1,18,201]. Natural intratypic reassortants have been identified within Bunyamwera, California, Simbu, and Group C serogroups [18]. While less common, there is evidence for intertypic reassortment, reassortment between more distantly related orthobunyaviruses [51]. Guaroa virus may be a reassortant virus that arose from parental viruses belonging to the California complex and the Bunyamwera complex – although this has been debated in the literature [202,203]. Whether intertypic reassortants are currently circulating is not known. However, there is evidence that ancestral strains were the result of intertypic reassortment (e.g. Guaroa virus [204], Murrumbidgee virus, Belem virus, Pacora virus, and Brazoran virus [51]). Ultimately, the ability for two genetically distinct viruses to reassort is dependent on a combination of sympatry, shared vector-host range, and molecular compatibility.

An in-depth understanding of shared sympatry and ecology can enable more strategic outbreak preparedness efforts. Rather than responding to an outbreak reactively, the goal is to respond proactively. Ideally, strategic surveillance could help pinpoint geographic areas with an increased potential for reassortment and emergence of novel viral strains. Therefore, the objective of this study was to determine which viruses have an increased risk for reassortment – based on sympatry and shared host-vector range. To do this, we utilized metadata from 1,850 orthobunyavirus sequences deposited to NCBI's Nucleotide database to curate a dataset of orthobunyavirus detections including isolation year, country of isolation, and isolation source. The dataset comprises metadata from true virus isolates as well as detection of viruses using metagenomic sequencing. For the sake of this chapter, we will refer to both as 'detections'. Analysis of this dataset provides insight into the strength of strategic surveillance and highlights vector and viral species with an increased risk for reassortment based on geographic and vector/host overlap.

3.2 Results

3.2.1 Overview of Metadata

The curated dataset is the culmination of metadata for 1,850 unique orthobunyavirus detections. Metadata included virus name and isolate, country of detection, year of detection, and source of detection. Detections of viruses included in this dataset have spanned 84 years, with the first isolation in 1937 (**Figure 3.1A**). Since that time, records of detections have occurred every decade with the greatest number of detections (n = 634) represented between 2010-2020. Orthobunyaviruses represented in this dataset were detected from invertebrate and vertebrate species sampled in 65

countries (**Figure 3.1B**). The greatest number of detections have been from samples collected within the USA (n= 342). Each of the 20 currently recognized serogroups is represented in the dataset (**Chapter 2 Figures 2.2-2.4** to visualize serogroup classifications), with the greatest number of virus detections belonging to the Simbu serogroup (n = 867) (**Figure 3.1C**). To identify what organism the viruses were detected in, the GenBank source modifiers 'host' and 'isolation source' were merged. Overall, detections have occurred in a large variety of vertebrate and invertebrate species (**Figure 3.1D**). Invertebrate species included mosquitoes, midges, ticks, bat flies, flies, and an Asian citrus psyllid. Detections originated from a wide variety of vertebrate species, ranging from cattle and sheep to rhinoceros and sloths. The greatest number of detections from invertebrates were from mosquitoes (n = 729) and from vertebrates, humans (n = 291). Together, this curated dataset represents the first large scale meta-analysis of all orthobunyavirus sequences deposited to the NCBI Nucleotide database. The curated dataset is available on GitHub (github.com/mllayton/dissertation/chapter3).

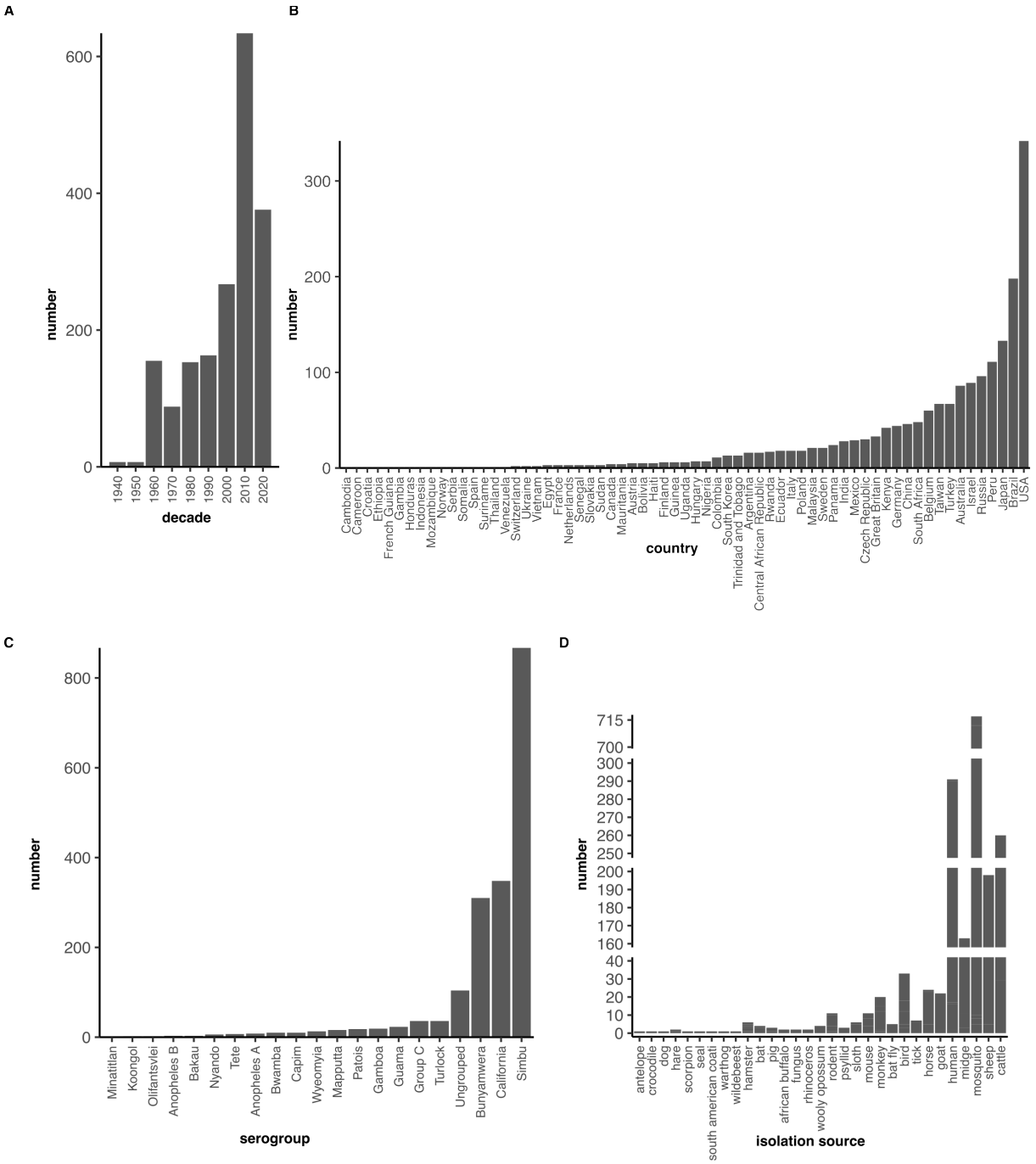

Figure 3.1. Summation of metadata
The curated dataset contains date and country of isolation, serogroup classification, and isolation source. A) histogram showing the number of isolations per decade B) histogram showing the number of isolations per country C) histogram showing number of isolations per serogroup classification and D) histogram showing number of isolations from source.

3.2.2 Orthobunyavirus geographic distribution

The first barrier to reassortment is sympatry – an overlap in geographic distribution. To determine which serogroups are sympatric, we plotted the location of where samples were collected (**Figure 3.2**). Because the specific latitude and longitude was not always present in the metadata, we plotted the centroid latitude and longitude for the country from which the organism hosting the viral strain was found. This gives an approximate overlap in geographic distribution. Detections originated on every continent, except Antarctica. Each of these continents support the circulation of more than one serogroup. There was substantial geographical overlap in the distribution of five serogroups in North and South America and Africa (**Figure 3.3**). While there is significant overlap on each continent, there is less overlap at the country level (**Figures 3.2 and 3.3**).

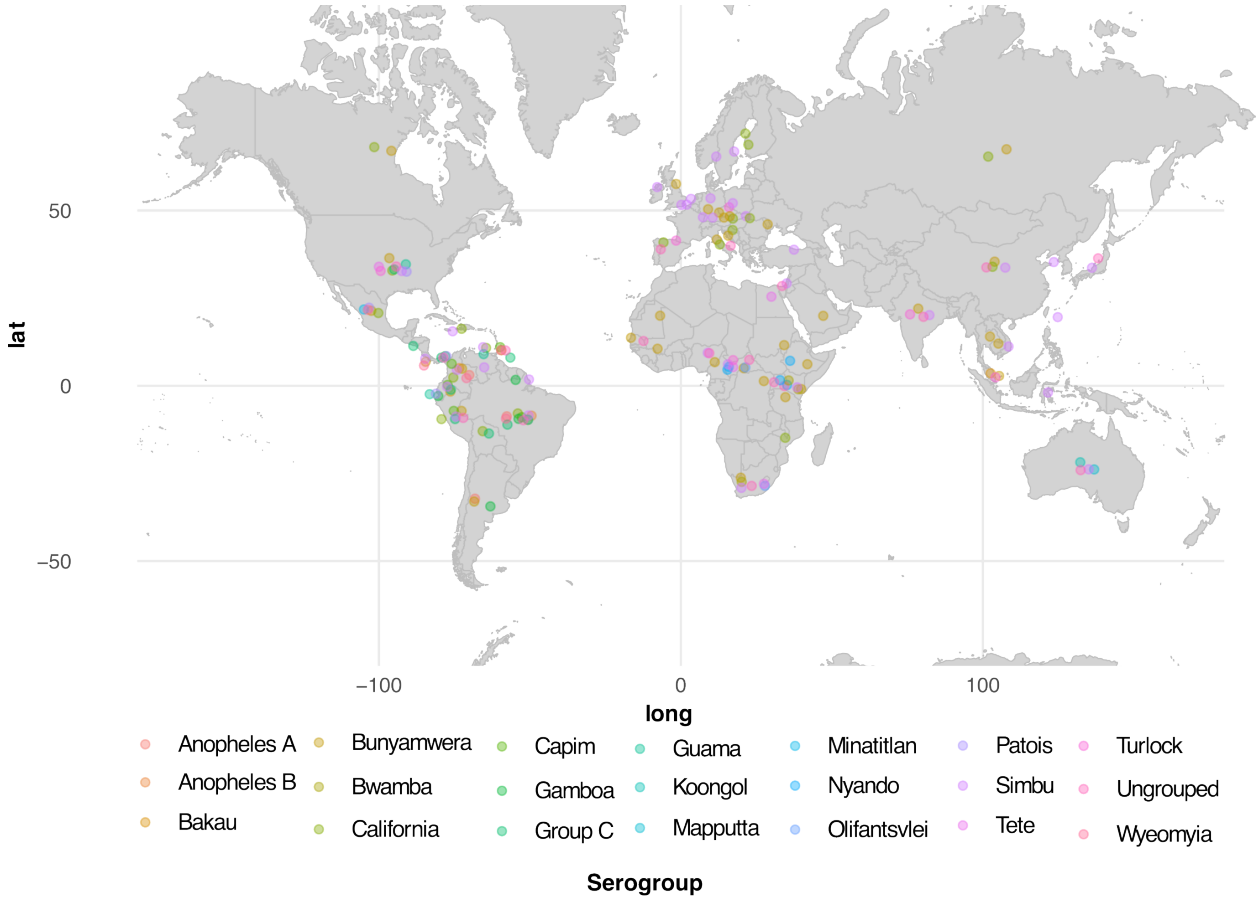

Figure 3.2. Many orthobunyavirus serogroups occupy the same country
World map showing the geographic distribution of orthobunyavirus isolations grouped by serogroup. Each colored dot corresponds to one or more virus isolations from that serogroup. Exact geographic locations are not shown, rather isolations within a country are shown.

Given the diversity of serogroups, it is difficult to discern any significant presence or lack of sympatry between serogroups using the map in **Figure 3.2**. To better evaluate sympatry we plotted the number of detections for each serogroup on an individual world map (**Figure 3.3**). Some serogroups have a limited geographic distribution, in that they've been isolated from one continent. For example, members of the Anopheles A, Anopheles B, Capim, and Gamboa serogroups were only isolated from South America; members of Bakau were only isolated from Asia; members of Bwamba, Nyando, and Olifanstvlei serogroups were only isolated from Africa; members of Minatitlan were only

isolated from North America; members of Koongol and Mapputta were only isolated from Australia. Alternatively, some serogroups have a broad geographic distribution and are present in more than one country. For example, members of the Bunyamwera and California and Simbu serogroups were isolated from every continent, except Australia; members of the Group C, Wyeomyia, and Guama serogroups were isolated from North and South America; members of the Tete serogroup were isolated from North America and Africa; members of the Turlock serogroup were isolated from North America, Europe, Africa, and Asia. Taken together, we determined which serogroups are sympatric on a continental-level.

Next, we aimed to fine-tune our analysis of sympatric serogroups to a within-country level (**Supplemental Table 3.2**). Countries from which five or more serogroups were detected include Brazil, USA, Panama, Trinidad & Tobago, Central Africa Republic, Ecuador, Colombia, Peru, South Africa, Kenya, and Mexico. Together, we show that serogroups are sympatric within continents and countries, providing opportunity for reassortment potential if all other barriers are overcome.

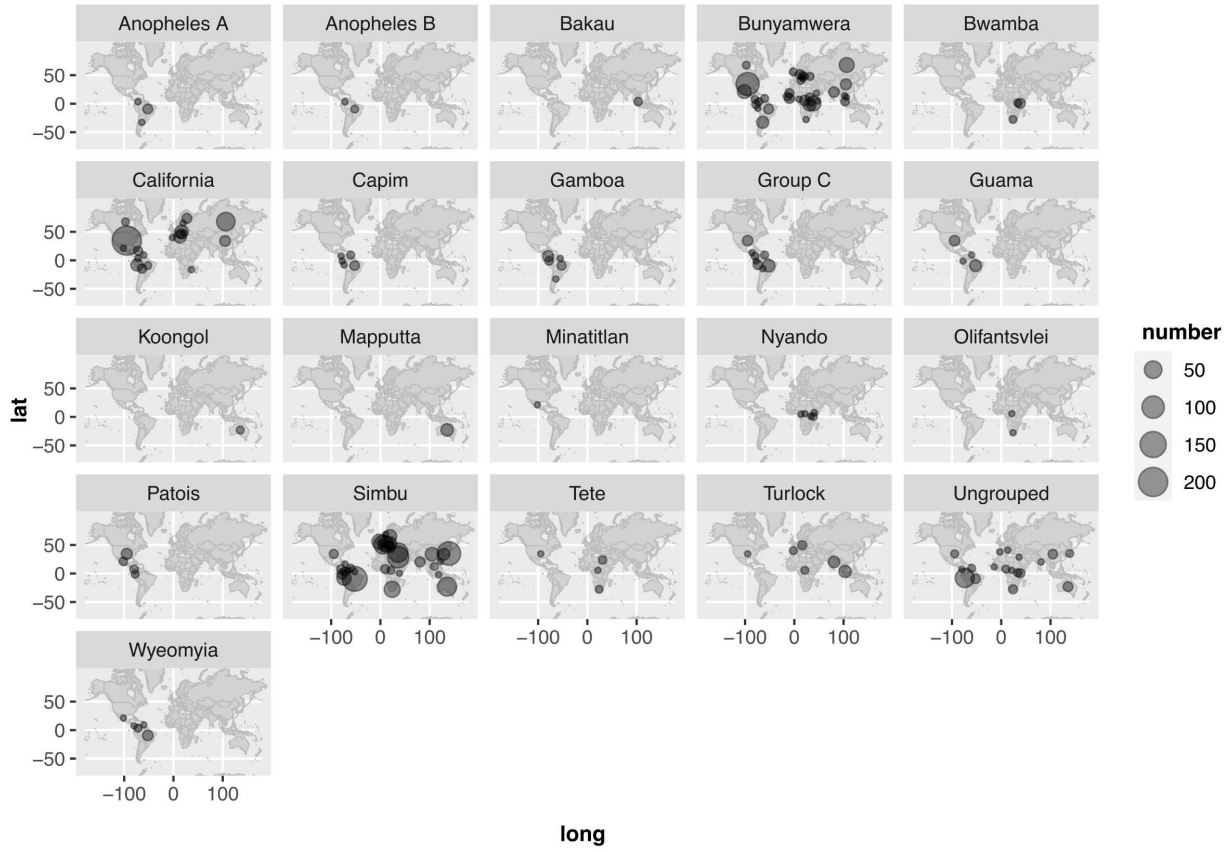

Figure 3.3. Geographic distribution of virus isolations within serogroups
Each map shows the country of isolation for viruses within a serogroup. The exact location is not given, rather the center latitude and longitude for the country from which viruses were isolated. The size of the dot depends on the number of viruses isolations in that country.

To assess sympatry within serogroups, and therefore potential for intratypic reassortment, we tabulated the extent to which viruses within the same serogroup had been detected in the same country (**Figure 3.4A-S**). There were two main findings: 1) some serogroups lack sympatry of viral strains within the serogroup and 2) some serogroups exhibit sympatry of viral strains within the serogroup. For example, three virus species (Anopheles A virus, Las Maloyas virus, and Tacaiuma virus) belonging to the Anopheles A serogroup are not sympatric: each of these viruses were isolated from different countries within South America. While viruses don't have any regard for

political borders, the observation may be due to differing climates, or vector and host species, or sampling bias. An example of shared sympatry within a serogroup are viruses belonging to the Group C serogroup in which 5 viruses are co-circulating in Brazil.

Figure 3.4. Orthobunyavirus sympatry within serogroups

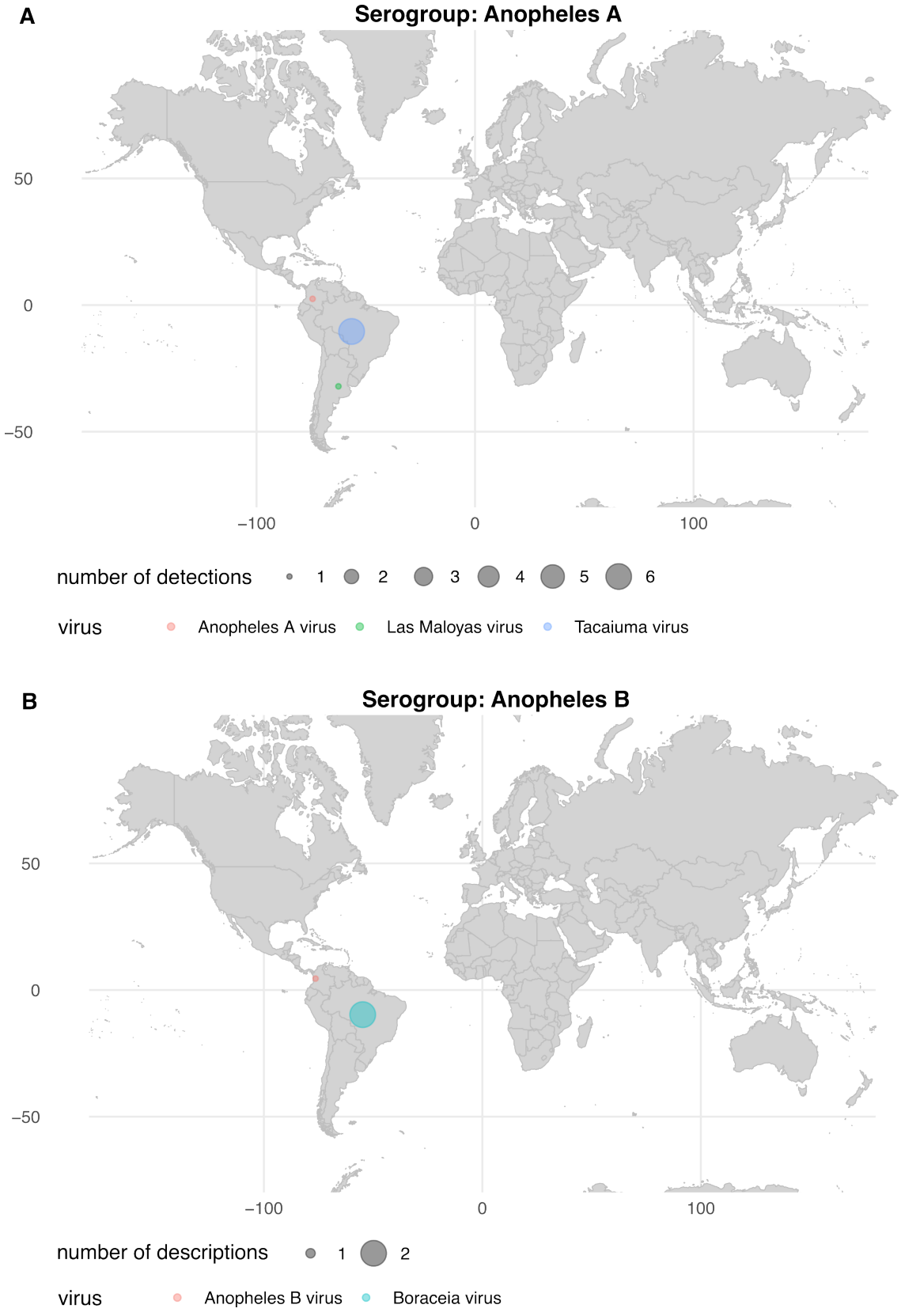

C

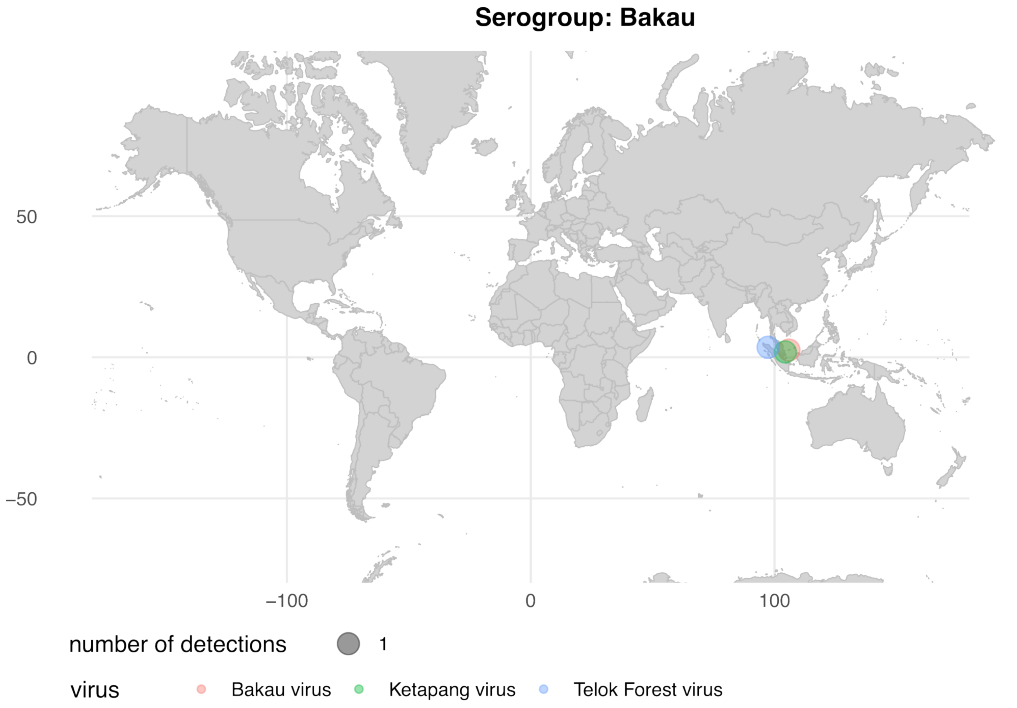
Serogroup: Bakau
50
0
−50
−100
0
100
number of detections
1
virus
Bakau virus
Ketapang virus
Telok Forest virus

D

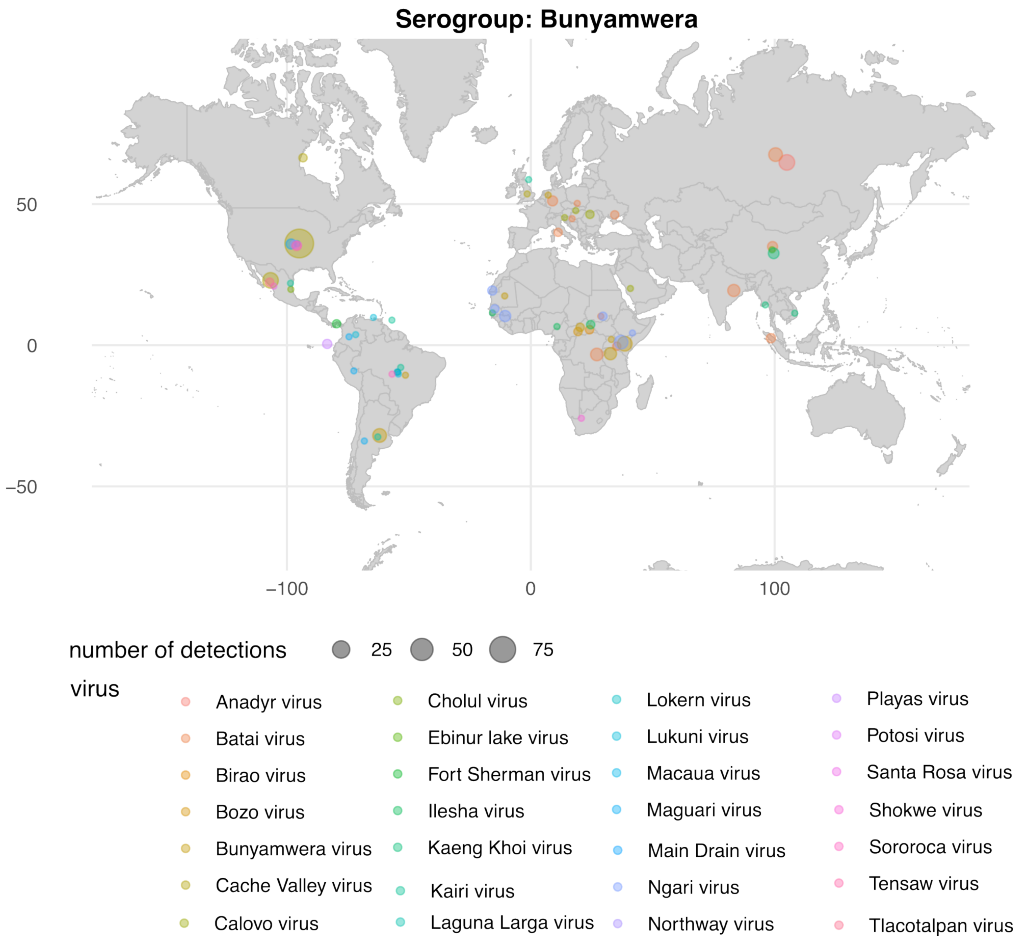
Serogroup: Bunyamwera
50
0
−50
−100
0
100
number of detections
25
50
75
virus
Anadyr virus
Batai virus
Birao virus
Bozo virus
Bunyamwera virus
Cache Valley virus
Calovo virus
Cholul virus
Ebinur lake virus
Fort Sherman virus
Ilesha virus
Kaeng Khoi virus
Kairi virus
Laguna Larga virus
Lokern virus
Lukuni virus
Macaua virus
Maguari virus
Main Drain virus
Ngari virus
Northway virus
Playas virus
Potosi virus
Santa Rosa virus
Shokwe virus
Sororoca virus
Tensaw virus
Tlacotalpan virus

E

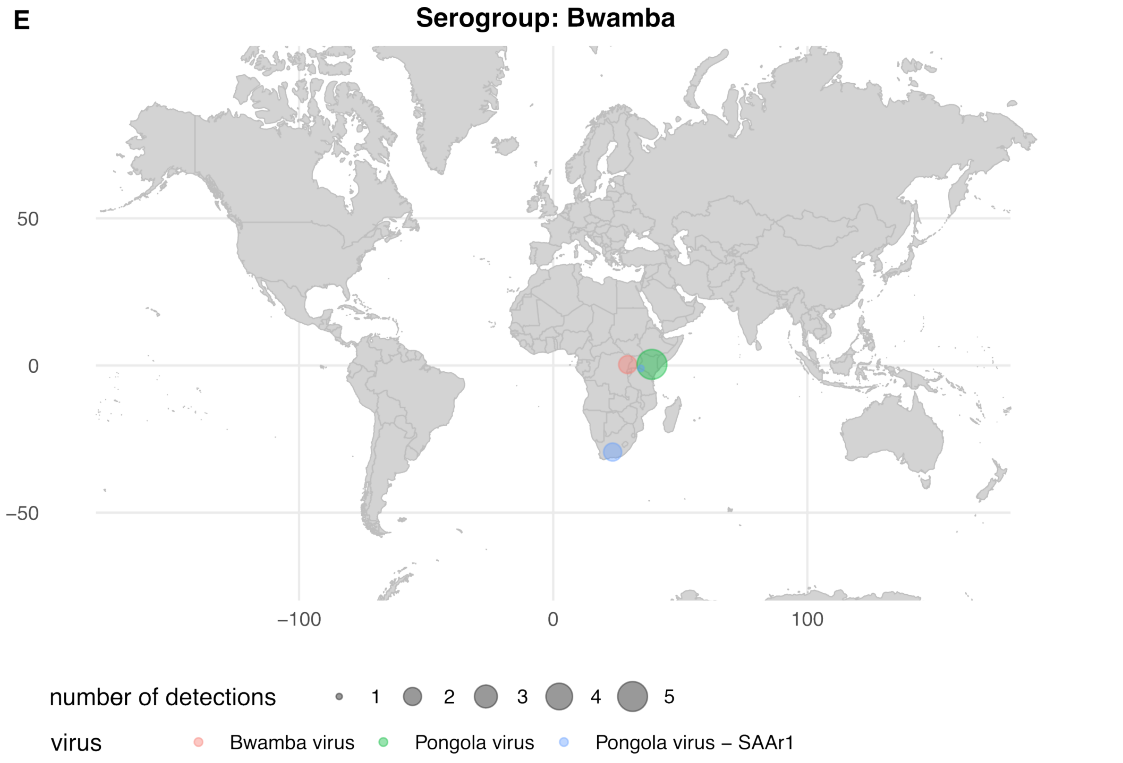
Serogroup: Bwamba
50
0
−50
−100
0
100
number of detections
1
2
3
4
5
virus
Bwamba virus
Pongola virus
Pongola virus – SAAr1

F

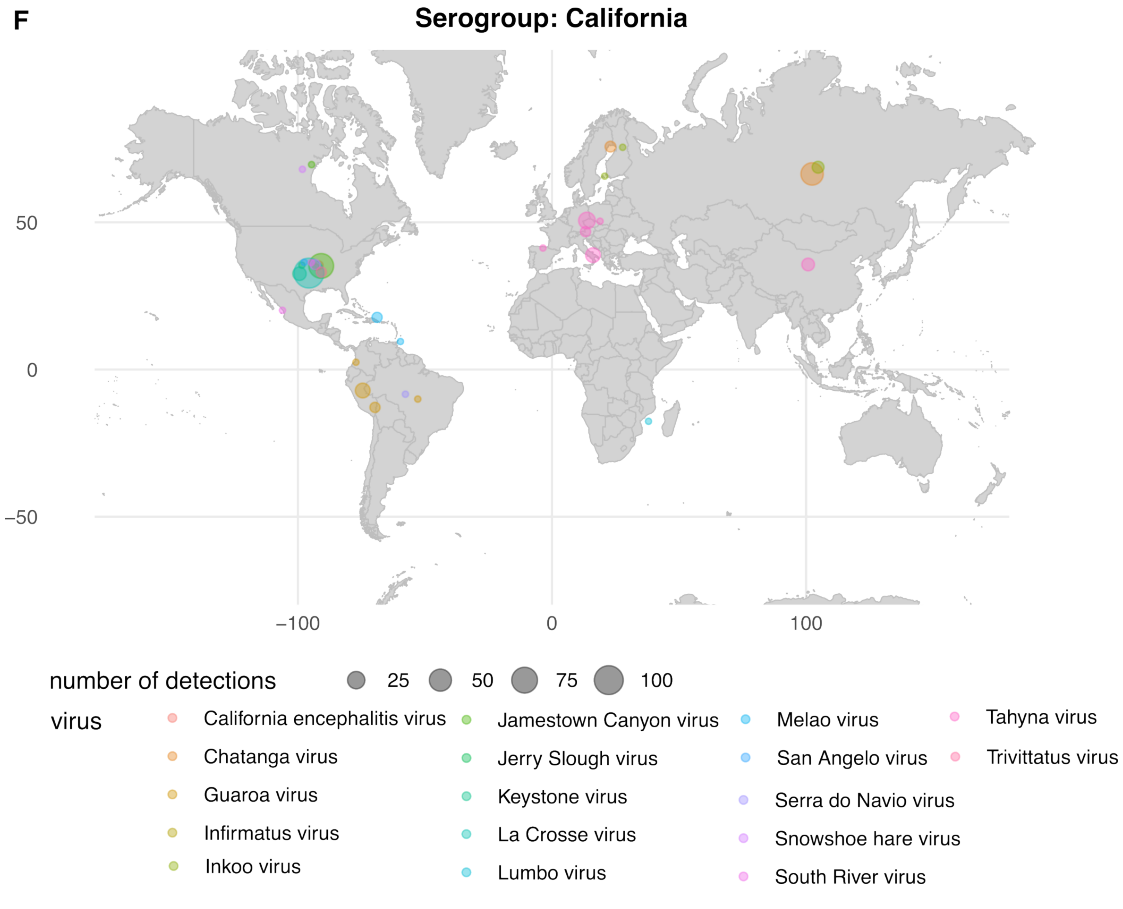
Serogroup: California
50
0
−50
−100
0
100
number of detections
25
50
75
100
virus
California encephalitis virus
Chatanga virus
Guaroa virus
Infirmatus virus
Inkoo virus
Jamestown Canyon virus
Jerry Slough virus
Keystone virus
La Crosse virus
Lumbo virus
Melao virus
San Angelo virus
Serra do Navio virus
Snowshoe hare virus
South River virus
Tahyna virus
Trivittatus virus

G

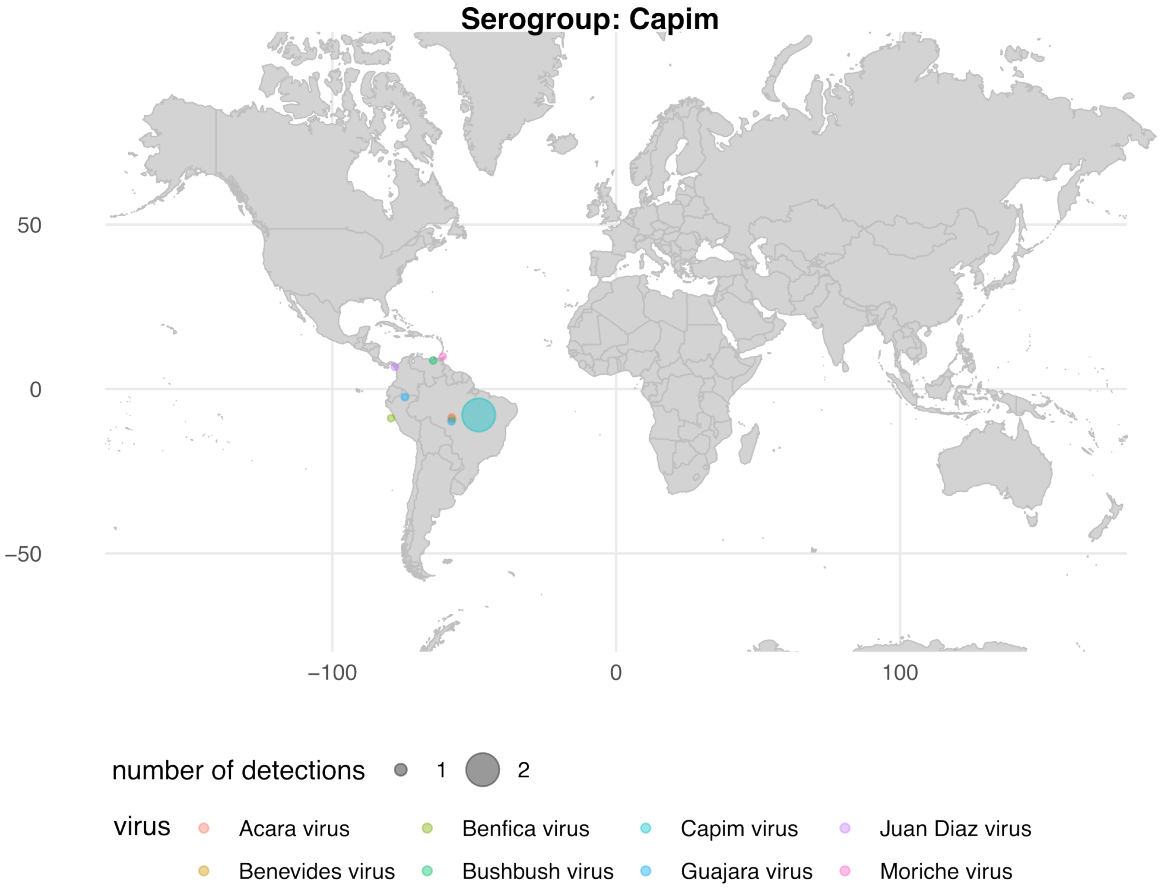
Serogroup: Capim
50
0
−50
−100
0
100
number of detections
1
2
virus
Acara virus
Benfica virus
Capim virus
Juan Diaz virus
Benevides virus
Bushbush virus
Guajara virus
Moriche virus

H

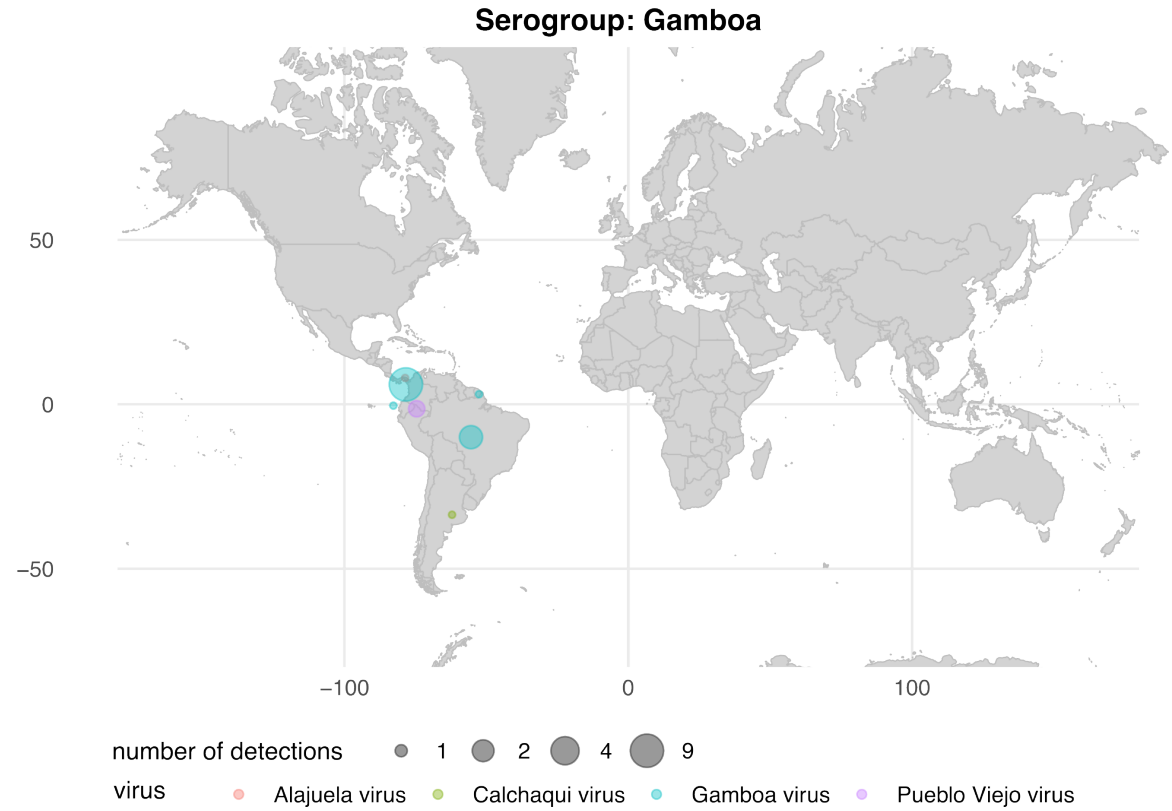
Serogroup: Gamboa
50
0
−50
−100
0
100
number of detections
1
2
4
9
virus
Alajuela virus
Calchaqui virus
Gamboa virus
Pueblo Viejo virus

I

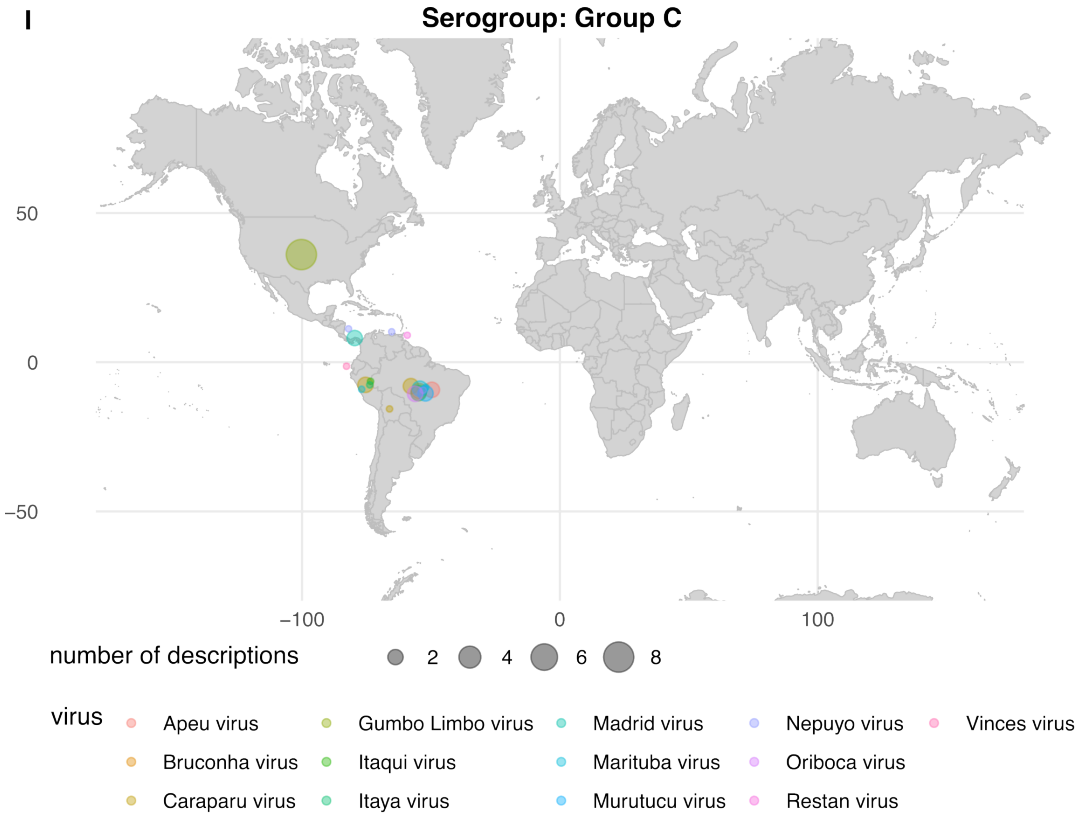
Serogroup: Group C
50
0
−50
−100
0
100
number of descriptions
2
4
6
8
virus
Apeu virus
Bruconha virus
Caraparu virus
Gumbo Limbo virus
Itaqui virus
Itaya virus
Madrid virus
Marituba virus
Murututucu virus
Nepuyo virus
Oriboca virus
Restan virus
Vinces virus

J

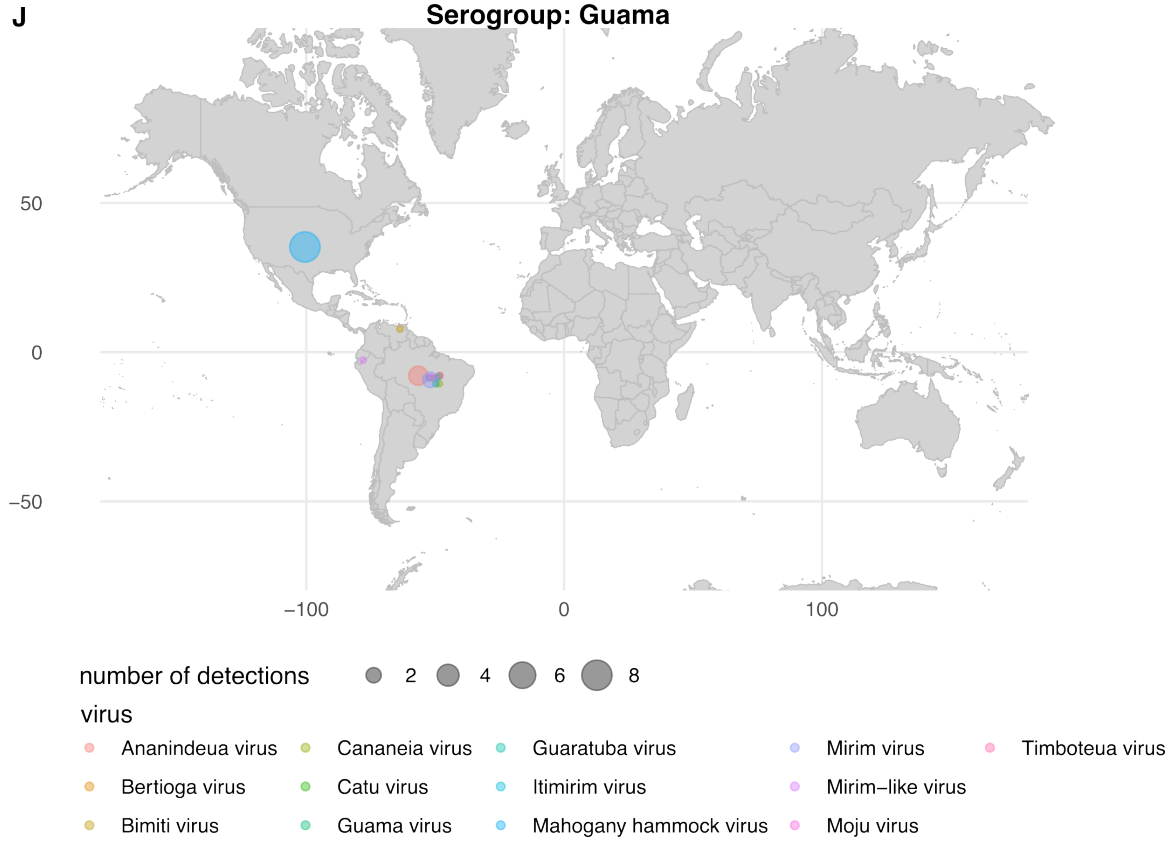
Serogroup: Guama
50
0
−50
−100
0
100
number of detections
2
4
6
8
virus
Ananindeua virus
Bertioga virus
Bimiti virus
Cananeia virus
Catu virus
Guama virus
Guaratuba virus
Itimirim virus
Mahogany hammock virus
Mirim virus
Mirim−like virus
Moju virus
Timboteua virus

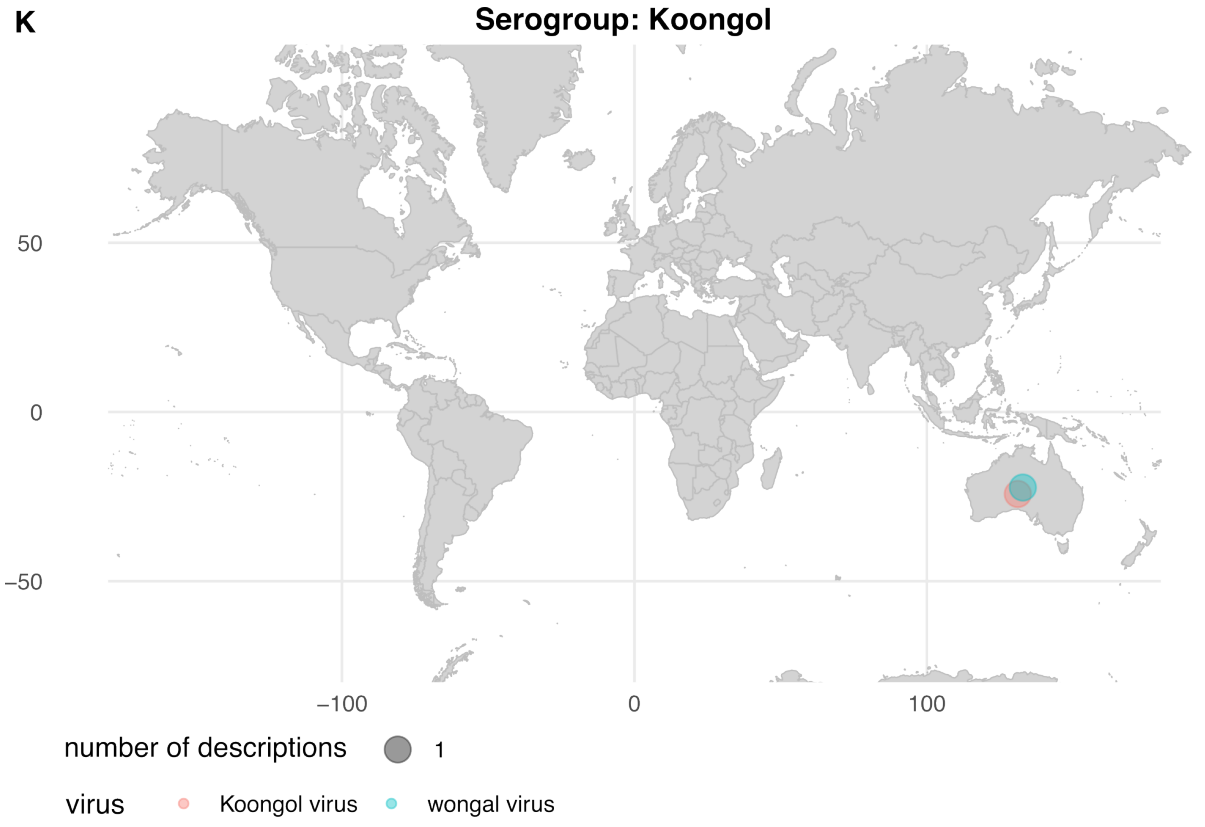
K
Serogroup: Koongol
50
0
−50
−100
0
100
number of descriptions
1
virus
Koongol virus
wongal virus

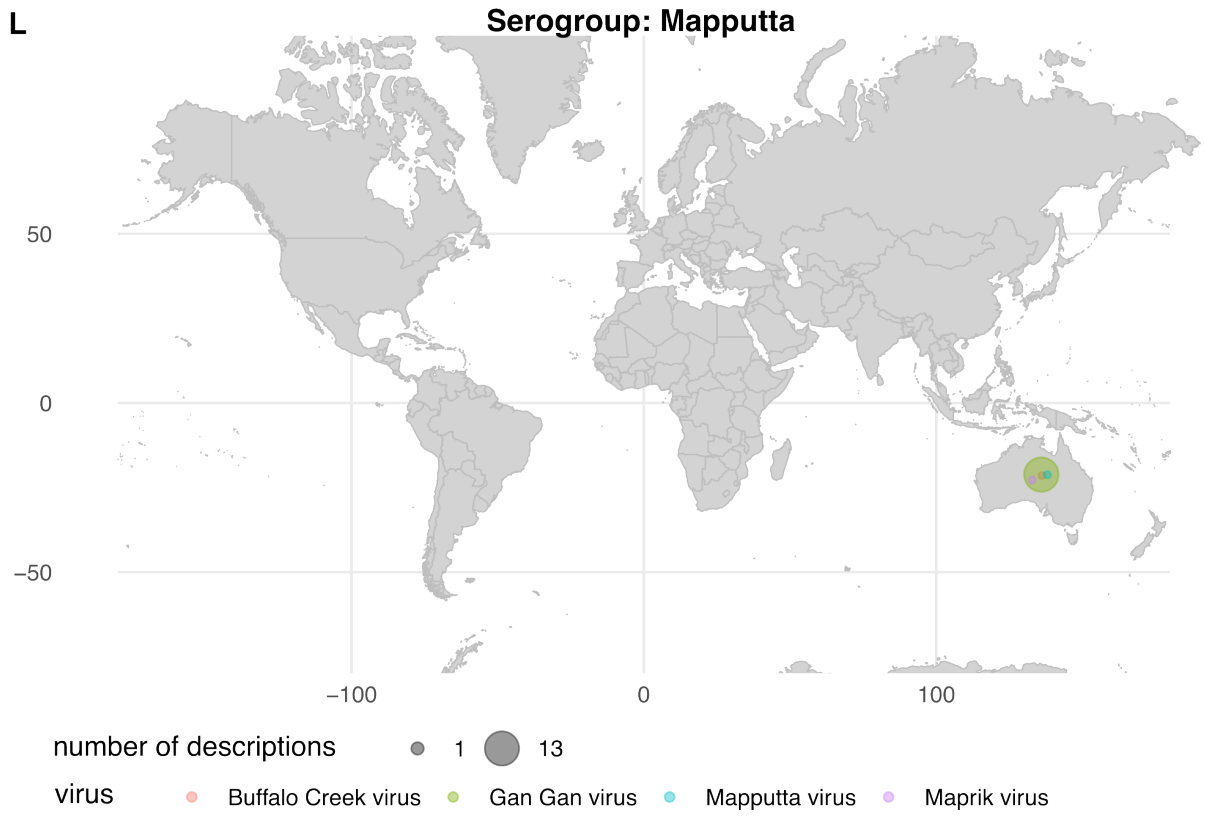
L
Serogroup: Mapputta
50
0
−50
−100
0
100
number of descriptions
1
13
virus
Buffalo Creek virus
Gan Gan virus
Mapputta virus
Maprik virus

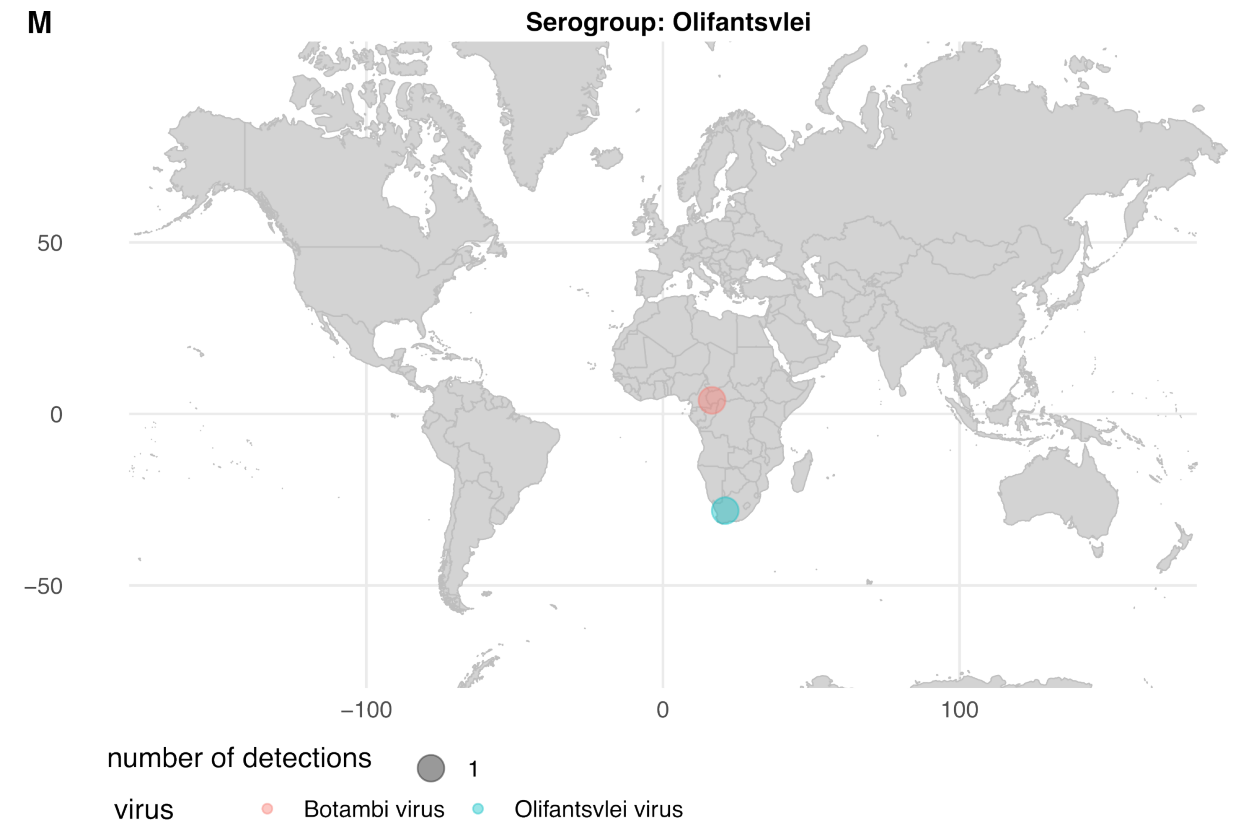
M
Serogroup: Olifantsvlei
50
0
−50
−100
0
100
number of detections
1
virus
Botambi virus
Olifantsvlei virus

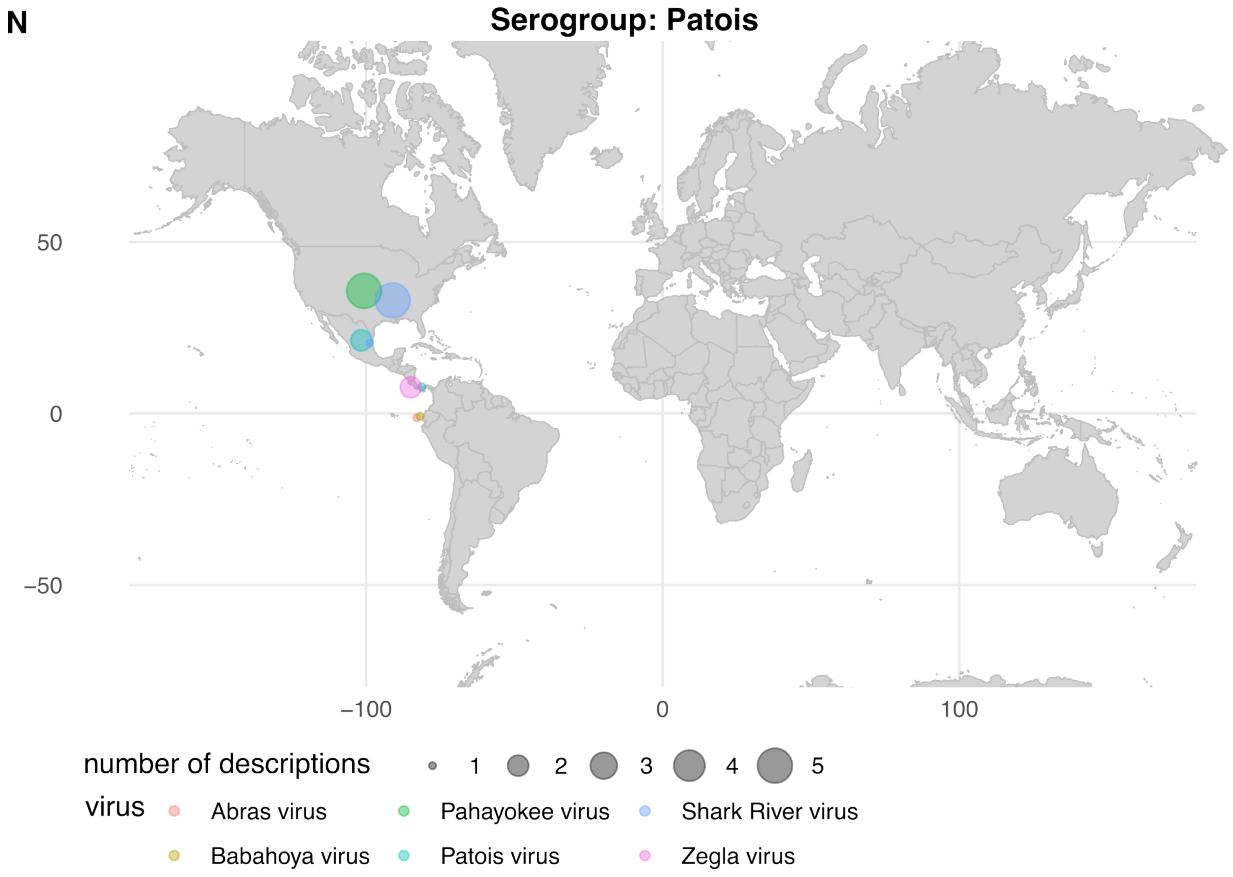
N
Serogroup: Patois
50
0
−50
−100
0
100
number of descriptions
1
2
3
4
5
virus
Abras virus
Babahoya virus
Pahayokee virus
Patois virus
Shark River virus
Zegla virus

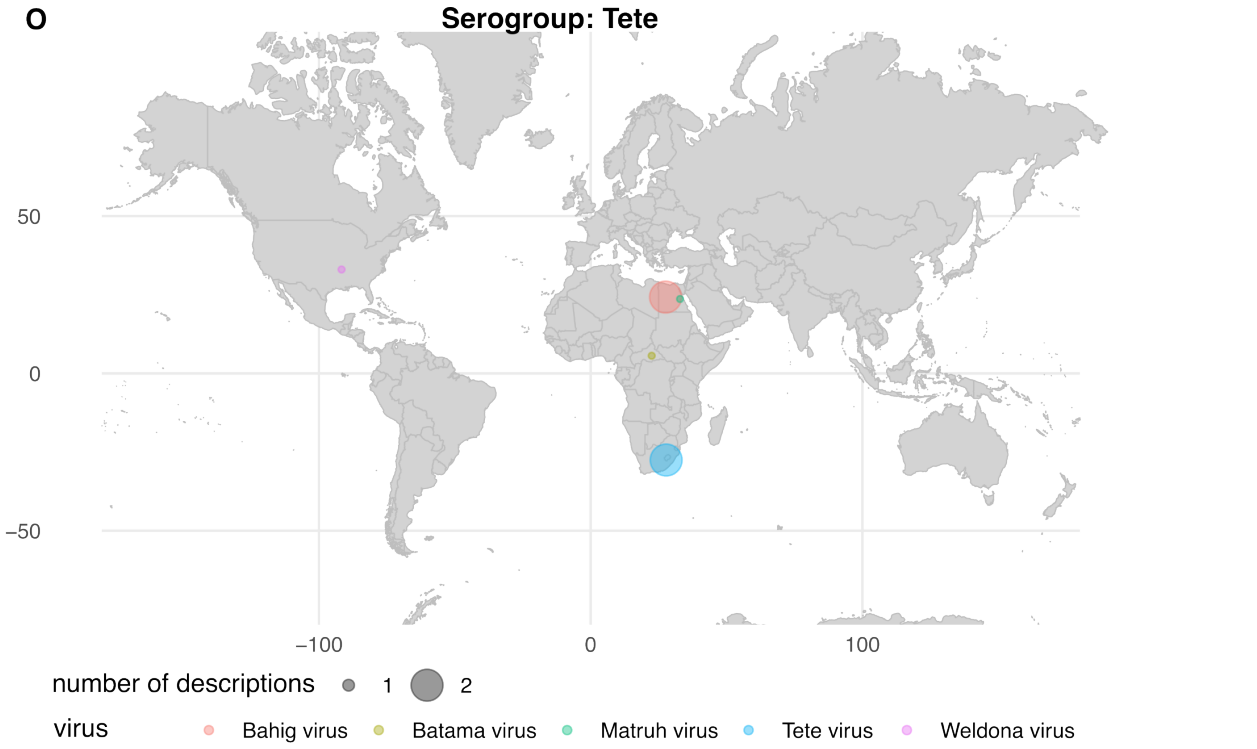
O
Serogroup: Tete
50
0
−50
−100
0
100
number of descriptions
1
2
virus
Bahig virus
Batama virus
Matruh virus
Tete virus
Weldona virus

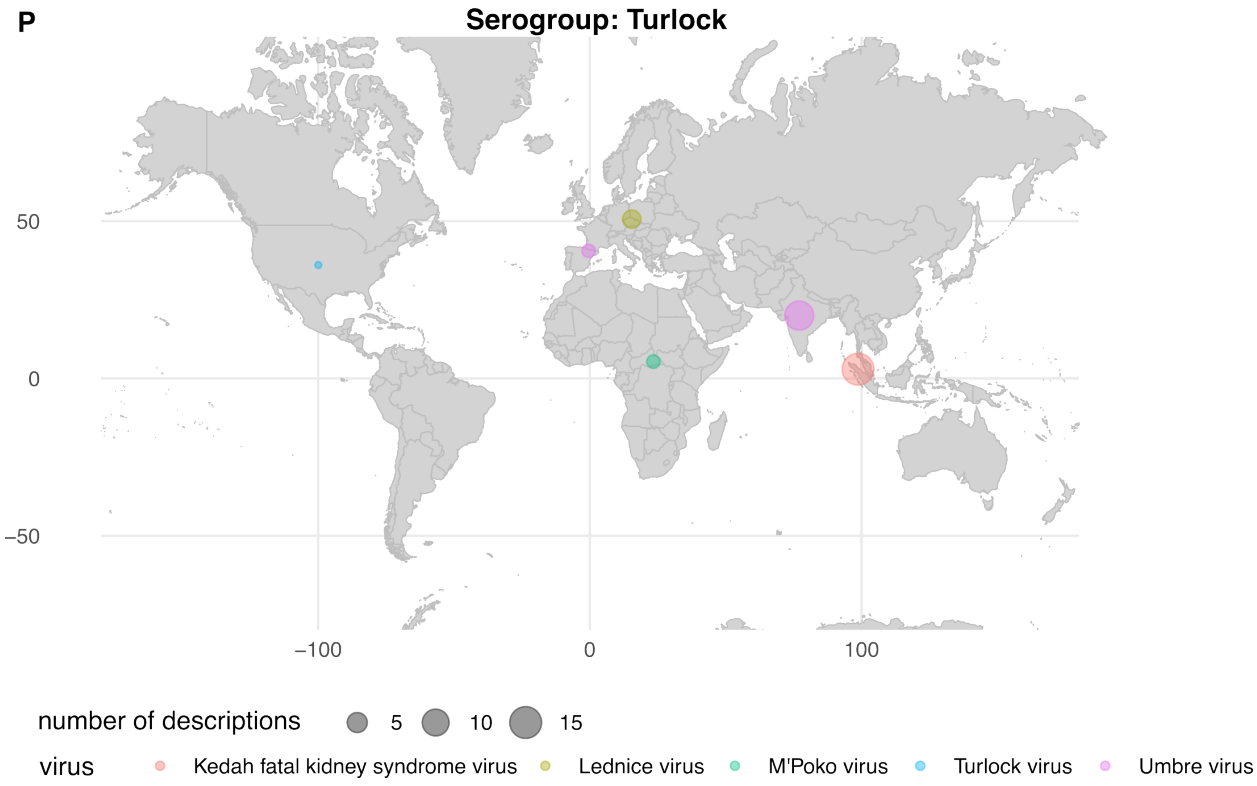
P
Serogroup: Turlock
50
0
−50
−100
0
100
number of descriptions
5
10
15
virus
Kedah fatal kidney syndrome virus
Lednice virus
M'Poko virus
Turlock virus
Umbre virus

Q

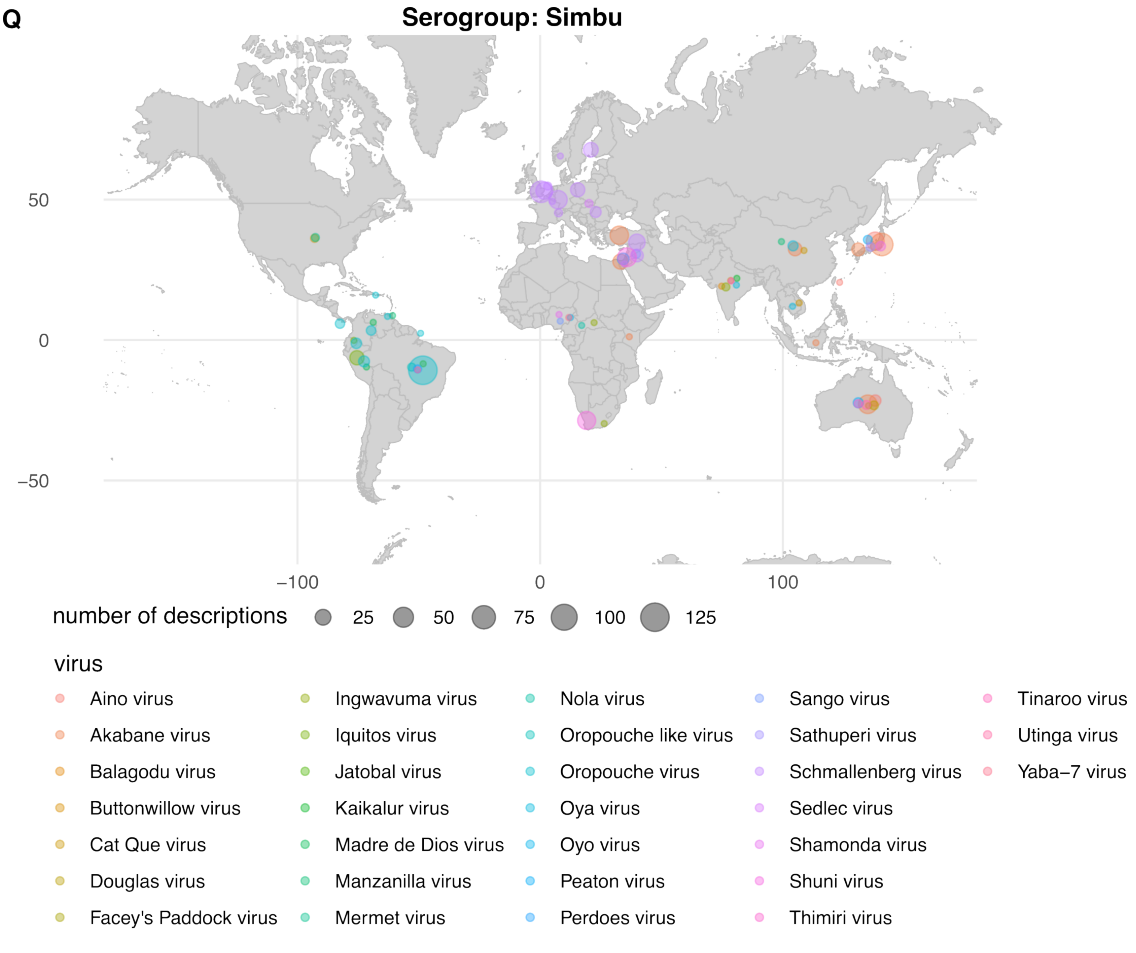
Serogroup: Simbu
50
0
−50
−100
0
100
number of descriptions
25
50
75
100
125
virus
Aino virus
Akabane virus
Balagodu virus
Buttonwillow virus
Cat Que virus
Douglas virus
Facey's Paddock virus
Ingwavuma virus
Iquitos virus
Jatobal virus
Kaikalur virus
Madre de Dios virus
Manzanilla virus
Mermet virus
Nola virus
Oropouche like virus
Oropouche virus
Oya virus
Oyo virus
Peaton virus
Perdoes virus
Sango virus
Sathuperi virus
Schmallenberg virus
Sedlec virus
Shamonda virus
Shuni virus
Thimiri virus
Tinaroo virus
Utinga virus
Yaba−7 virus

R

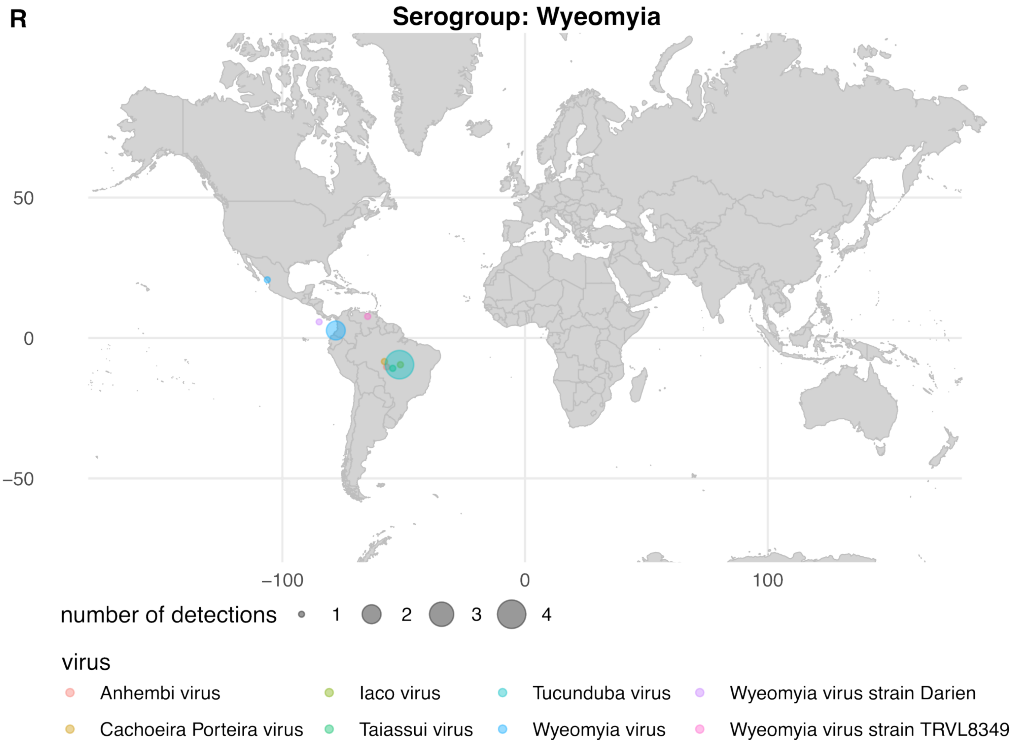
Serogroup: Wyeomyia
50
0
−50
−100
0
100
number of detections
1
2
3
4
virus
Anhembi virus
Cachoeira Porteira virus
Iaco virus
Taiassui virus
Tucunduba virus
Wyeomyia virus
Wyeomyia virus strain Darien
Wyeomyia virus strain TRVL8349

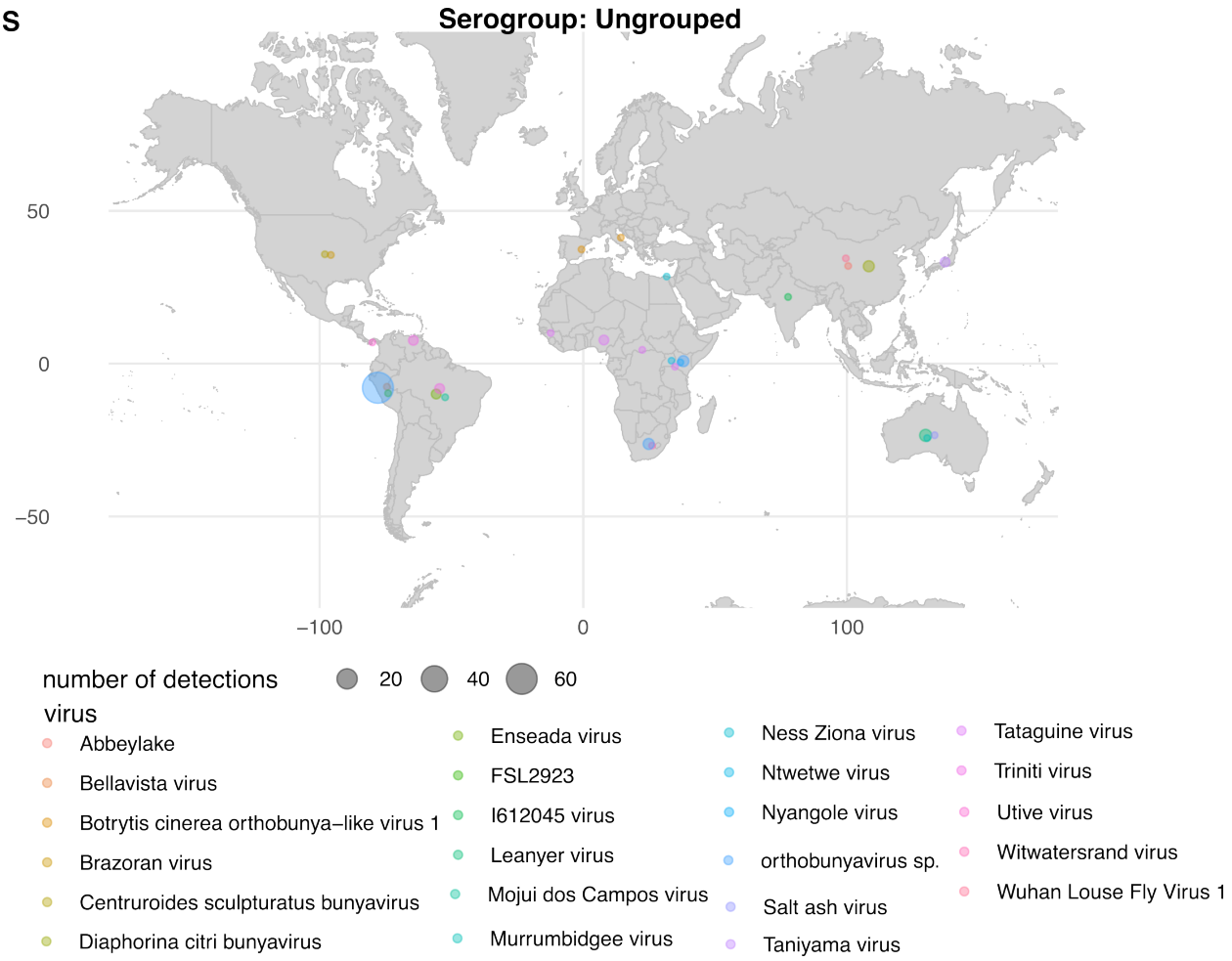

3.2.3 Orthobunyavirus vector and host range

The second barrier to reassortment potential is a shared vector-host range. In order to reassort, two viruses must co-infect the same vertebrate host or vector. To determine the breadth of organisms from which orthobunyaviruses have been isolated, as one component of shared ecology, we plotted the number of virus detections from vertebrate and invertebrate taxon. Vertebrate isolations span a wide range of species types. Multiple serogroups were isolated from several vertebrate species including, cattle, sheep, humans, goats, horse, bird, monkey, mouse, sloth, rodent, wooly opossum, pig, bat, hamster, and hare (**Figure 3.5A**). Viruses from Anopheles B,

Olifantsvlei, Koongol, Mapputta, and Nyando serogroup have never been isolated from vertebrates.

We chose to focus the analysis on shared vector ecology. Biting midges in the genus *Culicoides* vector most Simbu serogroup viruses. Here, we show shared vector ecology for Bunyamwera, Simbu, and Tete serogroups within the *Culicoides* genus (**Figure 3.5B**). However, these three serogroups do not share vector ecology at the level of vector species. Therefore, reassortment between strains of the same serogroup (intratypic) is possible, but not between serogroups (intertypic). A few orthobunyaviruses, all belonging to the Bunyamwera serogroup, have been isolated from ticks (**Figure 3.5C**). Similarly, a small number of Bunyamwera serogroup viruses have been isolated from bat flies (**Figure 3.5D**). Additionally, a few ungrouped orthobunyaviruses were isolated from an Asian citrus psyllid. Finally, the primary vector of orthobunyaviruses are mosquitoes. Our analysis revealed a significant number of viruses that shared a common vector species (**Figure 3.5**). Isolations from mosquitoes comprised the largest number of isolations and included 17 genera of mosquito including *Aedomyia*, *Aedes*, *Anopheles*, *Culex*, *Eretmapodites*, *Haemogogus*, *Limatus*, *Lutzia*, *Mansonia*, *Psorophora*, *Trichoprosopon*, *Verallina*, and *Wyeomyia* (**Figure 3.6**). Viruses from each serogroup have been isolated from a mosquito species, except for the Tete and Minatitlan serogroups. While each genus of mosquito vectors viruses from different serogroups, shared sympatry on a species level occurred less frequently. Mosquito species that vectored viruses from more than one serogroup include (more than one virus species were detected within the vector): *Ae. albopictus, Ae. nigripes*,

Ae. vexans, *An. funestus*, *An. maculipennis*, *Cx. melanconion*, *Cx. cedecei*, *Ma. uniformis*.

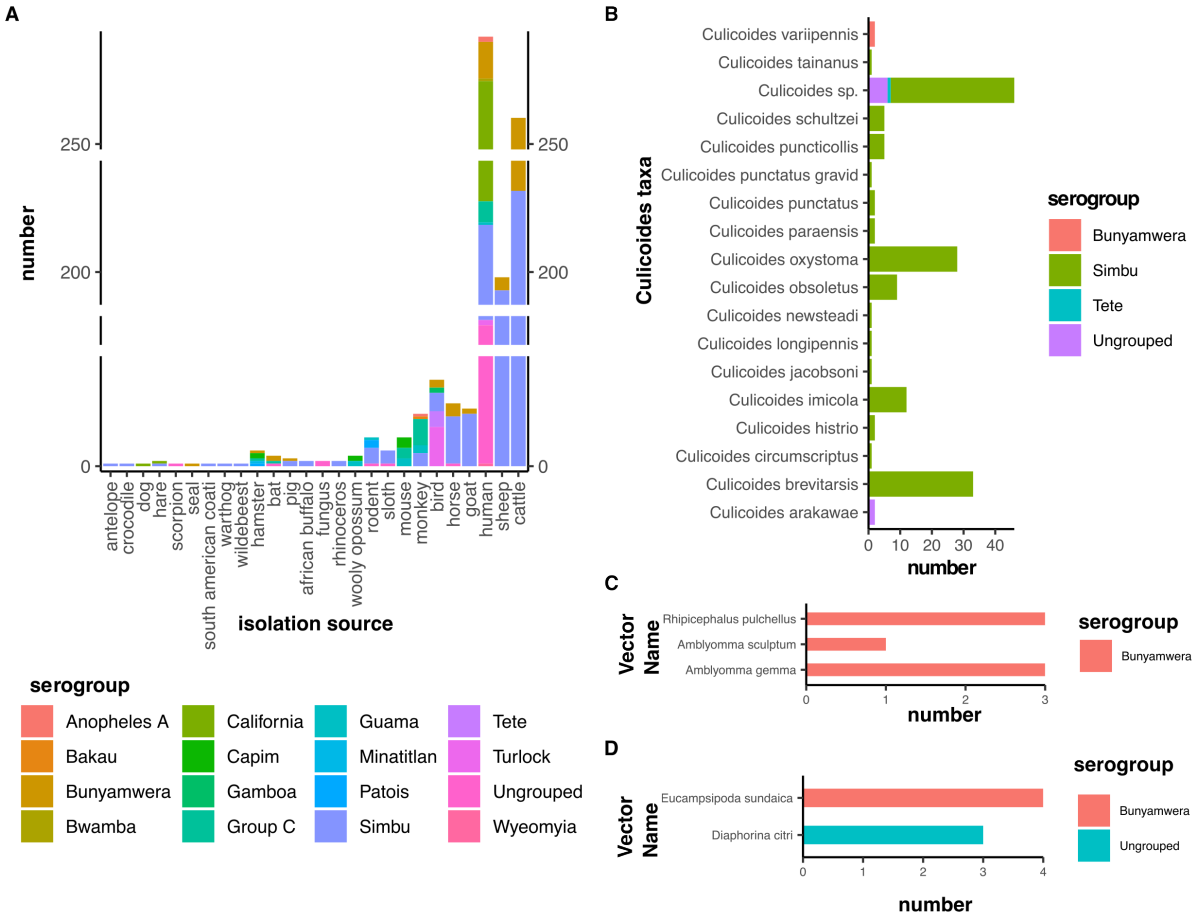

Figure 3.5. Isolation sources sans mosquito species
Histograms showing number of virus isolations for each serogroup, isolated from various sources. A) isolations from non-vector hosts, mainly vertebrate species B) isolations from midges C) isolations from ticks D) isolations from bat fly and psyllid.

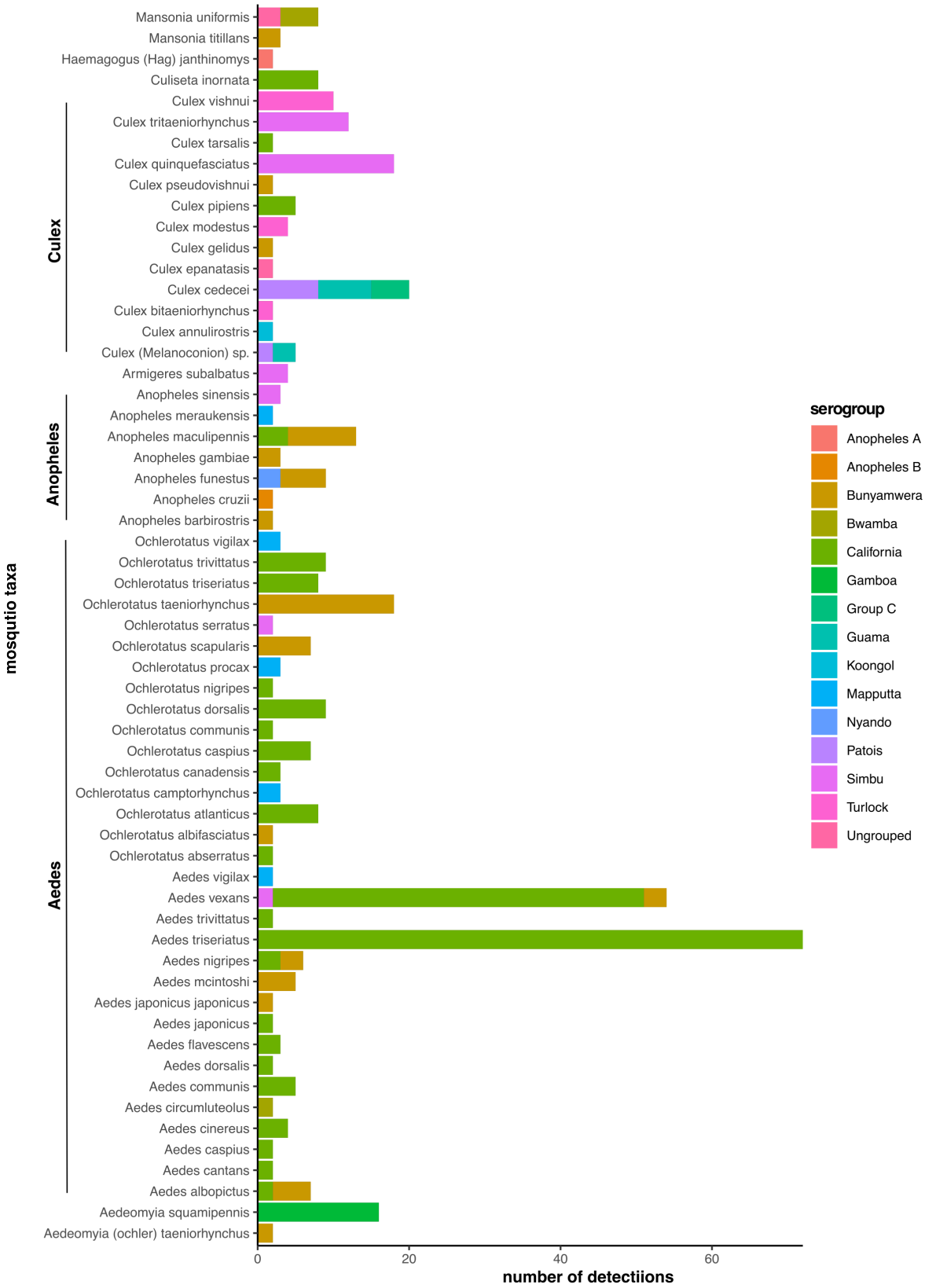

Figure 3.6. Orthobunyavirus ecology within mosquito species
Histogram showing the number of virus isolations per serogroup within a mosquito vector.

3.2.4 Delineating reassortment potential

We aimed to determine which viruses might present a relatively high risk for reassortment based on shared sympatry and ecology. To determine potential risk, the following parameters were used. Primarily, different virus species must have been isolated from the same vector species. Due to vector range expansion, the likelihood that geographically isolated viruses will eventually occupy the same region is probable. Therefore, if viruses vectored by the same species are currently geographically isolated, they are still considered a risk for reassortment. Using these parameters, we found several instances of intertypic and intratypic reassortment (**Table 3.1**).

Intratypic reassortment occurs between viruses within the same serogroup. The following serogroups have a possibly elevated potential risk for intratypic reassortment because more than one virus species within a serogroup was detected in the same vector species: **Gamboa serogroup** (*Aedeomyia squamipennis*), **Bunyamwera serogroup** (*Aedes albopictus*, *Aedes vexans*, *Amblyomma gemma*, *Anopheles gambiae*, *Mansonia titillans*, *Ochlerotatus albifasciatus*, *Ochlerotatus scapularis*, *Ochlerotatus taeniorhynchus*, *Rhipicephalus pulchellus*), **California serogroup** (*Aedes cantans*, *Aedes caspius*, *Aedes cinereus*, *Aedes communis*, *Aedes dorsalis*, *Aedes mcintoshi*, *Aedes nigripes*, *Aedes vexans*, *Anopheles maculipennis*, *Culiseta inornate*, *Ochlerotatus canadensis*, *Ochlerotatus communis*, *Ochlerotatus dorsalis*, *Ochlerotatus dorsalis*, *Ochlerotatus taeniorhynchus*), **Mapputta serogroup** (*Anopheles meraukensis*), **Simbu serogroup** (*Armigeres subalbatus*, *Culex quinquefasciatus*, *Culex tritaeniorhynchus*, *Culicoides brevitarsis*, *Culicoides imicola*, *Culicoides oxystoma*, *Culicoides punctatus*, *Culicoides puncticollis*), **Guama serogroup** (*Culex*

(*Melanoconion*), **Koongol serogroup** (*Culex annulirostris*), **Patois serogroup** (*Culex cedecei*).

Intertypic reassortment occurs between viruses belonging to different serogroups. The following serogroups have a potential risk for intertypic reassortment because viruses from different serogroups were detected in the same vector species: **Bunyamwera and California serogroups** (*Aedes albopictus, Aedes communis*, *Aedes nigripes*, *Aedes trivittatus*, *Anopheles crucians*, *Anopheles maculipennis*, *Culiseta inornate*, *Ochlerotatus scapularis*, *Ochlerotatus taeniorhynchus*), **Bunyamwera and Simbu serogroups** (*Aedes communis*, *Culex quinquefasciatus*, *Culex tritaeniorhynchus*), **Bunyamwera, California, and Simbu serogroups** (*Aedes vexans*), **Mapputta and Ungrouped serogroups** (*Aedes vigilax*, *Anopheles meraukensis*), **Anopheles A and Anopheles B serogroups** (*Anopheles boliviensis*), **Bunyamwera, Bwamba, Nyando, Simbu, and Ungrouped serogroups** (*Anopheles funestus*), **Group C, Guama, and Patois serogroups** (*Culex* (*Melanoconion*), *Culex cedecei*), **Capim and Group C serogroups** (*Culex accelerans*), **Bunyamwera, California, Turlock, and Ungrouped serogroups** (*Culex modestus*), **Guama and Patois serogroups** (*Culex paracrybda*), **California and Olifantsvleiserogroups** (*Culex pipiens*), **Bunyamwera,**

California, and Turlock serogroups (*Culex tarsalis*), **Bunyamwera, Bwamba, and Ungrouped serogroups** (*Mansonia uniformis*).

Table 3.1. List of viruses with shared vector ecology.

	Isolation source	serogroup	country	number[2]	risk type
Aedeomyia squamipennis					
Alajuela virus	mosquito	Gamboa	Panama	1	intratypic
Calchaqui virus	mosquito	Gamboa	Argentina	1	intratypic
Gamboa virus	mosquito	Gamboa	Brazil	2	intratypic
Gamboa virus	mosquito	Gamboa	Ecuador	1	intratypic
Gamboa virus	mosquito	Gamboa	Panama	9	intratypic
Pueblo Viejo virus	mosquito	Gamboa	Ecuador	2	intratypic
Aedes albopictus					
Cache Valley virus	mosquito	Bunyamwera	USA	3	intratypic/intertypic
Potosi virus	mosquito	Bunyamwera	USA	2	intratypic/intertypic
La Crosse virus	mosquito	California	USA	2	intertypic
Aedes cantans					
Chatanga virus	mosquito	California	Russia	1	intratypic
Tahyna virus	mosquito	California	Czech Republic	1	intratypic
Aedes caspius					
Chatanga virus	mosquito	California	Russia	1	intratypic
Tahyna virus	mosquito	California	Czech Republic	1	intratypic
Aedes cinereus					
Chatanga virus	mosquito	California	Russia	1	intratypic
La Crosse virus	mosquito	California	USA	3	intratypic
Aedes communis					

[2] number = number of detections for virus species including different strains.

	Isolation source	serogroup	country	number[2]	risk type
Cache Valley virus	mosquito	Bunyamwera	USA	1	intertypic
Chatanga virus	mosquito	California	Russia	3	intertypic/intratypic
Inkoo virus	mosquito	California	Finland	1	intertypic/intratypic
Inkoo virus	mosquito	California	Russia	1	intertypic/intratypic
Aedes dorsalis					
California encephalitis virus	mosquito	California	USA	1	intratypic
Tahyna virus	mosquito	California	China	1	intratypic
Aedes mcintoshi					
Bunyamwera virus	mosquito	Bunyamwera	Kenya	4	intertypic/intratypic
Ngari virus	mosquito	Bunyamwera	Kenya	1	intertypic/intratypic
Shuni virus	mosquito	Simbu	South Africa	1	intertypic
Aedes nigripes					
Anadyr virus	mosquito	Bunyamwera	Russia	3	intertypic
Chatanga virus	mosquito	California	Russia	2	intertypic/intratypic
Inkoo virus	mosquito	California	Russia	1	intertypic/intratypic
Aedes trivittatus					
Cache Valley virus	mosquito	Bunyamwera	USA	1	intertypic
Trivittatus virus	mosquito	California	USA	2	intertypic
Aedes vexans					
Anadyr virus	mosquito	Bunyamwera	Russia	1	intertypic/intratypic

	Isolation source	serogroup	country	number[2]	risk type
Batai virus	mosquito	Bunyamwera	Ukraine	1	intertypic/intratypic
Main Drain virus	mosquito	Bunyamwera	USA	1	intertypic/intratypic
Chatanga virus	mosquito	California	Russia	1	intertypic/intratypic
Jamestown Canyon virus	mosquito	California	USA	19	intertypic/intratypic
Snowshoe hare virus	mosquito	California	USA	2	intertypic/intratypic
Tahyna virus	mosquito	California	Austria	2	intertypic/intratypic
Tahyna virus	mosquito	California	China	2	intertypic/intratypic
Tahyna virus	mosquito	California	Czech Republic	18	intertypic/intratypic
Tahyna virus	mosquito	California	Italy	2	intertypic/intratypic
Tahyna virus	mosquito	California	Slovakia	1	intertypic/intratypic
Trivittatus virus	mosquito	California	USA	2	intertypic/intratypic
Akabane virus	mosquito	Simbu	Australia	1	intertypic/intratypic
Akabane virus	mosquito	Simbu	Japan	1	intertypic/intratypic
Aedes vigilax					
Gan Gan virus	mosquito	Mapputta	Australia	2	intertypic
Salt ash virus	mosquito	Ungrouped	Australia	1	intertypic
Amblyomma gemma					
Bunyamwera virus	tick	Bunyamwera	Kenya	1	intratypic
Ngari virus	tick	Bunyamwera	Kenya	2	intratypic
Anopheles boliviensis					

	Isolation source	serogroup	country	number[2]	risk type
Anopheles A virus	mosquito	Anopheles A	Colombia	1	intertypic
Anopheles B virus	mosquito	Anopheles B	Colombia	1	intertypic
Anopheles crucians					
Tensaw virus	mosquito	Bunyamwera	USA	1	intertypic
South River virus	mosquito	California	USA	1	intertypic
Anopheles funestus					
Bunyamwera virus	mosquito	Bunyamwera	Kenya	4	intertypic/intratypic
Ngari virus	mosquito	Bunyamwera	Kenya	2	intertypic/intratypic
Bwamba virus	mosquito	Bwamba	Uganda	1	intertypic
Nyando virus	mosquito	Nyando	Central African Republic	1	intertypic/intratypic
Nyando virus	mosquito	Nyando	Kenya	1	intertypic/intratypic
Nyando virus	mosquito	Nyando	Uganda	1	intertypic/intratypic
Akabane virus	mosquito	Simbu	Kenya	1	intertypic
Tataguine virus	mosquito	Ungrouped	Kenya	1	intertypic
Anopheles gambiae					
Batai virus	mosquito	Bunyamwera	Kenya	2	intratypic
Ilesha virus	mosquito	Bunyamwera	Central African Republic	1	intratypic
Anopheles maculipennis					
Batai virus	mosquito	Bunyamwera	Austria	1	Intertypic
Batai virus	mosquito	Bunyamwera	Germany	1	Intertypic
Batai virus	mosquito	Bunyamwera	Italy	1	Intertypic
Batai virus	mosquito	Bunyamwera	Russia	6	Intertypic

	Isolation source	serogroup	country	number[2]	risk type
Chatanga virus	mosquito	California	Russia	1	Intertypic
Tahyna virus	mosquito	California	Italy	3	intertypic
Anopheles meraukensis					
Buffalo Creek virus	mosquito	Mapputta	Australia	1	intertypic/intratypic
Mapputta virus	mosquito	Mapputta	Australia	1	intertypic/intratypic
Leanyer virus	mosquito	Ungrouped	Australia	1	intertypic
Armigeres subalbatus					
Aino virus	mosquito	Simbu	Taiwan	2	intratypic
Akabane virus	mosquito	Simbu	Taiwan	2	intratypic
Culex (Melanoconion) sp.					
Bruconha virus	mosquito	Group C	Brazil	1	intertypic
Bertioga virus	mosquito	Guama	Brazil	1	intertypic/intratypic
Mahogany hammock virus	mosquito	Guama	USA	1	intertypic/intratypic
Moju virus	mosquito	Guama	Brazil	1	intertypic/intratypic
Pahayokee virus	mosquito	Patois	USA	2	intertypic
Culex accelerans					
Bushbush virus	mosquito	Capim	Trinidad and Tobago	1	intertypic
Nepuyo virus	mosquito	Group C	Trinidad and Tobago	1	intertypic
Culex annulirostris					
Koongol virus	mosquito	Koongol	Australia	1	intratypic
wongal virus	mosquito	Koongol	Australia	1	intratypic
Culex cedecei					

	Isolation source	serogroup	country	number[2]	risk type
Gumbo Limbo virus	mosquito	Group C	USA	5	intertypic
Mahogany hammock virus	mosquito	Guama	USA	7	intertypic
Pahayokee virus	mosquito	Patois	USA	3	intertypic/intratypic
Shark River virus	mosquito	Patois	USA	5	intertypic/intratypic
Culex modestus					
Ebinur lake virus	mosquito	Bunyamwera	China	1	intertypic
Tahyna virus	mosquito	California	China	1	intertypic
Lednice virus	mosquito	Turlock	Czech Republic	4	intertypic
Abbeylake	mosquito	Ungrouped	China	1	intertypic
Culex paracrybda					
Mirim-like virus	mosquito	Guama	Ecuador	1	intertypic
Abras virus	mosquito	Patois	Ecuador	1	intertypic
Culex pipiens					
Tahyna virus	mosquito	California	Austria	2	intertypic
Tahyna virus	mosquito	California	Italy	3	intertypic
Olifantsvlei virus	mosquito	Olifantsvlei	South Africa	1	intertypic
Culex quinquefasciatus					
Bunyamwera virus	mosquito	Bunyamwera	Argentina	1	intertypic
Aino virus	mosquito	Simbu	Taiwan	3	intertypic/intratypic
Akabane virus	mosquito	Simbu	China	1	intertypic/intratypic
Akabane virus	mosquito	Simbu	Taiwan	1	intertypic/intratypic

	Isolation source	serogroup	country	number[2]	risk type
Oropouche virus	mosquito	Simbu	Brazil	13	intertypic/intratypic
Culex tarsalis					
Lokern virus	mosquito	Bunyamwera	USA	1	intertypic
Jamestown Canyon virus	mosquito	California	USA	2	intertypic
Turlock virus	mosquito	Turlock	USA	1	intertypic
Culex tritaeniorhynchus					
Batai virus	mosquito	Bunyamwera	India	1	intertypic
Aino virus	mosquito	Simbu	Japan	2	intertypic/intratypic
Aino virus	mosquito	Simbu	Taiwan	7	intertypic/intratypic
Akabane virus	mosquito	Simbu	Taiwan	1	intertypic/intratypic
Kaikalur virus	mosquito	Simbu	India	1	intertypic/intratypic
Manzanilla virus	mosquito	Simbu	China	1	intertypic/intratypic
Culicoides brevitarsis					
Aino virus	midge	Simbu	Australia	6	intratypic
Akabane virus	midge	Simbu	Australia	19	intratypic
Douglas virus	midge	Simbu	Australia	1	intratypic
Peaton virus	midge	Simbu	Australia	4	intratypic
Tinaroo virus	midge	Simbu	Australia	3	intratypic
Culicoides imicola					
Akabane virus	midge	Simbu	Turkey	1	intratypic
Peaton virus	midge	Simbu	Israel	4	intratypic
Schmallenberg virus	midge	Simbu	Israel	4	intratypic
Shuni virus	midge	Simbu	Israel	3	intratypic
Culicoides oxystoma					
Aino virus	midge	Simbu	Japan	9	Intratypic

	Isolation source	serogroup	country	number[2]	risk type
Aino virus	midge	Simbu	Taiwan	2	Intratypic
Akabane virus	midge	Simbu	Japan	5	Intratypic
Akabane virus	midge	Simbu	Taiwan	2	Intratypic
Peaton virus	midge	Simbu	Israel	2	Intratypic
Peaton virus	midge	Simbu	Taiwan	1	Intratypic
Sathuperi virus	midge	Simbu	Israel	1	Intratypic
Sathuperi virus	midge	Simbu	Japan	1	Intratypic
Schmallenberg virus	midge	Simbu	Israel	3	Intratypic
Shuni virus	midge	Simbu	Israel	2	Intratypic
Culicoides punctatus					
Aino virus	midge	Simbu	Japan	1	intratypic
Schmallenberg virus	midge	Simbu	Poland	1	Intratypic
Culicoides puncticollis					
Peaton virus	midge	Simbu	Israel	2	Intratypic
Schmallenberg virus	midge	Simbu	Israel	2	Intratypic
Shuni virus	midge	Simbu	Israel	1	intratypic
Culiseta 90ocktail					
Cache Valley virus	mosquito	Bunyamwera	USA	1	intertypic
Jamestown Canyon virus	mosquito	California	USA	7	Intertypic/intratypic
Jerry Slough virus	mosquito	California	USA	1	Intertypic/intratypic
Mansonia titillans					
Bunyamwera virus	mosquito	Bunyamwera	Argentina	2	intratypic
Tlacotalpan virus	mosquito	Bunyamwera	Mexico	1	intratypic

	Isolation source	serogroup	country	number[2]	risk type
Mansonia uniformis					
Bunyamwera virus	mosquito	Bunyamwera	Central African Republic	1	intertypic
Pongola virus	mosquito	Bwamba	Kenya	5	intertypic
Shuni virus	mosquito	Simbu	South Africa	1	intertypic
orthobunyavirus sp.	Mosquito	Ungrouped	Kenya	3	intertypic
Ochlerotatus albifasciatus					
Bunyamwera virus	mosquito	Bunyamwera	Argentina	1	intratypic
Laguna Larga virus	mosquito	Bunyamwera	Argentina	1	intratypic
Ochlerotatus canadensis					
Jamestown Canyon virus	mosquito	California	USA	2	intratypic
Snowshoe hare virus	mosquito	California	USA	1	intratypic
Ochlerotatus communis					
Chatanga virus	mosquito	California	Russia	1	intratypic
Inkoo virus	mosquito	California	Sweden	1	intratypic
Ochlerotatus dorsalis					
California encephalitis virus	mosquito	California	USA	1	intratypic
Jamestown Canyon virus	mosquito	California	USA	8	intratypic
Ochlerotatus scapularis					
Bunyamwera virus	mosquito	Bunyamwera	Argentina	4	Intertypic/intratypic
Kairi virus	mosquito	Bunyamwera	Brazil	1	Intertypic/intratypic

	Isolation source	serogroup	country	number[2]	risk type
Kairi virus	mosquito	Bunyamwera	Trinidad and Tobago	1	Intertypic/intratypic
Lukuni virus	mosquito	Bunyamwera	Trinidad and Tobago	1	Intertypic/intratypic
Melao virus	mosquito	California	Trinidad and Tobago	1	Intertypic
Ochlerotatus taeniorhynchus					
Cache Valley virus	mosquito	Bunyamwera	Mexico	17	Intertypic/intratypic
Cholul virus	mosquito	Bunyamwera	Mexico	1	Intertypic/intratypic
South River virus	mosquito	California	Mexico	1	Intertypic
Rhipicephalus pulchellus					
Bunyamwera virus	tick	Bunyamwera	Kenya	1	intratypic
Ngari virus	tick	Bunyamwera	Kenya	2	intratypic

3.3 DISCUSSION

The ability of orthobunyaviruses to reassort poses a significant risk to both animals and humans. Fortunately, there are several barriers to reassortment that must be overcome in order for a reassortant virus to emerge in a population. These barriers include sympatry, ecology, co-infection, and several molecular and immunological barriers within the host. We aimed to create a comprehensive dataset, using publicly available data, to evaluate sympatry and shared host range between orthobunyaviruses. This dataset highlights several viruses that have overcome the first two barriers to reassortment – shared sympatry and ecology. Overall, the dataset

provides a proof-of-concept for the value of surveillance in evaluating reassortment potential.

Reassortment occurs frequently in nature and it is hypothesized that most, if not all bunyavirus isolates, are reassortants [18]. Our genomic analysis, discussed in Chapter 2, highlights the frequency of orthobunyavirus reassortment [51]. Specifically, our phylogenetic analysis provides evidence for frequent intratypic reassortment and limited instances of intertypic reassortment. Therefore, we asked: if the barriers of sympatry and shared host range are overcome, can we predict which viruses will reassort within the same serogroup? We list several examples of potential intratypic reassortment in **Table 3.1**. To emphasize the validity of using shared host range to predict intratypic reassortment, we highlight an example within the Gamboa serogroup. Reassortment analyses, using whole genome sequencing, shows evidence of reassortment between three members of the Gamboa serogroup (Gamboa virus, Alajuela virus, and Pueblo Viejo virus (**Chapter 2 Figure 2.8 and 2.9**) [51]. The analysis presented here shows that these three viruses were detected in *Aedeomyia squamipennis* and circulate in South America – demonstrating sympatry and a shared vector range. The synthesis of sympatry and shared host range can reveal potential reassortment events.

While there are several examples of confirmed intratypic reassortment [18,51,52,55,69,163,169,170,205], evidence for intertypic reassortment is rare. Our analysis shows extensive sympatry between serogroups, but a lack of shared vector range between serogroups. This helps to explain why intertypic reassortment does not

occur frequently – opportunity is not provided because of a lack of shared vector range. One of the few possible examples of intertypic reassortment is Guaroa virus – a bridge between Bunyamwera and California serogroups. Here we provide data to support the potential for reassortment between these two serogroups. Viruses belonging to both serogroups have been detected in the USA from *Aedes albopictus*, *Aedes trivittatus*, *Anopheles crucians, Culex tarsalis*, and *Culiseta inornata;* in Russia from *Aedes nigripes*; in Russia and the USA from *Aedes vexans*; from Italy in *Anopheles maculipennis*; from China in *Culex modestus*; from South America in *Ochlerotatus scapularis*; and from Mexico in *Ochlerotatus taeniorhynchus*. Furthermore, our analysis shows shared sympatry and vector range between a few serogroups, such as Bunyamwera and Simbu, for which no reassortment has been documented. This suggests that barriers beyond geography and shared vector-host range inhibit intertypic reassortment or a reassortant hasn't been detected yet. We hypothesize that something on a molecular level acts as a relatively strong barrier to block intertypic reassortment (discussed in **Chapter 4**).

While this study has strengths and maximizes on previous virus isolations, there are limitations. First, the dataset represents non-exhaustive and likely biased sampling over an 80-year timespan. A more targeted surveillance study would greatly increase the strength of this type of analysis. Second, the dataset is missing some virus isolations for two reasons: 1) viruses have been isolated but not sequenced and therefore we missed them because we only pulled metadata for viruses that have been sequenced 2) metadata were missing from the GenBank submission and therefore the

isolation was not used in the analysis. For example, Tete virus and Bakau virus have been isolated from ticks [158], however our analysis lacks these vector associates.

The frequent reassortment among orthobunyaviruses provides an evolutionary advantage by increasing genetic diversity. However, this propensity to reassort presents a significant risk to animals and humans across the globe. Our analysis highlights the importance of strategic surveillance to bolster outbreak preparedness efforts. Increasing the number of isolations will enhance our ability to characterize the extent to which viruses have sympatry and ecology. Here, we've shown that the frequent intratypic reassortment is plausible due to a shared sympatry and ecology. However, the lack of intertypic reassortment is baffling given the extent to which different serogroups share the same geographic region and vector. Therefore, directing research efforts at understanding the molecular barriers to reassortment will be imperative to predicting which geographic areas have a high risk for reassortment.

This analysis takes advantage of years of research to present a detailed picture of sympatry and ecological dynamics for viruses within the *Orthobunyavirus* genus. It also highlights the wealth of epidemiologically relevant information that can be drawn from metadata associated with sequencing records, and how valuable this is for developing hypotheses and guiding future surveillance efforts. We hope that the curated dataset will be valuable to other researchers and that the trends we presented with the meta-analysis will inform future research.

3.4 Materials & Methods

3.4.1 Data Curation

The original dataset was assembled by downloading GenBank files from NCBI's Nucleotide database using the search term 'orthobunyavirus'. This analysis includes all sequences available as of April 25, 2023. Additionally, the accompanying GI accession numbers for all entries were downloaded. Metadata was extracted from the original dataset using a custom python script (*github.com/mllayton/dissertation/chapter3/extract_genbank.py*). The extract_genbank.py script searches the original dataset for GenBank source modifiers 'ogranism', 'isolate', 'df.xref', 'country', 'lat/lon', 'year', 'isolation source', 'host', 'paper'. The resulting file contained 5,411 entries. To validate that the number of entries in the metadata file matched those of the original dataset, the custom script check_parsed_genbank was used (*github.com/mllayton/dissertation/chapter3/check_parsed_genbank*).

To create a curated dataset that contained a single entry for each unique isolation, we used a custom R script for automated curation (*github.com/mllayton/dissertation/chapter3/script_analyze_metadata.R*) in addition to Excel for minimal manual curation.Using the metadata file, a curated dataset was made (*github.com/mllayton/dissertation/chapter3/curated_dataset*). First, the collection date, which had various date formats, was replaced with the year of isolation. The original collection date column was removed. Next, duplicate entries were removed. Duplicate entries were those with the same organism, strain, isolate, db.xref, country, lat.lon, collection.year, isolation.source, host, paper.title, segment. There were 309 duplicates.

Then, the dataframe was condensed to eliminate multiple entries for L/M/S segments from the same isolation. To do this, pivot_wider was used to move lines with L/M/S from one virus isolation were placed into one row while retaining the GenBank accession ID for each segment. This narrowed the dataset down to 2,774 entries. To tidy the curated dataset, the word 'orthobunyavirus' was replaced with 'virus' in the organism ID column. An important piece of metadata was the country of isolation. Unfortunately, the specific latitude and longitude are rarely included. Therefore, we chose to use the country name of isolation for plotting. In order to do this, we added a new column and included the centroid latitude and longitude for the country. Centroid latitude and longitude were found using a combination of the R packages 'rgeos', 'rworldmap', rworldxtra', and google maps. At this point, the curated dataset was read back into R and duplicate entries were still found. For example, strain and isolate information are often used interchangeably. Therefore, the strain and isolate columns were merged to preserve the isolate identification. Entries lacking data for country.norm, centroid.lat, centroid.long, and collection.year were removed because these isolations could not be plotted. The remaining 30 duplicates were manually verified and found to be truly unique except for Shuni/275/1/14. To add serogroup classification, the ArboCat Reference Catalog and literature searches were performed. Serogroup designations were added to a new column. The final curated dataset contained 1,850 unique virus isolations and is publicly available (*github.com/mllayton/dissertation/chapter3*).

Another dataset was used to evaluate host and vector patterns. To do this, the curated dataset was used to expand on the isolation source information present in the

original dataset. Specifically, the ‘host.scientific’ and ‘host.common’ columns were added. The ‘host.scientific’ column was used to add the scientific name for the organism from which the virus was isolated. The ‘host.common’ column was added to use a common name to identify the type of organism.

3.4.2 Data Visualization

The curated dataset was used to visualize the year of isolation, country of isolation, source of isolation, and serogroup assignments. The custom R script, script_analyze_metadata.R, includes all of the packages, commands, and notes.

Chapter 4: Minigenome Melees: A novel high throughput method to evaluate reassortment potential between orthobunyaviruses

4.1 Introduction

The emergence of novel reassortants with altered phenotype can lead to high consequence pathogens with devastating economic and health impacts. With increased climate change and human travel, ecological niches are changing, allowing for overlap between host and vectors which increases the opportunity for coinfection. Because these environmental barriers continue to be removed, a deeper understanding of the molecular compatibility between viruses is warranted. Determining the molecular limitations/boundaries to segmented RNA virus reassortment will better inform outbreak preparedness strategies by identifying viruses that occupy the same geographic areas and are molecularly compatible for reassortment.

One way reassortment has traditionally been studied is through the use of minigenome/replicon assays. These assays are limited in throughput because reassortment can only be studied between two viruses at a time. We've enhanced traditional minigenome assays by including unique barcodes that enables quantification of the minigenome RNA using next-generation sequencing and strand-specific RT-qPCR (ss-RT-qPCR). This allows us to evaluate the molecular compatibility of the viral machinery (RdRp and nucleoprotein) for untranslated regions (UTR) in high-throughput. Using novel minigenome melees, in concert with traditional techniques, we can answer

targeted questions about the molecular compatibility between segmented RNA viruses, using the orthobunyavirus genus as a prototype.

We chose to develop our minigenome melee system using viruses belonging to the orthobunyavirus genus (*Bunyavirales:Peribunyaviridae*) for several reasons. First, orthobunyaviruses are a large group of segmented RNA viruses with high genetic diversity. Second, this group of viruses is vector-borne, sustaining the viral lifecycle and increasing geographic spread of viruses. Third, this group infects a wide range of hosts and include several zoonotic diseases. Fourth, disease presentation varies widely among this group of viruses, from mild febrile disease to encephalitis and hemorrhagic fever. Finally, natural reassortment is ubiquitous among this group and has driven the viral evolution of this group for many years. All of these factors increase the likelihood for the emergence of a high consequence reassortant as environmental barriers to coinfection continue to be removed.

The genomes of orthobunyaviruses are composed of three segments: the small segment (S) encodes a viral nucleoprotein, the medium (M) segment encodes a glycoprotein for cell entry, and the large (L) segment encodes the RNA dependent RNA polymerase (RdRp) for replication and transcription of viral genomes [8,206]. The viral RdRp replicates and transcribes genomes for which it recognizes the 5' and 3' untranslated regions (UTR). Signals for replication, transcription, and packaging are all contained within the UTR [8,207–211]. The terminal 11 nucleotides of the UTRs are highly conserved among viruses in the orthobunyavirus genus [8,212,213] and form a panhandle which allows for the RdRp to initiate replication [1]. By using the UTR and

removing the coding region, minigenome systems can study replication, transcription, and packaging dynamics in a safe way.

In the experiments below, we present data that support the use of the novel minigenome melee system to evaluate reassortment potential. Additionally, we show important molecular compatibility dynamics between orthobunyaviruses that inform reassortment potential. Specifically, we show that the replication machinery is functional on a surprising number of genetically diverse UTRs. First, we present data to show proof-of-concept for this technique. Secondly, we use this system to determine what limits, if any, exist for the molecular compatibility between closely related (intertypic) and distantly related (intratypic) viruses. Together, we've shown that novel minigenome melees can be used to evaluate molecular limitations to reassortment and that by combining this knowledge with known environmental barriers, we can identify locations, vectors, and hosts, with an increased potential for the emergence of a reassortant of high consequence. This proactive approach will aid in minimizing the economic and health burdens that result from unexpected outbreaks.

4.2 Results

4.2.1 Overview of Minigenome Melees

Minigenome melees evaluate reassortment potential between segmented viruses in high-throughput. Traditional minigenomes replace the protein coding sequence with a reporter gene, making this a safe system. While this system has contributed much to the field, it is low-throughput – allowing researchers to evaluate molecular compatibility between two viruses at once. This results in time intensive and expensive research.

With so many viruses capable of reassortment, and environmental barriers continuing to breakdown, it is important to efficiently evaluate reassortment potential. Therefore, we aimed to create a system that increases the throughput of traditional minigenome systems.

Barcoded minigenomes build on traditional minigenomes while increasing throughput. **Figure 4.1A** compares a traditional minigenome to a barcoded minigenome. There are two differences: 1) two unique barcodes flanking the nanoluciferase gene, (b1/b2) and 2) conserved primer binding sites (P1/P2) flanking the unique barcodes. The unique barcodes correspond to the viral genome segment from which the UTRs are derived. Because each minigenome contains a unique barcode, the minigenomes can be multiplexed to make a 'minigenome library' (**Figure 4.1B**). This library of minigenomes can then be transfected into cell culture expressing the replication machinery of one orthobunyavirus. This results in the ability to test the compatibility of a single virus replication machinery (RdRp and nucleoprotein) for a large number of genome segments at one time.

Although the general principles remain, our minigenome melees have two major differences in the experimental protocol. First, traditional minigenome systems measure reporter activity to determine molecular compatibility (**Figure 4.1C**). Reporter activity represents a successful replication, transcription, and translation of the viral UTRs by the RdRp and nucleoprotein. Because our system uses a minigenome library for which all minigenomes have the same reporter gene, we cannot determine which minigenomes are contributing what fraction of the reporter signal. Therefore, we

designed two parallel methods to evaluate molecular compatibility: a strand-specific-RT-qPCR assay and an amplicon library preparation for next-generation sequencing (**Figure 4.1D**). These methods enable reliable identification of compatible minigenomes with the helper proteins and provide insight into variable replication and transcription efficiencies. Second, traditional minigenome systems typically transfect plasmids containing a promoter for expression of viral helper proteins and minigenome RNA inside the tissue culture system (**Figure 4.1C**). In the minigenome melee system, this method resulted in significant levels of background minus strand RNA from minigenomes transcribed from cellular T7 polymerase instead of viral transcription (data not shown). Therefore, we switched to transfecting *in vitro* transcribed minigenome RNA to bypass the need for cellular T7 polymerase to make minigenome RNA (**Figure 4.1D**). Molecular compatibility can be measured using traditional luciferase assays, ss-RT-qPCR, or amplicon-based sequencing, thereby increasing the robustness of the minigenome melee system.

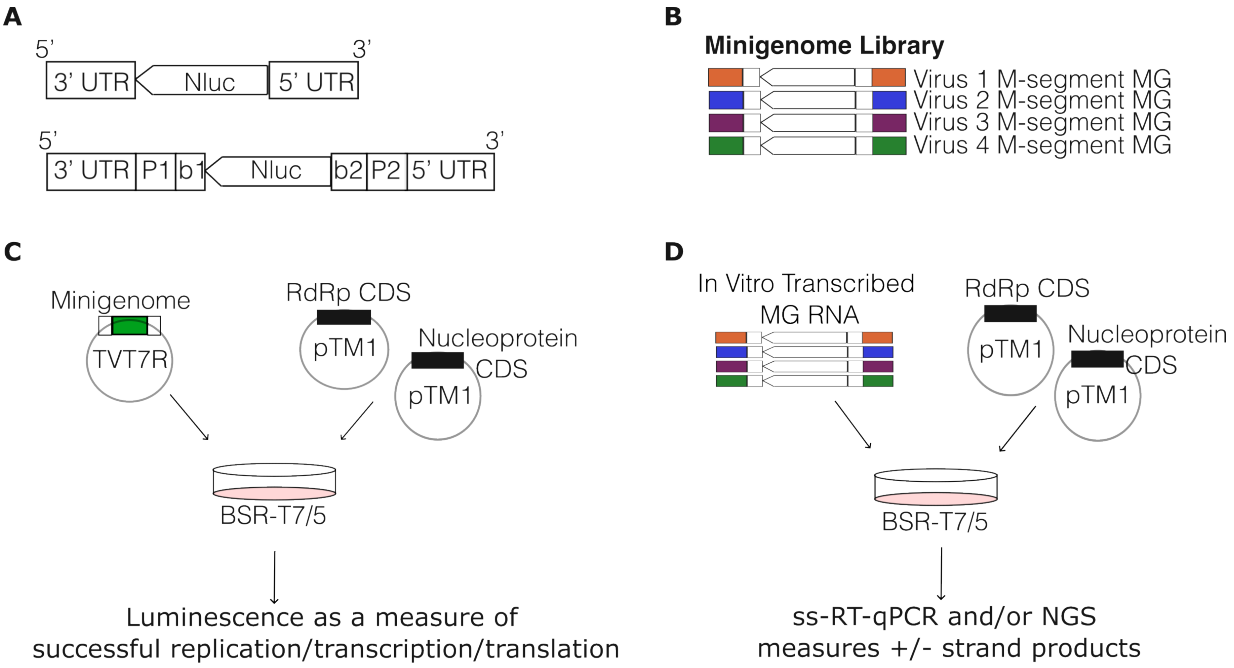

Figure 4.1. Design of minigenome melee system
Minigenome melees improve traditional minigenome assays by increasing throughput. A) Minigenome melees use unique barcodes to identify which minigenome corresponds to which viral M-segment (b1/b2). Conserved P1/P2 primer sequences are used to develop strand-specific libraries for next-generation sequencing B) Minigenome libraries are created by adding equal amounts of each in vitro transcribed minigenome RNA C) Traditional minigenome assays use luminescence as a measure of compatibility and does not distinguish between replication/transcription/translation products D) The minigenome melee assay utilizes in vitro transcribed RNA and tests the compatibility for viral RdRp and nucleoprotein to replicate/transcribe/translate all minigenomes in the minigenome library. Using ss-RT-qPCR and/or NGS, replication (+/- strand) can be distinguished from the transcription products (+strand).

The strand-specific-RT-qPCR and amplicon-based sequencing methods provide measures of replication and transcription efficiency by quantifying plus and minus strand transcripts. Replication of the minigenome RNA results in plus and minus strand products, while transcription produces only plus strand products. By measuring the number of plus strand products, we can evaluate compatibility of the helper proteins to replicate and transcribe the viral UTRs present in the minigenome. Similarly, we can evaluate the compatibility for replication by measuring the minus strand products. However, measuring minus strand products is not reliable since the transfected *in vitro*

transcribed RNAs are also minus strand. To mitigate this, use of an N-only control provides a baseline for background levels of *in vitro* transcribed RNA.

The amplicon-based library preparation creates strand-specific libraries to enable identification of plus and minus strand products as well as detangle which minigenome RNAs were compatible with the viral RdRp and nucleoproteins (**Figure 4.2A**). Briefly, RNA undergoes first-strand synthesis using P1/P2 primers containing the i5 adapter. For plus strand: P1. For minus strand: P2. First-strand synthesis is followed by second-strand synthesis using the P2-i7 primer (plus strand products) or the P1-i7 primer (minus strand products). This results in an amplicon containing the P1/P2, b1/b2, and nanoluciferase sequences. The amplicons are amplified using full-length adapters compatible with Illumina sequencing platforms. Finally, we quantified the number of plus strand and minus strand reads that correspond to each M-segment minigenome based on the orientation of the i5/i7 index, P1/P2 sequence, and unique b1/b2 barcodes.

The strand-specific-RT-qPCR (ss-RT-qPCR) assay allows for cost-effective and targeted evaluation of 1) *in vitro* transcribed minigenome RNAs prior to transfection and 2) experimental minigenome melees (**Figure 4.2B**). The ss-RT-qPCR assay is faster and cheaper than next-generation sequencing and allows for optimization of minigenome melees before proceeding with next-generation sequencing. Briefly, reverse transcription is performed using a strand-specific primer containing a tag sequence, that binds in the nanoluciferase gene [214]. The reverse transcription products are then quantified using qPCR that incorporates a tag-primer, which binds to the tag sequence, and a minigenome-specific primer, which binds within the

nanoluciferase reporter gene. For validating *in vitro* transcribed RNAs, we measure the amount of plus and minus strand from RNA and DNA to determine the quality of the *in vitro* transcribed RNA. To measure the compatibility of viral replication machinery for minigenomes within the minigenome library, we screen for plus and minus strand.

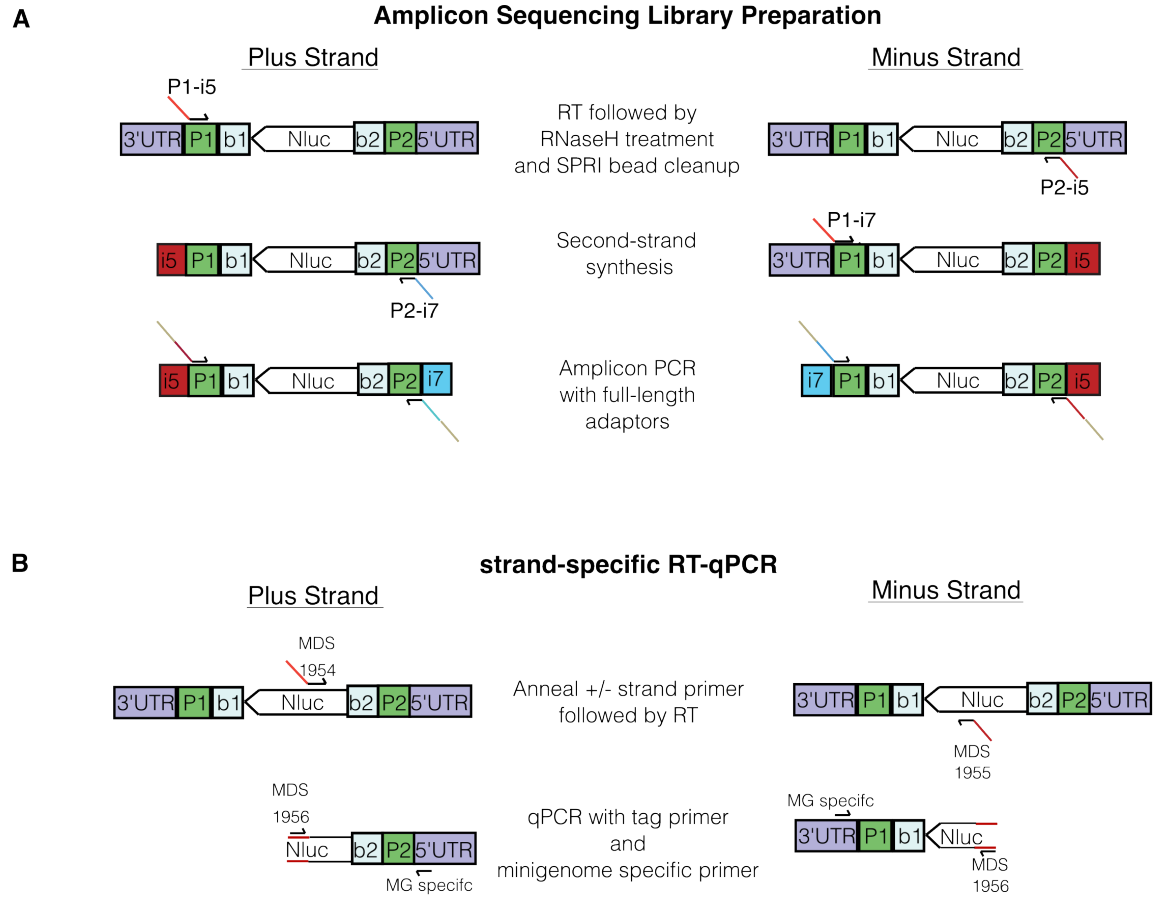

Figure 4.2. Strand-specific RT-qPCR and Next-Generation Sequencing Library Prep Design
Minigenome melees enable multiple forms of measuring compatibility for RdRp and nucleoproteins for a variety of M-segment minigenomes. A) Strand-specific libraries can be made using the conserved P1/P2 primer sequences in the minigenome. The number of sequencing reads for plus and minus strand measure replication and transcription efficiency B) strand-specific-RT-qPCR is an efficient way to measure the amount of plus and minus strand for validating in vitro transcribed minigenome RNA as well as measuring replication and transcription efficiencies during minigenome melees.

4.2.2 Composition of the barcoded minigenome library

Our aim was to increase throughput of traditional minigenome systems by making a library of barcoded minigenomes. The goals of the barcoded minigenome

library were three-fold: 1) To create a library with more than one barcoded minigenome 2) To test viruses that are closely related and distantly related, resulting in a range of genetic diversity and 3) To include some viruses belonging to serogroups known to cause disease in animals and humans in order to evaluate the potential for reassortment between non-pathogenic and pathogenic orthobunyaviruses. Therefore, we chose to design barcoded M-segment minigenomes for the following viruses: Kairi virus (Bunyamwera serogroup), Cache Valley virus (Bunyamwera serogroup), Boraceia virus (Anopheles B serogroup), Gamboa virus (Gamboa serogroup), La Crosse virus (California serogroup), Oropouche virus (Simbu serogroup), and Brazoran virus (not classified). **Figure 4.3** shows the relatedness of these viruses and that the distribution contains viruses closely and distantly related to Kairi virus – the replication machinery used for the minigenome melee shown here.

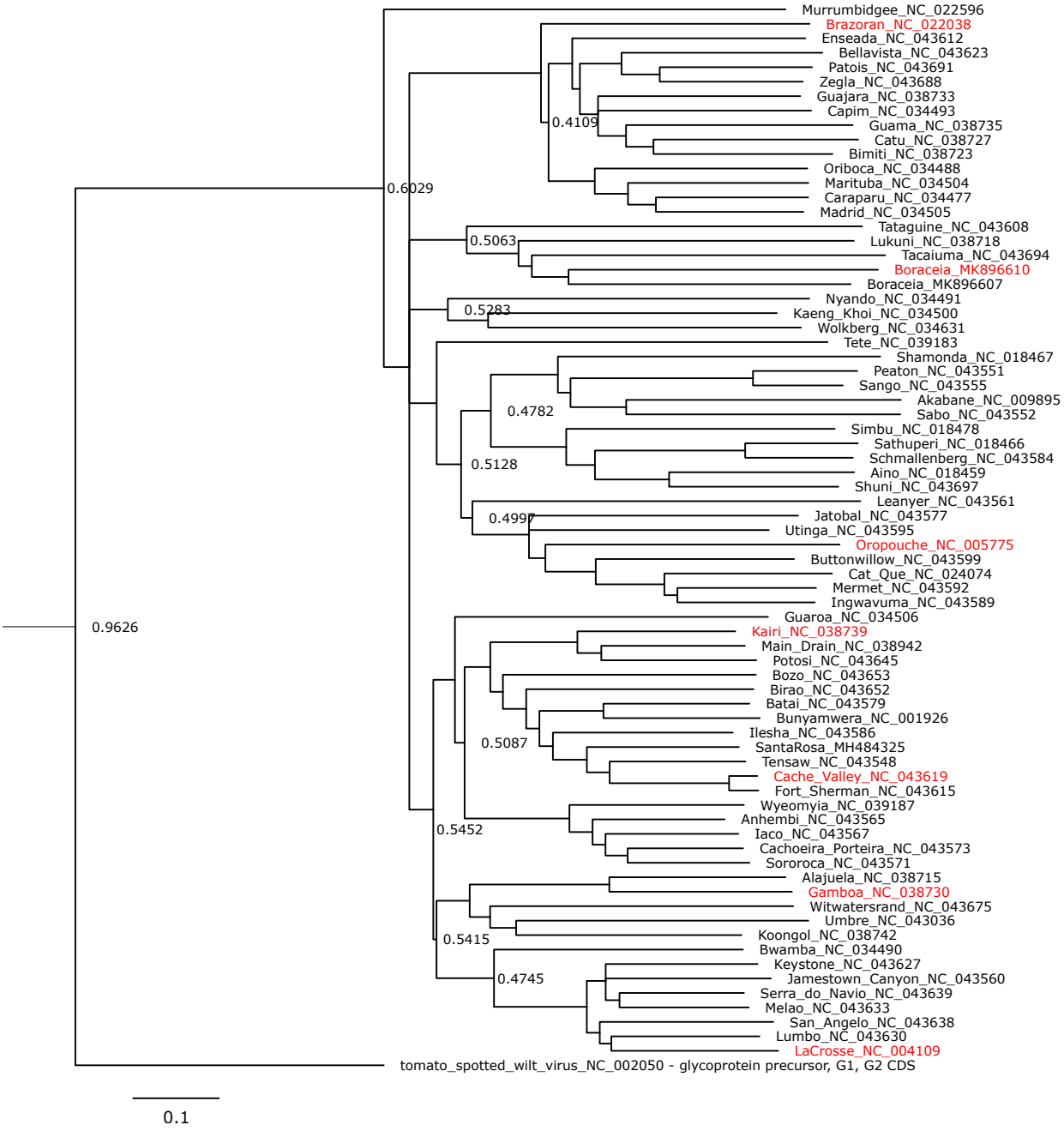

Figure 4.3. M-segment minigenomes represent a wide range of genetic diversity within the orthobunyavirus genus. M-segment phylogeny made using the glycoprotein coding region of all orthobunyavirus RefSeqs available on NCBI.

To determine the nucleotide similarity of the minigenome viral UTRs, we performed a pairwise alignment of the 5' and 3' UTRs individually (**Figure 4.4 A and B**).

Additionally, the percent nucleotide similarity to Kairi virus M-segment UTRs was determined using NCBI BLAST (**Figure 4.4C**). Here, we show that the viral UTRs are quite different from each other, except for the highly conserved terminal 11 nucleotides. Interestingly, the 3' UTRs have an overall higher nucleotide similarity than the 5' UTRs; minimum percent similarity for 5' UTR is 43% compared to maximum 3' UTR similarity of 37% (**Figure 4.4C**). La Crosse virus UTRs have the highest nucleotide similarity to Kairi virus (52% 3' UTR and 37% 5' UTR). With such low nucleotide similarity, we hypothesized that Kairi virus L+N proteins would be less compatible, if at all, on minigenomes outside of the Bunyamwera serogroup. And that this molecular compatibility would present a significant barrier to reassortment potential.

We designed negative control minigenomes for Kairi virus and Cache Valley virus M-segment minigenomes. These negative controls lack most of the UTR and therefore should not be replicated or transcribed.

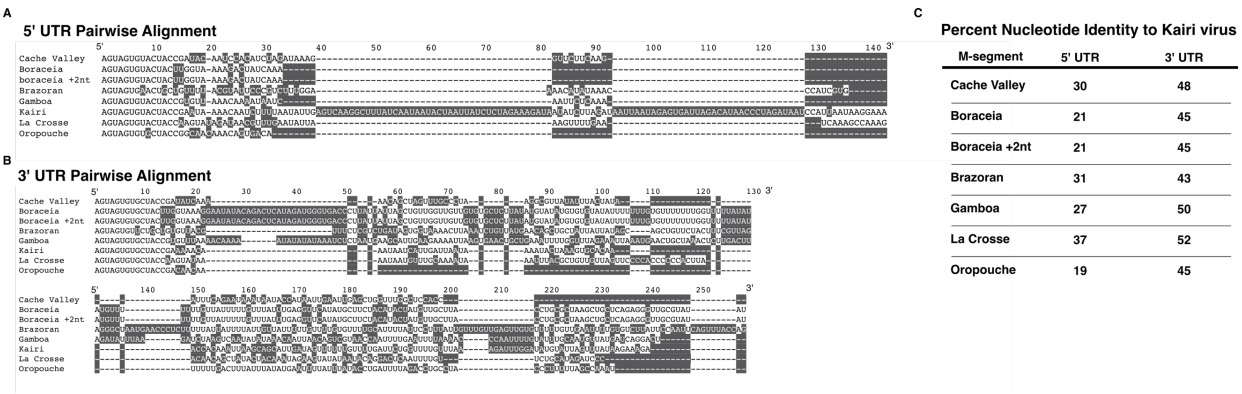

M-segment	5' UTR	3' UTR
Cache Valley	30	48
Boraceia	21	45
Boraceia +2nt	21	45
Brazoran	31	43
Gamboa	27	50
La Crosse	37	52
Oropouche	19	45

Figure 4.4. Nucleotide similarity between UTRs of viruses used.

Pairwise alignments were made using the Geneious Pairwise Alignment tool. Percent nucleotide identity was determined using BLAST.

4.2.3 Barcoded minigenomes are functional

We next confirmed that extra primer binding and barcode sequences didn't interfere with the minigenome function. To determine if the addition of these sequences would interfere with the function of the minigenome system, we measured nanoluciferase expression. Using 6 well plates of BSR T7/5 cells, pTM1-Kairi-L and pTM1-Kairi-S helper plasmids were transfected using TransIT-LT1 (MirusBio) and then a single M-segment minigenome was transfected 24 hours later using TransIT-X2 (MirusBio). To control for background expression, a pTM1-Kairi-N only transfection was performed for each M-segment minigenome. All transfections were done in triplicate. Cells were harvested in 1X passive lysis buffer and then imaged for nanoluciferase and firefly luciferase expression using Promega's Dual-Luciferase Reporter Assay Kit, according to manufacturer's instructions. Kairi virus L+N proteins were functional on Kairi virus M-segment minigenome, as expected (**Figure 4.5**). Additionally, the negative control minigenomes (Cache Valley negative control and Kairi virus negative control) did not express any nanoluciferase, as expected. Kairi virus L+N proteins were not functional on Brazoran or Oropouche M-segment minigenomes (there are caveats to these two minigenomes, see discussion). Finally, Kairi virus L+N proteins were functional on Cache Valley virus, La Crosse virus, Boraceia +2nt, Gamboa, and Boraceia virus M-segment minigenomes – at variable efficiencies. From this we determined that barcoded minigenomes are functional and can be used to evaluate reassortment potential, similarly to the traditional minigenome system.

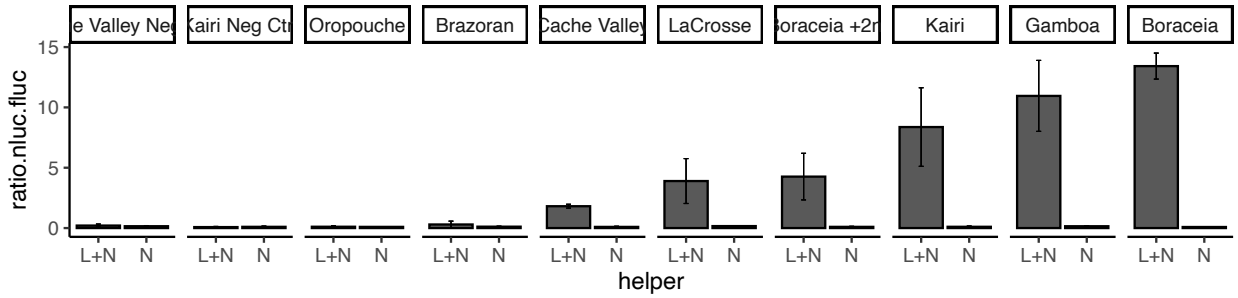

Figure 4.5. Barcoded minigenomes are functional.
Individual *in vitro* transcribed barcoded minigenomes were transfected into BSR T7/5 cells previously transfected with pTM1-Kairi-L and pTM1-Kairi-S plasmids. To measure functionality, nanoluciferase and firefly express (control plasmid) were measured 24 hours post-minigenome transfection. Minigenome expression is shown as the ratio of nanoluciferase (RLU) over firefly luciferase (RLU).

4.2.4 ss-RT-qPCR and NGS as readouts for barcoded minigenomes

To evaluate reassortment potential using traditional minigenomes is time intensive because it is low-throughput – only two viruses can be tested at once. The primary goal of the minigenome melee system is to increase throughput. We aimed to accomplish this by generating a barcoded minigenome library that would allow simultaneous transfection of multiple M-segment minigenomes into one well. RNA from BSR T7/5 cells transfected with Kairi virus L+N plasmids plus the minigenome library, were prepared for amplicon sequencing using our custom strand-specific amplicon library protocol. As a negative control, cells were transfected in the same way, but without the L plasmid (N-only). Libraries were deep-sequenced using the MiSeq. The number of plus strand reads were determined using our custom pipeline, as described in the methods section. The sequencing data shows an increase in plus strand reads for Kairi, La Crosse, Oropouche, Gamboa, Boraceia, Boraceia +2nt, and Cache Valley M-segment minigenomes (**Figure 4.6**). Additionally, there is no increase in plus strand RNA from Brazoran, Cache Valley negative control, and Kairi negative control M-segment minigenomes. The plus strand RNA levels present in the N-only samples

provide a control for background levels of expression. These levels are all below that of the samples transfected with L+N plasmids.

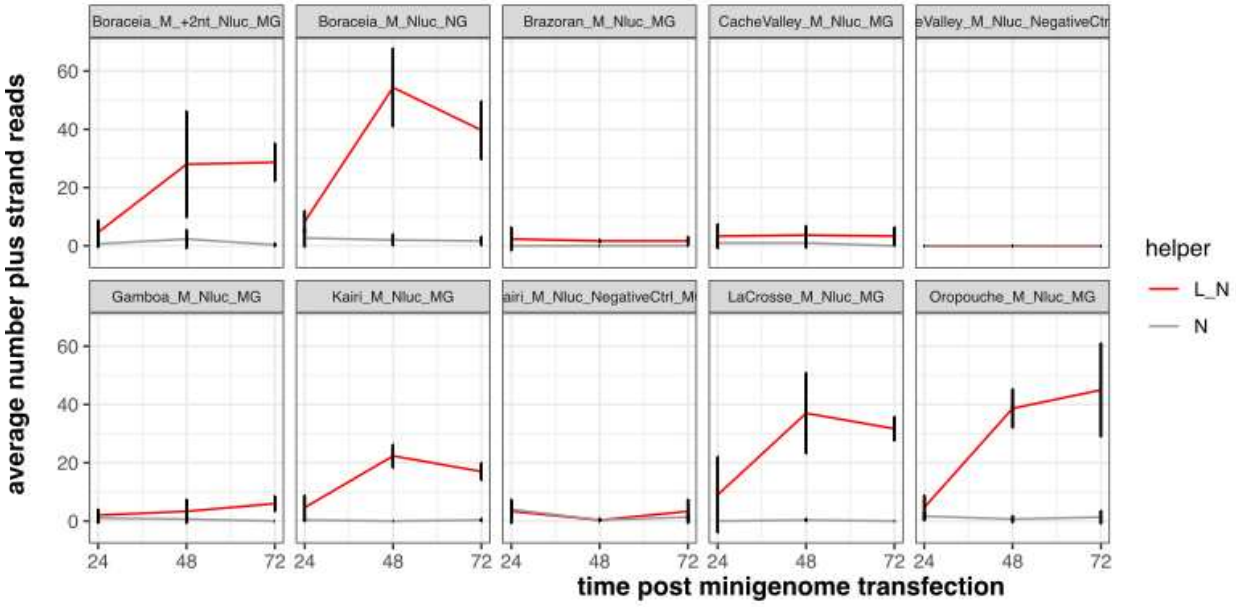

Figure 4.6. Amplicon sequencing measures replication and transcription efficiency.
RNA from minigenome melee was prepared for sequencing using a custom amplicon library preparation that preserves strand information. Cells were harvested at 24, 48, and 72 hours post-minigenome transfection. RNA from cells transfected with pTM1-Kair-L and pTM1-Kairi-S are shown in red. RNA from cells transfected with pTM1-Kairi-S only are shown in grey. The number average number of plus strand reads for each minigenome are shown. Standard deviation is shown in black.

As an independent validation of our NGS-based methods, we performed strand-specific RT-qPCR using the same RNA extracted from the minigenome melee. Briefly, the strand-specific RT-qPCR assay selectively reverse transcribes either the plus or minus strand of all minigenome RNA. The cDNA is then amplified using a tag primer and a minigenome specific primer (**Figure 4.2B**). Kairi virus M-segment minigenome had the highest fold change of plus strand RNA products (**Figure 4.7**). Other minigenomes with a fold change above background levels included La Crosse, Oropouche, Gamboa, Cache Valley, and Boraceia. Brazoran minigenome did not have

any levels of plus strand RNA above background. Because we used this system to validate the sequencing data, the negative control minigenomes and Boraceia +2nt were not tested using this method.

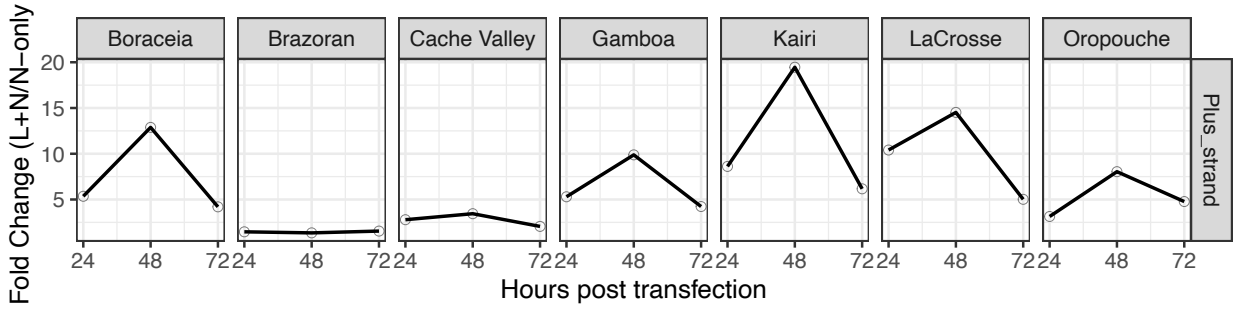

Figure 4.7. strand-specific RT-qPCR measures replication and transcription efficiencies. Cellular RNA from the minigenome melee was used to validate the amount of plus strand RNA determined by amplicon sequencing. The amount of plus strand RNA is shown as the fold change of minigenome present in cells expressing pTM1-Kairi-L and pTM1-Kairi-S versus cells expressing only pTM1-Kairi-S.

4.3 Discussion

Novel minigenome melees enhance traditional minigenome systems by increasing throughput. Here, we've shown that the addition of a unique barcode sequence to the minigenome allows for increased throughput and fine-tuned readouts such as amplicon sequencing and ss-RT-qPCR. While traditional minigenomes have led to significant discoveries about reassortment potential, we are hopeful the minigenome melee system will prove to be a valuable tool in increasing the efficiency at which we can evaluate reassortment potential.

Using Kairi virus as a prototype, we've shown that the minigenome system can increase our understanding of molecular compatibility between viruses within a large group of viruses. The replication machinery of Kairi virus is functional on the M-segments of Boraceia virus, Cache Valley virus, Gamboa virus, and La Crosse virus.

However, the M-segment of Brazoran virus is not compatible with Kairi virus L+N proteins. Here, we've demonstrated that Kairi virus is able to replicate and transcribe a surprising number of M-segments with significantly different nucleotide composition. This suggests that replication and transcription may not pose a significant barrier to reassortment.

While reassortment between orthobunyaviruses occurs frequently [18,51], we do not know the molecular mechanisms that permit or inhibit reassortment. Traditional minigenomes have been used to understand if two viruses might reassort, were they given the opportunity. One such study showed that the replication machinery of Schmallenberg virus is capable of replicating and transcribing the M-segment of Oropouche virus [215] Currently, these two viruses are not sympatric, but the data suggests that were these two Simbu serogroup viruses to meet in nature, reassortant progeny are possible. Similarly, Cache Valley virus and Kairi virus have been shown to replicate and transcribe each others M-segments [216] These are both examples of intratypic reassortment – within serogroup. We've shown that Kairi virus is capable of replicating and transcribing M-segment genomes from outside the Bunyamwera serogroup. This suggests that replication and transcription are not significant barriers to intertypic or intratypic reassortment.

The Oropouche M-segment minigenome resulted in an interesting phenotype. Plus strand RNA accumulation was evident by amplicon sequencing and ss-RT-qPCR, suggesting the minigenome was compatible with Kairi virus L+N proteins. However, Oropouche M-segment minigenome did not express any nanoluciferase protein,

suggesting it was not compatible with Kairi virus L+N proteins. Together, this phenotype suggests that the Oropouche M-segment minigenome was successfully replicated, but not transcribed by Kairi virus replication machinery. Upon further investigation, we realized that the nucleotide at position 9 relative to the 5' end of the genome was incorrect in the GenBank reference sequence (NC_005775.1). An 'A' base at this position of the genome is necessary for successful transcription [217], and so the lack of transcription was not surprising. Fortunately, it does provide evidence that our minigenome melee system can distinguish between replication and transcription compatibility.

Ideally, the minigenome melee system enables the quantification of replication and transcription products by measuring the number of RNAs originating from the plus strand (replication and transcription products) and minus strand (replication products). However, we are unable to distinguish between replication and transcription products because of the high number of minus strand RNA inherent in the *in vitro* transcribed minigenome library. To mitigate this, future experiments are aimed at developing an isolation protocol that would mitigate the high amount of background from the *in vitro* transcribed RNA. One such technique is to use a cap-specific antibody to pull-down transcription products (plus strand) and reserve the eluate that contains replication products (plus and minus strand) and *in vitro* transcribed RNA (minus strand). These experiments are ongoing and would further enhance the power of the minigenome melee system.

The minigenome melee system can be used to study reassortment potential for any segmented virus. The effects of reassortment have clearly resulted in significant human health impacts and agricultural losses. The frequent reassortment of Influenza virus, a segmented RNA virus, has resulted in significant health burdens and economic losses globally. Bluetongue virus, another segmented RNA virus, frequently reassorts and causes significant disease in ruminants resulting in significant agricultural losses. We believe that our minigenome melee system will improve research efforts to understand reassortment potential within segmented viruses and ultimately aid in discoveries that support outbreak preparedness.

Reassortment of RNA viruses results in significant economic and health burdens. To aid in outbreak preparedness, we've developed a novel minigenome melee system that builds upon traditional minigenomes to enable the investigation of molecular compatibility between viruses in high-throughput. Here, we've shown proof-of-concept using the orthobunyavirus genus as a prototype. Using the minigenome melees, we've shown that Kairi virus has the ability to function on a wide range of M-segments within the orthobunyavirus genus. This suggests that this aspect of molecular compatibility is not a significant barrier to reassortment. Ultimately, we present a novel system that will aid in understanding reassortment potential between any segmented virus.

4.4 Materials and Methods

4.4.1 Cells

BSR-T7/5 cells (golden hamster cells stably expressing T7 polymerase) were grown in GMEM media supplemented with 10% FBS, 0.5% Pen/Strep, 2% MEM amino acids,

and 1% tryptose phosphate broth. To select for T7 expressing cells, cultures were subjected to 1mg/mL G418 selection prior to plating for experiments.

4.4.2 Plasmids

To generate T7-driven helper plasmids, the viral coding region for Kairi virus L and S segments were amplified in multiple fragments and then cloned into the pTM1 backbone using NEB Builder/Gibson Assembly. A list of primers used to clone the viral coding region is provided (**Supplemental Table 4.1**). Colonies were screened by restriction digest and validated using Sanger sequencing. Helper plasmids used for this study are: 1) pTM1-Kairi-L and 2) pTM1-Kairi-S.

Additional plasmids were used for various conditions. Promega's pGL4.53[luc2/PGK] plasmid (PN: E5011) which expresses firefly luciferase was used for normalization in nanoluciferase assays. An empty vector (pMDS 511 = pTrc99) was used when pTM1-Kairi-L was not included to normalize the amounts of plasmid added to each transfection.. To visualize transfection efficiency, pMDS_710 (GFP-expressing plasmid) was transfected.

4.4.3 Barcoded Minigenomes

4.4.3.1 Construction of barcoded minigenomes

Barcoded minigenomes were designed using Geneious Prime software, version 2020.0.3. Specifically, the negative sense orientation of the nanoluciferase gene was flanked by barcodes b1/b2, and followed by the conserved primer binding sites P1/P2 (**Figure 4.1A**). The viral 3' UTR, in the negative sense, was upstream of P1/b1 and the viral 5' UTR, in the negative sense, was downstream of P2/b2. Finally, the T7 promoter

sequence was added upstream of the viral 3' UTR and the hammerhead ribozyme sequence was added downstream of the 5' UTR. GenBank files for these sequence constructs are available (*https://github.com/mllayton/Dissertation/blob/main/Chapter%204/gblocks_dissertation.geneious*).

To clone the constructs into the TVT7R plasmid, gBlocks (IDT) were cloned into TVT7R using the NEB Builder HiFi DNA Assembly kit. TVT7R was linearized using MDS 1626/1262 followed by a DPN1 treatment to remove remaining template. Reactions were assembled on ice and consisted of a 2:1 molar ratio of minigenome PCR to TVT7R linear plasmid in a 10μL reaction volume containing 5μL of NEB Builder HiFi DNA assembly master mix. Reactions were incubated at 50˚C for 15 minutes with the lid off. Cloning reactions were transformed into chemically competent DH5alpha cells following standard protocol with 1μL of cloning reaction. Transformed cells were streaked onto LB plates containing carbenicillin and incubated at 37˚C overnight.

To screen colonies, overnight miniprep cultures containing 3 ml of LB and 3μl of carbenicillin (100mg/mL) were incubated at 37˚C overnight in a shaking incubator at 250rpm. DNA was extracted using Zymo's Zyppy Plasmid Miniprep Kit, according to manufacturer's protocol. Samples were screened by restriction digest and/or PCR (MDS_886 and MDS_1650). Candidate samples were then Sanger sequenced for validation. Midipreps were made from one successful candidate colony for each minigenome.

4.4.3.2 In vitro transcription of barcoded minigenomes

PCR was performed using Q5 polymerase (NEB). PCR amplification was performed in a 100μl volume with the following components: 1X Q5 reaction buffer, 10mM dNTPs, 10μM MDS 1622, 10μM MDS 1623, Q5 HiFi DNA polymerase (1U), 500ng of plasmid. Reactions underwent the following thermal-cycling conditions: 98˚C for 2 minutes, followed by 25 rounds of 98˚C for 30 seconds, 55˚C for one minute and 30 seconds, and 72˚C for 3 minutes, followed by a final extension step at 72˚C for 5 minutes and a 4˚C infinite hold. Amplified PCR products were run on a 1.1% agarose gel with ethidium bromide, size selected and purified using the Zymo Gel DNA Recovery Kit according to manufacturer's protocol. Purified PCR product was quantified using the Nanodrop.

Barcoded minigenomes were *in vitro* transcribed using T7 polymerase (NEB). Reactions were performed in a 100μl volume with the following components: 500ng of PCR product, 1X reaction buffer, NTP mixture (2mM each NTP), 1U/μL RNase inhibitor murine, 5mM fresh DTT, and 250U T7 polymerase. Reactions were incubated at 37˚C for 8.5 hours. To remove DNA, samples were treated with 5U DNaseI (NEB) in 1X reaction buffer and incubated at 37˚C for 10 minutes.

Samples were purified using a lithium chloride (LiCl) precipitation. Samples were incubated in a 2.5M LiCl solution overnight at -20˚C. RNA was pelleted by centrifugation at >=12,000 x g for 20 minutes at 4˚C. Supernatant was discarded and the pellet washed in 500μl of 75% ethanol, followed by centrifugation at >=7500 x g for 15 minutes at 4˚C. Supernatant was removed and the pellet resuspended in 25μl of 1X TE. RNA was stored on at -20˚C. and the concentration and quality determined by

Nanodrop. RNA size was determined using Agilent's RNA High Sensitivity screen tape (**Supplemental Figure 4.1**).

4.4.3.3 Validation of in vitro transcribed RNA

Concentration, purity, and size were determined for the purified *in vitro* transcribed RNAs. Concentration and purity were determined using Nanodrop. The size of RNAs were determined using Agilent's RNA High Sensitivity screen tape (**tapestation traces provided in Supplemental Figure 4.1**).

4.4.3.4 Making the barcoded minigenome library

Purified *in vitro* transcribed minigenome RNAs were pooled to make the barcoded minigenome library. Minigenomes were added in equal concentrations (determined by Qubit) for equal representation in the minigenome library. The barcoded minigenome library contained a total of 10 minigenomes.

4.4.4 Cell Culture Transfections

4.4.4.1 Individual minigenome transfections

BSR T7/5 cells were plated in 6 well plates with 200,000 cells/well in 3ml of complete GMEM media. Cells were incubated at 37˚C for 24 hours before being transfected with plasmid mixtures. One plate was dedicated to each minigenome. Three of the 6 wells were transfected with pTM1-Kairi-L and pTM1-Kairi-S and the other three wells were transfected with pTM1-Kairi-S only to control for background expression. Cells were transfected with 650ng of pTM1-Kairi-L and 325ng of pTM1-Kairi-S for dually-transfected wells. For wells lacking pTM1-Kairi-L, pMDS-511 was transfected to ensure equal mass. To normalize nanoluciferase expression, 25ng of the firefly expressing plasmid (pMDS-120) was transfected. To visualize transfection efficiency,

25ng of pMDS-710 (GFP) was transfected. Transfections were made using 3μl of TransIT-LT1 reagent (MirusBio) per well. Plates were incubated at 37˚C for 24 hours.

After a 24-hour incubation, cells were transfected with *in vitro* transcribed minigenome RNA– one minigenome per well. Transfection mixtures contained 500 ng of *in vitro* transcribed RNA, 100μL serum-free MEM, and 3μl TransIT-X2 reagent (MirusBio). Mixtures were incubated for 2-5 minutes and then added drop-wise to the wells. Cells were incubated at 37˚C for 24 hours before being harvested for nano-luciferase assays.

4.4.4.2 Minigenome Melee transfections

BSR T7/5 cells were plated in 6 well plates with 200,000 cells per well. Cells were incubated at 37˚C for 24 hours and then transfected with pTM1-Kairi-L and pTM1-Kairi-S or only pTM1-Kairi-S plasmids. Transfection mixtures contained 650ng of pTM1-Kairi-L and 325ng of pTM1-Kairi-S for dually-transfected wells. For wells lacking pTM1-Kairi-L, pMDS-511 was transfected to ensure equal mass. To normalize nanoluciferase expression, 25ng of the firefly expressing plasmid (pMDS-120) was transfected. To visualize transfection efficiency, 25ng of pMDS-710 (GFP) was transfected. Transfections were made using 3μl of TransIT-LT1 reagent (MirusBio) per well. Plates were incubated at 37˚C for 24 hours. Transfection mixtures were incubated at room temperature for 15 minutes and then added dropwise to each well. Cells were incubated at 37˚C for 24 hours and then transfected with the minigenome library.

Media was refreshed prior to minigenome library transfection. Minigenome library transfection mixes contained 100μl of serum-free MEM, 500ng of the minigenome

library, and 3μl of TransIT-X2 transfection reagent (MirusBio). Transfection mixes were incubated at room temperature for 2-5 minutes and then added dropwise to the wells. Plates were incubated at 37˚C until harvested at 24, 48, and 72 hours post-minigenome library transfection.

4.4.5 Harvesting cells

4.4.5.1 Individual transfections

Twenty-four hours post-minigenome RNA transfection, cells were harvested to measure levels of nano-luciferase expression. Cell culture media was removed and cells were washed once with 500μl of 1X PBS. To lyse the cells, 500μl of 1x passive lysis buffer (Promega) was added to each well. Plates were placed on a rocking platform to gently agitate the cells for 15 minutes at room temperature. Cell lysates were transferred to 1.5ml microcentrifuge tubes and stored at -20˚C.

4.4.5.2 Minigenome Melees

Cells were harvested for nanoluciferase expression and RNA extraction. First, cell culture media was removed from all wells and cells were washed once with 500μL of 1X PBS. Cells were then trypsinized in 250μl of 0.25% Trypsin and incubated at 37˚C for 2 minutes or until cells were no longer adherent. Cells were resuspended in 250μl of complete-GMEM media and transferred to a 1.5ml microcentrifuge tube. Cells were pelleted for 5 minutes at 1,000 x g, supernatant removed, and cell pellet washed in 200μL of 1X PBS. This step was repeated twice. After the last 1X PBS wash, cells were resuspended in 200μL of 1X PBS. For RNA extraction, 160μL of cells in 1X PBS were transferred to a new tube. The remaining 40μL of cells in 1x PBS were transferred to a new tube for nanoluciferase expression assays. Cells were then pelleted by

centrifugation at 1,000 x g for 5 minutes. To the tube containing 80% of the cells, 1ml of TRIzol was added and cells resuspended. To the tube containing 20% of the cells, 90μl of 1X passive lysis buffer was added and cells resuspended. Samples were stored at -80˚C until ready for further processing. Cells placed in TRIzol were used for RNA extraction and downstream amplicon sequencing and strand-specific RT-qPCR. Cells placed in 1X passive lysis buffer were used to measure nanoluciferase expression using Promega's Nano-Glo Dual-Luciferase Reporter Assay System (data not shown).

4.4.6 Nano-luciferase assays

Nanoluciferase expression was measured using Promega's Nano-Glo Dual-Luciferase Reporter Assay System (Promega: N1610). Cell lysates and reagents were allowed to equilibrate to room temperature. To measure firefly luminescence, 80μl of cell lysates in 1X passive lysis buffer were added to a white 96-well plate followed by 80μl of ONE-Glo Ex Reagent. Cells were incubated at room temperature for at least three minutes on an orbital shaker (300-600rpm). Firefly luminescence was measured using the Enspire plate reader (Perkin-Elmer) using settings suggested by Promega's Nano-Glo Dual-Luciferase Reporter Assay System manual. Next, nanoluciferase expression was measured by adding 80μl of NanoDLR Stop&Glo reagent to the cells and mixing well. Plates were placed on an orbital shaker (300-600 rpm) for at least 10 minutes. Then, levels of nanoluciferase expression were measured using the plate reader and settings suggested by the manufacturer's manual. Expression of the nanoluciferase gene is expressed as a fold-change of nanoluciferase RLU over firefly RLU.

4.4.7 RNA Extraction

Cells stored in TRIzol were processed for RNA extraction. Samples were thawed and allowed to equilibrate to room temperature. To each tube, 200μL of chloroform was added, shaken by hand for 15 seconds, and then incubated at room temperature for 2 minutes. Samples were spun at 12,000 x g for 10 minutes for phase separation. The RNA layer was removed and placed into a fresh tube. RNA from the aqueous layer was purified using a standardized protocol for on-column purification and DNase treatment using Zymo's CC-5 RNA columns [218]. RNA was stored at -80˚C.

4.4.8 Amplicon library preparation and sequencing

We developed a strand-specific amplicon-based library preparation protocol. Cellular RNA (1000ng) was reverse transcribed using MDS-1820 and MDS-1821 primers (1μM each) which selectively bind to the P1i5 and P2i5 sequences, respectively (**Figure 4.2A**) and incubated at 65˚C for 1 minute and then immediately placed on ice. Reverse transcription was performed in a 12μL volume with the following components: 1X Superscript III buffer (Thermo), 5mM DTT, 1mM dNTP mixture, and 0.5μL Superscript III reverse transcriptase. Reverse transcription reactions were incubated at 55˚C for 1 hour, heat inactivated at 70˚C for 15 minutes, and then cooled to 4˚C. Using ampure RNA beads, the reactions were purified using a 1.8X ratio of beads:RNA. RNA was eluted in 15μl of nuclease-free water. Second strand synthesis was performed in a 25μL volume with the following components: 0.15μL of RNaseH (NEB), 1x Q5 buffer, 200μm dNTPs, 0.5μM MDS-1822, 0.5μM MDS-1823, 15μL of purified RT product, and 0.25μL Q5 HiFi DNA polymerase (NEB). Reactions were incubated at 37˚C for 15 minutes to degrade RNA:DNA hybrids, followed by denaturation at 95˚C for 2 minutes

and primer extension at 70˚C for 10 minutes, and a 4˚C hold. Samples were stored at -20˚C before undergoing another 1.8X ampure DNA bead cleanup. DNA was eluted in 15μL of nuclease free water. Using PCR, Illumina adapters were added to the amplicons. Reactions were performed in 25μL and included: 5.8μL of the purified amplicon, 1X Kapa Library Amplification mix (KK2612 or KK2702), 0.33μM of MDS-143/MDS-445 primer mix (5μM each), and 0.02μM Nextera indexed oligos. Adapter ligation was performed with the following thermocycling conditions: initial denaturation at 98˚C for 30 seconds, 15 cycles of [98˚C for 15 seconds, 63˚C for 30 seconds, and 72˚C for 3 minutes] and a 4˚C hold. Concentration was determined using Qubit High Sensitivity DNA kit and size was determined using Agilent's DNA High Sensitivity screentape. The size was as expected, but the yield was low. Therefore, we performed an additional 0.6X ampure bead cleanup to clean and concentrate the libraries. Libraries were eluted in 15μL of nuclease free water. Concentration and size were determined for final libraries. Final library sizes ranged from 730-800 base pairs.

Libraries were sequenced on the MiSeq using a v2 300 cycle nano kit; 2 x 151 reads. Fastq reads were quality filtered and collapsed for PCR duplicates using FastQC and cutadapt. A *key* containing the sequence information for the 'tag type' (tagID), 'tag_seq' (sequence of tag), 'bc_id' (unique barcode ID), 'bc_type' (b1/b2), 'seq' (sequence of barcode), 'mg_id' (minigenome ID), and 'mg_description'. The tag sequences were extracted from the fastq files using the script (*count_all_tags*) available on GitHub. The number of reads corresponding to plus strand and minus strand RNAs were counted using the custom script (*count_tags*) available on GitHub. **Table 4.1**

shows how reads were classified as originating from either the plus or minus strand: the orientation of the tag sequence comprised of P1/P2 and b1/b2 indicates which strand the sequence originated from. The custom script outputs a '*all_tag_counts.txt*' file containing the number of reads for each tagID and each minigenome. This 'all_tag_counts.txt' file is then processed in R using the script '*script_analyze_pilot3_sequencing_data.R*' to plot the number of plus strand reads (replication and transcription products) for each minigenome under L+N or N-only conditions.

Table 4.1. Scheme for differentiating plus and minus strand reads from NGS.

Read	Tag ID	Minus strand	Plus strand
Read 1	P1b1		X
Read 1	P2b2 reverse complement	X	
Read 2	P1b1	X	
Read 2	P2b2 reverse complement		X

4.4.9 Strand-specific reverse transcription quantitative PCR (ss-RT-qPCR)

We developed a strand-specific reverse transcription quantitative PCR (ss-RT-qPCR) to validate the amplicon sequencing results. This technique was previously developed for o'nyong-nyong virus [214] and we've adapted this protocol for minigenome melees. Total RNA is selectively reverse transcribed to preserve stranded-ness. Prior to reverse transcription, a strand-specific primer is incubated with the cellular RNA. The plus strand primer is MDS-1954 and the minus strand primer is MDS-1955 (**Figure 4.2B**). Both primers bind within the nanoluciferase gene so that all minigenome products are detected. Annealing of the strand-specific primer is performed in a 6.5μL reaction

volume with the following components: 0.125μM of the strand-specific primer, 0.5mM dNTP mix (10mM each), and 500ng of cellular RNA. RNAs are then reverse transcribed using SuperScript IV (Thermo). Reverse transcription reactions contain the following components in a 10μL reaction: 1X SuperScript IV buffer, 5mM DTT, 0.5μL Ribonuclease inhibitor, and 100U of SuperScript IV reverse transcriptase. Reactions were incubated at 50˚C for 10 minutes. Excess primer is degraded using 0.5U of Exonucelease I (NEB) in a final reaction volume of 11μL. The resulting cDNA was diluted 1:10 in a final volume of 100μL and stored at -20˚C. Next, qPCR is used to determine which minigenomes are present in the sample. This is accomplished with a tag-specific primer (MDS-1956) that binds the conserved tag sequence in the plus/minus strand primers and a minigenome-specific primer (**Supplemental Table 4.1**). Reactions were carried out in a 15μL volume with the following components: 1X qPCR mix (homebrew), 0.5μM of tag primer and minigenome-specific primer (3μM each), and 5μL of 1:10 diluted cDNA. Due to the high background from minus strand RNA in the *in vitro* transcribed minigenome RNA that was transfected into the cells, only plus strand RNA is reported for minigenome melees.

4.4.10 Phylogenetic analysis of the M-segment

To visualize the genetic relatedness of the M-segments chosen for minigenomes, we made a phylogenetic tree containing all reference sequences available for the M segment of orthobunyaviruses. Pairwise alignments of the glycoprotein coding region were made using Geneious Prime 2020.0.3. Also using Geneious, we created a neighbor-joining consensus tree from the pairwise alignment.

4.4.11 Pairwise alignment of minigenome UTRs

Pairwise alignments of the minigenome 5’ and 3’ UTRs were made using Geneious Prime 2020.0.3. To determine percent nucleotide identity, BLAST nucleotide was used with default settings.

Chapter 5: DISCUSSION

Together, this body of work is a substantial contribution to the field of bunyavirus research. Detailed discussions have already been provided within each chapter. It is my hope that this work will, in some way, highlight the importance of strategic viral surveillance and research into the molecular mechanisms underlying reassortment potential. I'd like to conclude with a brief discussion on the importance of combining virus surveillance with wet-lab research techniques and highlight some finer points within bunyavirus research.

Bunyaviruses will continue to circulate, and novel strains are likely to emerge. Every battle necessitates a battle plan, a strategy to ensure victory with the fewest number of lives lost. Vaccine development for bunyaviruses is a worthy strategy, however, the broad genetic diversity and rapid evolution of bunyaviruses complicates the development of a vaccine. In addition to vaccine development, increased viral surveillance and wet-lab techniques are warranted. Viral surveillance can provide an early warning system for the emergence or re-emergence of pathogenic bunyaviruses. Wet-lab techniques can continue to investigate the molecular underpinnings of bunyaviruses such as replication, transcription, packaging, vector capacity, and vector-host immune responses. The combination of viral surveillance and research utilizes traditional and modern techniques.

Before the advent of next-generation sequencing, virus hunters went out looking for viruses across the globe. Characterization of these viruses was based on traditional

techniques such as serology. The advent of next-generation sequencing bolstered our ability to characterize the genomes of viruses and our knowledge of the RNA virosphere is rapidly expanding. Unfortunately, the rise of next-generation sequencing has left traditional techniques and virus surveillance in its wake, resulting in a deficit for the field [219]. Here, we've shown the value in utilizing surveillance data to pinpoint geographic regions and vectors with an increased potential to host a reassortant bunyavirus. By combining epidemiological data with wet-lab techniques we can strengthen our ability to identify and respond to bunyavirus outbreaks. For example, Iroegbu et al. demonstrated the ability of Bunyamwera virus, Maguari virus, and Batai virus (*Peribunyaviridae*: Bunyamwera serogroup) to reassort *in vitro* and predict that their geographic isolation prevents reassortment in nature[201]. Our analysis in chapter 3 provides evidence that these viruses are no longer isolated geographically (**Supplemental Table 3.1**). Bunyamwera virus and Maguari virus have both been isolated from Argentina and Brazil. Bunyamwera virus and Batai virus have both been isolated from Germany, Kenya, and Rwanda. The barrier to reassortment between these viruses may simply be a shared vector-host range. From our analysis, these viruses have not been detected in the same vector species. Therefore, it may be wise to increase surveillance efforts within these countries.

The serogroup classification of orthobunyaviruses is particularly problematic when trying to determine patterns of reassortment that might aid in predicting reassortment potential. Throughout this dissertation, we've discussed and investigated intertypic and intratypic reassortment. However, it is difficult to infer the extent to which

either has occurred using the serogroup classification. Because there is frequent reassortment among orthobunyaviruses, the phylogenies for each segment are quite different. To more clearly explain, virus A may be closely related to virus B based on the L and S segments, but the M segment is actually more closely related to virus C. And in fact, when you begin to really tease apart the tanglegrams provided in chapter 2, there is evidence of between serogroup reassortment (Capim and Gamboa serogroups, Anopheles A and Anopheles B serogroups). We suggest a restructuring of orthobunyavirus classification may aid in better understanding the reassortment potential between orthobunyaviruses, ultimately aiding in more strategic surveillance and research efforts.

Finally, I leave you with a call for cohesive surveillance and research efforts to aid in our understanding of bunyaviruses and our ability to respond to an outbreak. Because there is not a question of if an outbreak will occur, it is a question of when, and if we will be prepared.

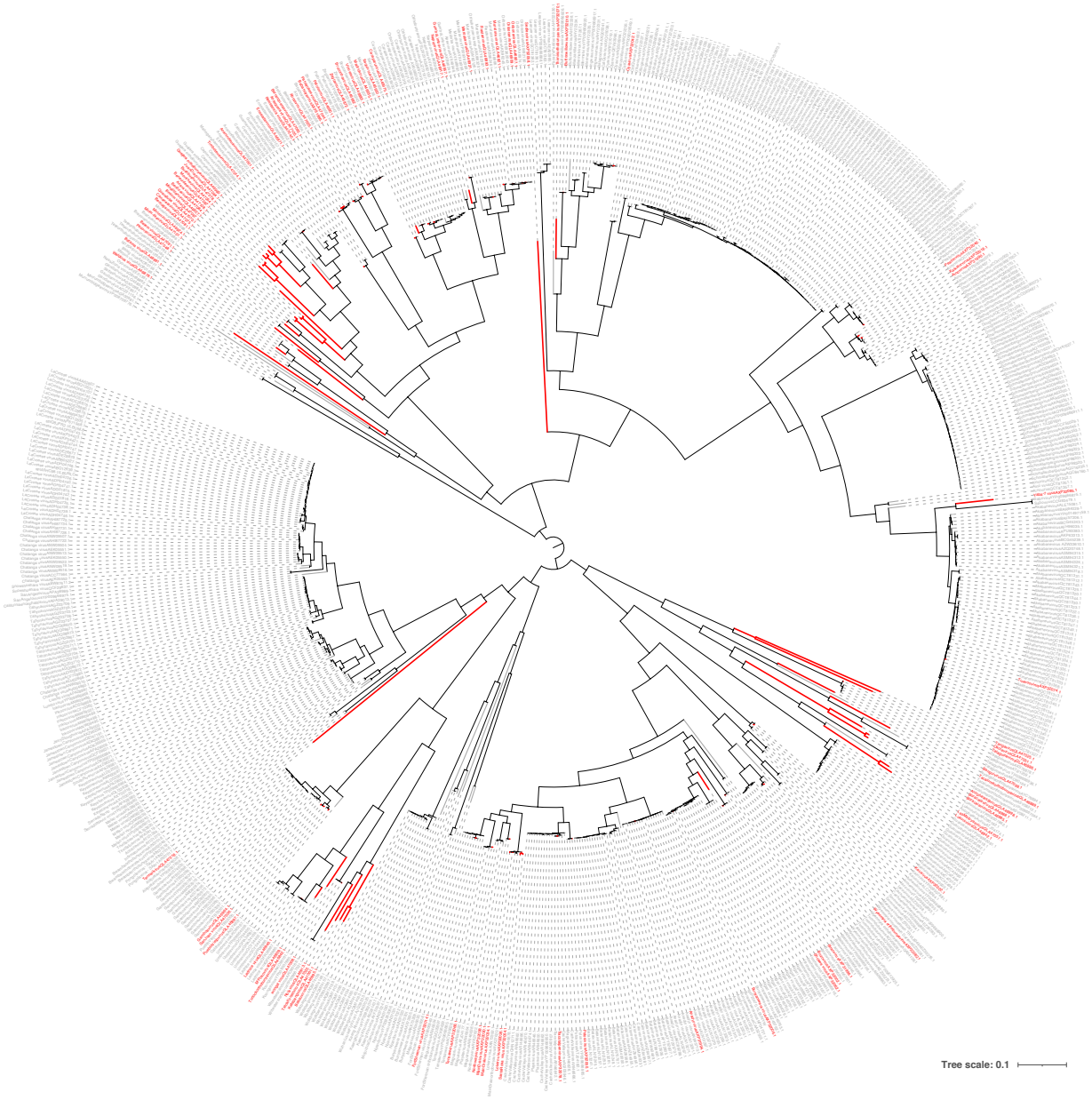

Supplemental Figure 2.2. Tree containing all available *Orthobunyavirus* sequences. All complete L protein sequences annotated under the *Orthobunyavirus* genus in the NCBI Taxonomy database were downloaded and used to infer a maximum likelihood phylogeny. Sequences that we generated in the course of this study are indicated in red. Tree is midpoint rooted. Scale bar indicates substitutions per site.

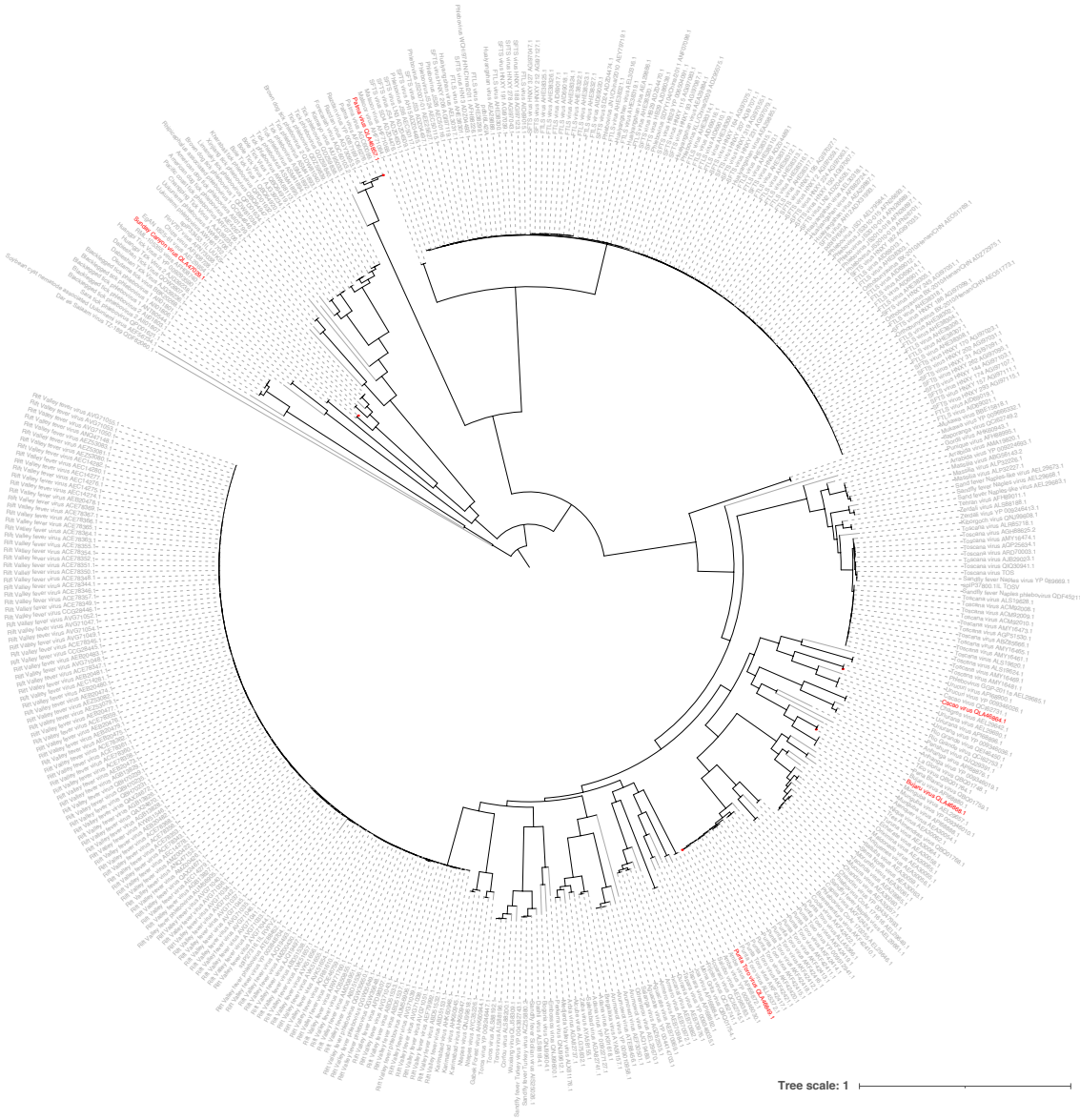

Supplemental Figure 2.3. Tree containing all available *Phlebovirus* sequences. All complete L protein sequences annotated under the *Phlebovirus* genus in the NCBI Taxonomy database were downloaded and used to infer a maximum likelihood phylogeny. Sequences that we generated in the course of this study are indicated in red. Tree is midpoint rooted. Scale bar indicates substitutions per site.

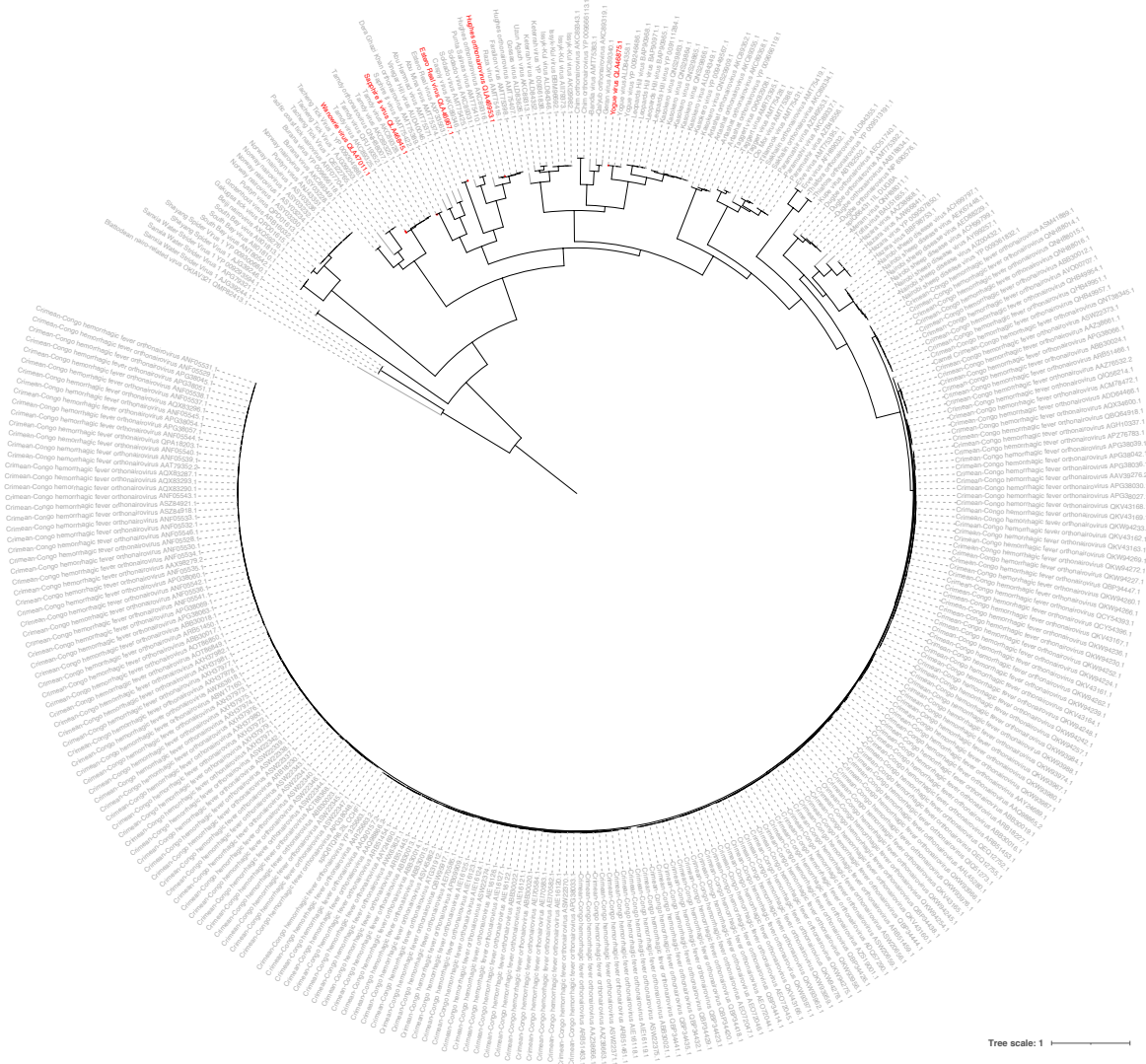

Supplemental Figure 2.4. Tree containing all available *Nairoviridae* sequences. All complete L protein sequences annotated under the *Nairoviridae* family in the NCBI Taxonomy database were downloaded and used to infer a maximum likelihood phylogeny. Sequences that we generated in the course of this study are indicated in red. Tree is midpoint rooted. Scale bar indicates substitutions per site.

Supplemental Figure 2.5. L segment phylogeny for viruses in *Peribunyaviridae: Pacuvirus*. The virus sequences we generated in this study are shown in black.

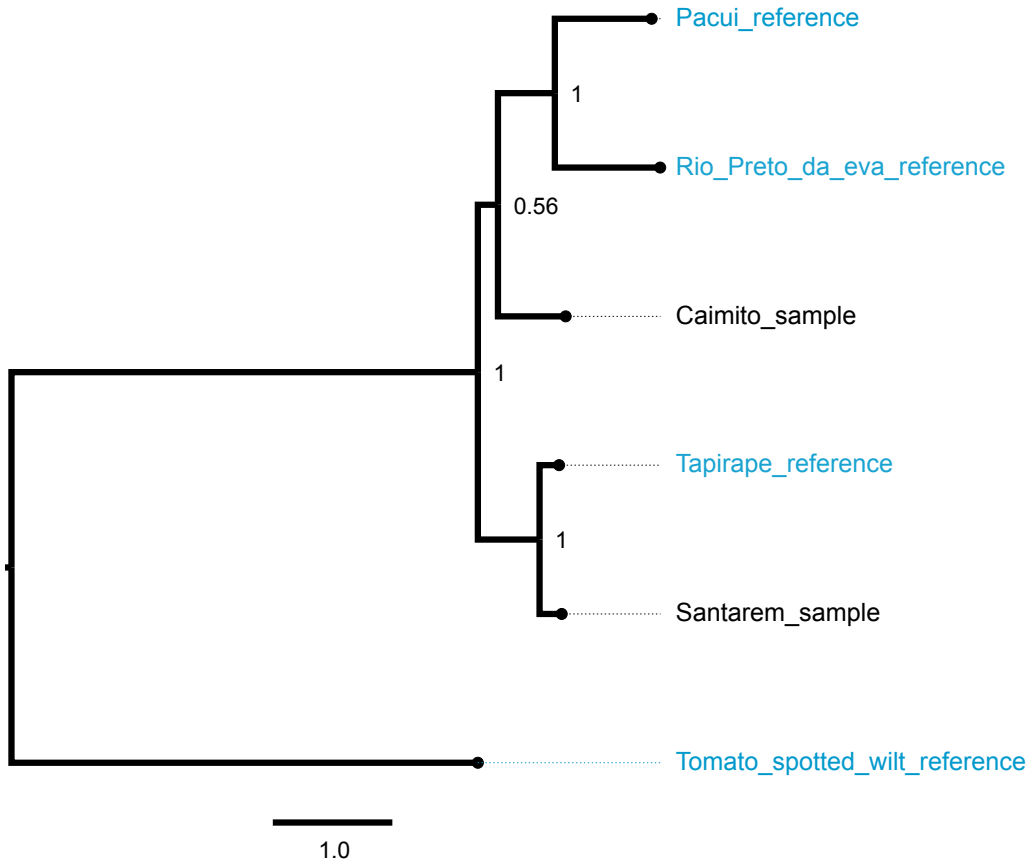

Supplemental Table 3.1. List of virus detections by country	serogroup	number
Argentina		
Las Maloyas virus	Anopheles A	1
Bunyamwera virus	Bunyamwera	12
Laguna Larga virus	Bunyamwera	1
Maguari virus	Bunyamwera	1
Calchaqui virus	Gamboa	1
Australia		
Koongol virus	Koongol	1
wongal virus	Koongol	1
Buffalo Creek virus	Mapputta	1
Gan Gan virus	Mapputta	13
Mapputta virus	Mapputta	1
Maprik virus	Mapputta	1
Aino virus	Simbu	8
Akabane virus	Simbu	40
Douglas virus	Simbu	3
Facey's Paddock virus	Simbu	1
Peaton virus	Simbu	5
Thimiri virus	Simbu	2
Tinaroo virus	Simbu	3
Leanyer virus	Ungrouped	4
Murrumbidgee virus	Ungrouped	1
Salt ash virus	Ungrouped	1
Austria		
Batai virus	Bunyamwera	1
Tahyna virus	California	4
Belgium		
Schmallenberg virus	Simbu	60
Bolivia		
Guaroa virus	California	4
Caraparu virus	Group C	1
Brazil		
Tacaiuma virus	Anopheles A	6
Boraceia virus	Anopheles B	2
Bunyamwera virus	Bunyamwera	1
Fort Sherman virus	Bunyamwera	1
Kairi virus	Bunyamwera	1
Macaua virus	Bunyamwera	1

Supplemental Table 3.1. List of virus detections by country	serogroup	number
Maguari virus	Bunyamwera	1
Sororoca virus	Bunyamwera	1
Guaroa virus	California	1
Serra do Navio virus	California	1
Acara virus	Capim	1
Benevides virus	Capim	1
Capim virus	Capim	2
Guajara virus	Capim	1
Gamboa virus	Gamboa	4
Apeu virus	Group C	2
Bruconha virus	Group C	2
Caraparu virus	Group C	2
Itaqui virus	Group C	2
Madrid virus	Group C	1
Marituba virus	Group C	2
Murutucu virus	Group C	2
Nepuyo virus	Group C	1
Oriboca virus	Group C	2
Ananindeua virus	Guama	3
Bertioga virus	Guama	1
Cananeia virus	Guama	1
Catu virus	Guama	1
Guama virus	Guama	1
Guaratuba virus	Guama	1
Itimirim virus	Guama	1
Mirim virus	Guama	2
Moju virus	Guama	1
Timboteua virus	Guama	1
Jatobal virus	Simbu	1
Oropouche like virus	Simbu	2
Oropouche virus	Simbu	125
Perdoes virus	Simbu	2
Utinga virus	Simbu	1
Enseada virus	Ungrouped	2
Mojui dos Campos virus	Ungrouped	1
Triniti virus	Ungrouped	2
Anhembi virus	Wyeomyia	1
Cachoeira Porteira virus	Wyeomyia	1
Iaco virus	Wyeomyia	1
Taiassui virus	Wyeomyia	1

Supplemental Table 3.1. List of virus detections by country	serogroup	number
Tucunduba virus	Wyeomyia	4
Cambodia		
Kaeng Khoi virus	Bunyamwera	1
Cameroon		
Nyando virus	Nyando	1
Canada		
Cache Valley virus	Bunyamwera	2
Jamestown Canyon virus	California	1
Snowshoe hare virus	California	1
Central African Republic		
Birao virus	Bunyamwera	2
Bozo virus	Bunyamwera	2
Bunyamwera virus	Bunyamwera	2
Ilesha virus	Bunyamwera	2
Nyando virus	Nyando	1
Botambi virus	Olifantsvlei	1
Ingwavuma virus	Simbu	1
Nola virus	Simbu	1
Batama virus	Tete	1
M'Poko virus	Turlock	2
Tataguine virus	Ungrouped	1
China		
Batai virus	Bunyamwera	4
Ebinur lake virus	Bunyamwera	1
Kaeng Khoi virus	Bunyamwera	5
Tahyna virus	California	9
Akabane virus	Simbu	15
Cat Que virus	Simbu	1
Manzanilla virus	Simbu	1
Oya virus	Simbu	5
Abbeylake	Ungrouped	1
Diaphorina citri bunyavirus	Ungrouped	3
Wuhan Louse Fly Virus 1	Ungrouped	1
Colombia		
Anopheles A virus	Anopheles A	1
Anopheles B virus	Anopheles B	1
Lukuni virus	Bunyamwera	1
Maguari virus	Bunyamwera	1

Supplemental Table 3.1. List of virus detections by country	serogroup	number
Guaroa virus	California	1
Oropouche virus	Simbu	4
Wyeomyia virus	Wyeomyia	2
Croatia		
Calovo virus	Bunyamwera	1
Czech Republic		
Batai virus	Bunyamwera	1
Calovo virus	Bunyamwera	1
Tahyna virus	California	22
Sedlec virus	Simbu	2
Lednice virus	Turlock	4
Ecuador		
Playas virus	Bunyamwera	3
Guajara virus	Capim	1
Gamboa virus	Gamboa	1
Pueblo Viejo virus	Gamboa	2
Vinces virus	Group C	1
Mirim-like virus	Guama	1
Abras virus	Patois	1
Babahoya virus	Patois	1
Iquitos virus	Simbu	1
Oropouche virus	Simbu	6
Egypt		
Bahig virus	Tete	2
Matruh virus	Tete	1
Ethiopia		
Nyando virus	Nyando	1
Finland		
Chatanga virus	California	5
Inkoo virus	California	1
France		
Tahyna virus	California	1
Umbre virus	Turlock	2
French Guiana		
Oropouche virus	Simbu	1
Gambia		
Tataguine virus	Ungrouped	1

Supplemental Table 3.1. List of virus detections by country	serogroup	number
Germany		
Batai virus	Bunyamwera	4
Bunyamwera virus	Bunyamwera	1
Schmallenberg virus	Simbu	39
Great Britain		
Cache Valley virus	Bunyamwera	1
Kairi virus	Bunyamwera	1
Schmallenberg virus	Simbu	31
Guinea		
Ngari virus	Bunyamwera	6
Haiti		
Melao virus	California	4
Oropouche virus	Simbu	1
Honduras		
Nepuyo virus	Group C	1
Hungary		
Schmallenberg virus	Simbu	7
India		
Batai virus	Bunyamwera	8
Balagodu virus	Simbu	1
Cat Que virus	Simbu	1
Ingwavuma virus	Simbu	2
Kaikalur virus	Simbu	1
Oya virus	Simbu	1
Thimiri virus	Simbu	1
Umbre virus	Turlock	12
I612045 virus	Ungrouped	1
Indonesia		
Akabane virus	Simbu	1
Israel		
Akabane virus	Simbu	22
Peaton virus	Simbu	9
Sango virus	Simbu	3
Sathuperi virus	Simbu	1
Schmallenberg virus	Simbu	12
Shuni virus	Simbu	41
Ness Ziona virus	Ungrouped	1

Supplemental Table 3.1. List of virus detections by country	serogroup	number
Italy		
Batai virus	Bunyamwera	2
Tahyna virus	California	15
Botrytis cinerea orthobunya-like virus 1	Ungrouped	1
Japan		
Batai virus	Bunyamwera	2
Aino virus	Simbu	38
Akabane virus	Simbu	76
Peaton virus	Simbu	6
Sathuperi virus	Simbu	4
Shamonda virus	Simbu	5
Taniyama virus	Ungrouped	2
Kenya		
Batai virus	Bunyamwera	2
Bunyamwera virus	Bunyamwera	15
Ngari virus	Bunyamwera	12
Pongola virus	Bwamba	5
Pongola virus - SAAr1	Bwamba	1
Nyando virus	Nyando	2
Akabane virus	Simbu	1
Tataguine virus	Ungrouped	1
orthobunyavirus sp.	Ungrouped	3
Malaysia		
Bakau virus	Bakau	1
Ketapang virus	Bakau	1
Telok Forest virus	Bakau	1
Batai virus	Bunyamwera	3
Kedah fatal kidney syndrome virus	Turlock	15
Mauritania		
Bunyamwera virus	Bunyamwera	1
Ngari virus	Bunyamwera	3
Mexico		
Cache Valley virus	Bunyamwera	18
Cholul virus	Bunyamwera	1
Kairi virus	Bunyamwera	1
Santa Rosa virus	Bunyamwera	1
Tlacotalpan virus	Bunyamwera	2
South River virus	California	1

Supplemental Table 3.1. List of virus detections by country	serogroup	number
Minatitlan virus	Minatitlan	1
Patois virus	Patois	2
Shark River virus	Patois	1
Wyeomyia virus	Wyeomyia	1
Mozambique		
Lumbo virus	California	1
Netherlands		
Schmallenberg virus	Simbu	3
Nigeria		
Ilesha virus	Bunyamwera	1
Oyo virus	Simbu	1
Sango virus	Simbu	1
Shamonda virus	Simbu	1
Yaba-7 virus	Simbu	1
Tataguine virus	Ungrouped	2
Norway		
Schmallenberg virus	Simbu	1
Panama		
Fort Sherman virus	Bunyamwera	2
Juan Diaz virus	Capim	1
Alajuela virus	Gamboa	1
Gamboa virus	Gamboa	9
Madrid virus	Group C	2
Patois virus	Patois	1
Zegla virus	Patois	2
Oropouche virus	Simbu	4
Utive virus	Ungrouped	1
Wyeomyia virus strain Darien	Wyeomyia	1
Peru		
Maguari virus	Bunyamwera	1
Guaroa virus	California	15
Benfica virus	Capim	1
Caraparu virus	Group C	2
Itaqui virus	Group C	1
Itaya virus	Group C	1
Marituba virus	Group C	1
Iquitos virus	Simbu	18
Madre de Dios virus	Simbu	1

Supplemental Table 3.1. List of virus detections by country	serogroup	number
Oropouche virus	Simbu	7
Bellavista virus	Ungrouped	1
FSL2923	Ungrouped	1
orthobunyavirus sp.	Ungrouped	61
Poland		
Schmallenberg virus	Simbu	18
Russia		
Anadyr virus	Bunyamwera	18
Batai virus	Bunyamwera	12
Chatanga virus	California	51
Inkoo virus	California	7
Ebinur lake virus	NA	8
Rwanda		
Batai virus	Bunyamwera	9
Bunyamwera virus	Bunyamwera	8
Senegal		
Ilesha virus	Bunyamwera	1
Ngari virus	Bunyamwera	2
Serbia		
Calovo virus	Bunyamwera	1
Slovakia		
Calovo virus	Bunyamwera	2
Tahyna virus	California	1
Somalia		
Ngari virus	Bunyamwera	1
South Africa		
Shokwe virus	Bunyamwera	1
Pongola virus - SAAr1	Bwamba	2
Olifantsvlei virus	Olifantsvlei	1
Ingwavuma virus	Simbu	1
Shuni virus	Simbu	37
Tete virus	Tete	2
Witwatersrand virus	Ungrouped	1
orthobunyavirus sp.	Ungrouped	3
South Korea		
Akabane virus	Simbu	13
Spain		

Supplemental Table 3.1. List of virus detections by country	serogroup	number
Botrytis cinerea orthobunya-like virus 1	Ungrouped	1
Sudan		
Batai virus	Bunyamwera	1
Ngari virus	Bunyamwera	2
Suriname		
Gamboa virus	Gamboa	1
Sweden		
Inkoo virus	California	1
Schmallenberg virus	Simbu	20
Switzerland		
Schmallenberg virus	Simbu	2
Taiwan		
Aino virus	Simbu	31
Akabane virus	Simbu	32
Peaton virus	Simbu	4
Thailand		
Kaeng Khoi virus	Bunyamwera	1
Trinidad and Tobago		
Kairi virus	Bunyamwera	1
Lukuni virus	Bunyamwera	1
Melao virus	California	1
Bushbush virus	Capim	1
Moriche virus	Capim	1
Nepuyo virus	Group C	1
Restan virus	Group C	1
Bimiti virus	Guama	1
Manzanilla virus	Simbu	1
Oropouche virus	Simbu	1
Triniti virus	Ungrouped	2
Wyeomyia virus strain TRVL8349	Wyeomyia	1
Turkey		
Akabane virus	Simbu	39
Schmallenberg virus	Simbu	28
USA		
Cache Valley virus	Bunyamwera	96
Lokern virus	Bunyamwera	1
Main Drain virus	Bunyamwera	4

Supplemental Table 3.1. List of virus detections by country	serogroup	number
Northway virus	Bunyamwera	2
Potosi virus	Bunyamwera	2
Tensaw virus	Bunyamwera	3
California encephalitis virus	California	2
Infirmatus virus	California	1
Jamestown Canyon virus	California	67
Jerry Slough virus	California	1
Keystone virus	California	11
La Crosse virus	California	108
San Angelo virus	California	1
Snowshoe hare virus	California	4
South River virus	California	1
Trivittatus virus	California	4
Gumbo Limbo virus	Group C	8
Mahogany hammock virus	Guama	8
Pahayokee virus	Patois	5
Shark River virus	Patois	5
Buttonwillow virus	Simbu	2
Mermet virus	Simbu	2
Weldona virus	Tete	1
Turlock virus	Turlock	1
Brazoran virus	Ungrouped	1
Centruroides sculpturatus bunyavirus	Ungrouped	1
Uganda		
Bunyamwera virus	Bunyamwera	1
Bwamba virus	Bwamba	2
Nyando virus	Nyando	1
Ntwetwe virus	Ungrouped	1
Nyangole virus	Ungrouped	1
Ukraine		
Batai virus	Bunyamwera	2
Venezuela		
Madre de Dios virus	Simbu	1
Vietnam		
Cat Que virus	Simbu	1
Oya virus	Simbu	1

Supplemental Table 3.3. Number of serogroups detected at a country-level

country	number of serogroups
Brazil	11
USA	9
Panama	8
Trinidad and Tobago	8
Central African Republic	7
Ecuador	7
Colombia	6
Peru	6
South Africa	6
Kenya	5
Mexico	5
Australia	4
China	4
Czech Republic	4
India	4
Uganda	4
Argentina	3
Italy	3
Japan	3
Malaysia	3
Nigeria	3
Austria	2
Bolivia	2
Canada	2
France	2
Germany	2
Great Britain	2
Haiti	2
Israel	2
Russia	2
Slovakia	2
Sweden	2

Belgium	1
Cambodia	1
Cameroon	1
Croatia	1
Egypt	1
Ethiopia	1
Finland	1
French Guiana	1
Gambia	1
Guinea	1
Honduras	1
Hungary	1
Indonesia	1
Mauritania	1
Mozambique	1
Netherlands	1
Norway	1
Poland	1
Rwanda	1
Senegal	1
Serbia	1
Somalia	1
South Korea	1
Spain	1
Sudan	1
Suriname	1
Switzerland	1
Taiwan	1
Thailand	1
Turkey	1
Ukraine	1
Venezuela	1
Vietnam	1

REFERENCES

1. Elliott RM. Orthobunyaviruses: recent genetic and structural insights. Nature Reviews Microbiology. 2014;12: 673–685. doi:10.1038/nrmicro3332

2. Roselló S, Díez MJ, Nuez F. Viral diseases causing the greatest economic losses to the tomato crop. I. The Tomato spotted wilt virus — a review. Scientia Horticulturae. 1996;67: 117–150. doi:10.1016/S0304-4238(96)00946-6

3. Kwaśnik M, Rożek W, Rola J. Rift Valley Fever – a Growing Threat To Humans and Animals. J Vet Res. 2021;65: 7–14. doi:10.2478/jvetres-2021-0009

4. Claine F, Coupeau D, Wiggers L, Muylkens B, Kirschvink N. Schmallenberg virus infection of ruminants: challenges and opportunities for veterinarians. Vet Med (Auckl). 2015;6: 261–272. doi:10.2147/VMRR.S83594

5. Wahid B, Altaf S, Naeem N, Ilyas N, Idrees M. Scoping Review of Crimean-Congo Hemorrhagic Fever (CCHF) Literature and Implications of Future Research. J Coll Physicians Surg Pak. 2019;29: 563–573. doi:10.29271/jcpsp.2019.06.563

6. Jiang H, Zheng X, Wang L, Du H, Wang P, Bai X. Hantavirus infection: a global zoonotic challenge. Virol Sin. 2017;32: 32–43. doi:10.1007/s12250-016-3899-x

7. Harding S, Greig J, Mascarenhas M, Young I, Waddell LA. La Crosse virus: a scoping review of the global evidence. Epidemiol Infect. 2018;147: e66. doi:10.1017/S0950268818003096

8. Elliott RM, Schmaljohn CS. Bunyaviridae. 6th ed. In: Knipe, D M, Howley, P M, editors. Fields Virology. 6th ed. Philadelphia, PA: Lippincott Williams & Wilkins; 2013. pp. 1244–1282.

9. Gould E, Pettersson J, Higgs S, Charrel R, de Lamballerie X. Emerging arboviruses: Why today? One Health. 2017;4: 1–13. doi:10.1016/j.onehlt.2017.06.001

10. Beaty BJ, Calisher CH. Bunyaviridae--natural history. Curr Top Microbiol Immunol. 1991;169: 27–78.

11. Rückert C, Ebel GD. How do virus-mosquito interactions lead to viral emergence? Trends Parasitol. 2018;34: 310–321. doi:10.1016/j.pt.2017.12.004

12. Vasconcelos PF, Travassos da Rosa AP, Rodrigues SG, Travassos da Rosa ES, Dégallier N, Travassos da Rosa JF. Inadequate management of natural ecosystem in the Brazilian Amazon region results in the emergence and reemergence of arboviruses. Cad Saude Publica. 2001;17 Suppl: 155–164. doi:10.1590/s0102-311x2001000700025

13. Leisnham PT, Juliano SA. Impacts of climate, land use, and biological invasion on the ecology of immature Aedes mosquitoes: implications for La Crosse emergence. Ecohealth. 2012;9: 217–228. doi:10.1007/s10393-012-0773-7

14. Elliott RM. Bunyaviruses and climate change. Clinical Microbiology and Infection. 2009;15: 510–517. doi:10.1111/j.1469-0691.2009.02849.x

15. Ellwanger JH, Kulmann-Leal B, Kaminski VL, Valverde-Villegas JM, Veiga ABGD, Spilki FR, et al. Beyond diversity loss and climate change: Impacts of Amazon deforestation on infectious diseases and public health. An Acad Bras Cienc. 2020;92: e20191375. doi:10.1590/0001-3765202020191375

16. Marklewitz M, Junglen S. Evolutionary and ecological insights into the emergence of arthropod-borne viruses. Acta Trop. 2019;190: 52–58. doi:10.1016/j.actatropica.2018.10.006

17. Lowen AC. It's in the mix: Reassortment of segmented viral genomes. PLOS Pathogens. 2018;14: e1007200. doi:10.1371/journal.ppat.1007200

18. Briese T, Calisher CH, Higgs S. Viruses of the family Bunyaviridae: Are all available isolates reassortants? Virology. 2013;446: 207–216. doi:10.1016/j.virol.2013.07.030

19. Piret J, Boivin G. Pandemics Throughout History. Frontiers in Microbiology. 2021;11. Available: https://www.frontiersin.org/articles/10.3389/fmicb.2020.631736

20. Carrasco-Hernandez R, Jácome R, López Vidal Y, Ponce de León S. Are RNA Viruses Candidate Agents for the Next Global Pandemic? A Review. ILAR Journal. 2017;58: 343–358. doi:10.1093/ilar/ilx026

21. Morens DM, Folkers GK, Fauci AS. Emerging infections: a perpetual challenge. Lancet Infect Dis. 2008;8: 710–719. doi:10.1016/S1473-3099(08)70256-1

22. Morens DM, Folkers GK, Fauci AS. The challenge of emerging and re-emerging infectious diseases. Nature. 2004;430: 242–249. doi:10.1038/nature02759

23. Ebel GD. Toward an Activist Agenda for Monitoring Virus Emergence. Cell Host & Microbe. 2014;15: 655–656. doi:10.1016/j.chom.2014.05.014

24. Rosenberg R. Detecting the emergence of novel, zoonotic viruses pathogenic to humans. Cell Mol Life Sci. 2015;72: 1115–1125. doi:10.1007/s00018-014-1785-y

25. Woolhouse M, Guant E. Ecological origins of novel human pathogens. Critical Reviews in Microbiology. 2007;33: 1–12.

26. Morens DM, Daszak P, Markel H, Taubenberger JK. Pandemic COVID-19 Joins History's Pandemic Legion. mBio. 2020;11: e00812-20. doi:10.1128/mBio.00812-20

27. Jones KE, Patel NG, Levy MA, Storeygard A, Balk D, Gittleman JL, et al. Global trends in emerging infectious diseases. Nature. 2008;451: 990–993. doi:10.1038/nature06536

28. Ebel GD. Promiscuous viruses – how do viruses survive multiple unrelated hosts? Curr Opin Virol. 2017;23: 125–129. doi:10.1016/j.coviro.2017.05.002

29. Sexton NR, Ebel GD. Effects of Arbovirus Multi-Host Life Cycles on Dinucleotide and Codon Usage Patterns. Viruses. 2019;11: 643. doi:10.3390/v11070643

30. Chala B, Hamde F. Emerging and Re-emerging Vector-Borne Infectious Diseases and the Challenges for Control: A Review. Front Public Health. 2021;9: 715759. doi:10.3389/fpubh.2021.715759

31. ter Horst S, Conceição-Neto N, Neyts J, Rocha-Pereira J. Structural and functional similarities in bunyaviruses: Perspectives for pan-bunya antivirals. Rev Med Virol. 2019;29: e2039. doi:10.1002/rmv.2039

32. Abudurexiti A, Adkins S, Alioto D, Alkhovsky SV, Avšič-Županc T, Ballinger MJ, et al. Taxonomy of the order Bunyavirales: update 2019. Arch Virol. 2019;164: 1949–1965. doi:10.1007/s00705-019-04253-6

33. Bente DA, Forrester NL, Watts DM, McAuley AJ, Whitehouse CA, Bray M. Crimean-Congo hemorrhagic fever: history, epidemiology, pathogenesis, clinical syndrome and genetic diversity. Antiviral Res. 2013;100: 159–189. doi:10.1016/j.antiviral.2013.07.006

34. Flick R, Bouloy M. Rift Valley fever virus. Curr Mol Med. 2005;5: 827–834. doi:10.2174/156652405774962263

35. Beer M, Conraths FJ, van der Poel WHM. 'Schmallenberg virus'--a novel orthobunyavirus emerging in Europe. Epidemiol Infect. 2013;141: 1–8. doi:10.1017/S0950268812002245

36. Doceul V, Lara E, Sailleau C, Belbis G, Richardson J, Bréard E, et al. Epidemiology, molecular virology and diagnostics of Schmallenberg virus, an emerging orthobunyavirus in Europe. Vet Res. 2013;44: 31. doi:10.1186/1297-9716-44-31

37. WHO to identify pathogens that could cause future outbreaks and pandemics. [cited 18 May 2023]. Available: https://www.who.int/news/item/21-11-2022-who-to-identify-pathogens-that-could-cause-future-outbreaks-and-pandemics

38. NIAID Emerging Infectious Diseases/ Pathogens | NIH: National Institute of Allergy and Infectious Diseases. [cited 28 Apr 2021]. Available: https://www.niaid.nih.gov/research/emerging-infectious-diseases-pathogens

39. Bridgen A, Weber F, Fazakerley JK, Elliott RM. Bunyamwera bunyavirus nonstructural protein NSs is a nonessential gene product that contributes to viral pathogenesis.

Proceedings of the National Academy of Sciences. 2001;98: 664–669. doi:10.1073/pnas.98.2.664

40. Weber F, Bridgen A, Fazakerley JK, Streitenfeld H, Kessler N, Randall RE, et al. Bunyamwera Bunyavirus Nonstructural Protein NSs Counteracts the Induction of Alpha/Beta Interferon. J Virol. 2002;76: 7949–7955. doi:10.1128/JVI.76.16.7949-7955.2002

41. Leventhal SS, Wilson D, Feldmann H, Hawman DW. A Look into Bunyavirales Genomes: Functions of Non-Structural (NS) Proteins. Viruses. 2021;13: 314. doi:10.3390/v13020314

42. The ends of La Crosse virus genome and antigenome RNAs within nucleocapsids are base paired. - PMC. [cited 24 May 2023]. Available: https://www.ncbi.nlm.nih.gov/pmc/articles/PMC247664/

43. Pettersson RF, Hewlett MJ, Baltimore D, Coffin JM. The genome of Uukuniemi virus consists of three unique RNA segments. Cell. 1977;11: 51–63.

44. Olschewski S, Cusack S, Rosenthal M. The Cap-Snatching Mechanism of Bunyaviruses. Trends in Microbiology. 2020;28: 293–303. doi:10.1016/j.tim.2019.12.006

45. Hopkins K, Cherry S. Bunyaviral cap-snatching vs. decapping. Cell Cycle. 2013;12: 3711–3712. doi:10.4161/cc.26878

46. Leisnham PT, Juliano SA. Impacts of climate, land use, and biological invasion on the ecology of immature Aedes mosquitoes: implications for La Crosse emergence. Ecohealth. 2012;9: 217–228. doi:10.1007/s10393-012-0773-7

47. Burkett-Cadena ND, Vittor AY. Deforestation and vector-borne disease: Forest conversion favors important mosquito vectors of human pathogens. Basic Appl Ecol. 2018;26: 101–110. doi:10.1016/j.baae.2017.09.012

48. Evans AB, Peterson KE. Throw out the Map: Neuropathogenesis of the Globally Expanding California Serogroup of Orthobunyaviruses. Viruses. 2019;11. doi:10.3390/v11090794

49. Elbers ARW, Koenraadt CJM, Meiswinkel R. Mosquitoes and Culicoides biting midges: vector range and the influence of climate change. Rev Sci Tech. 2015;34: 123–137. doi:10.20506/rst.34.1.2349

50. McDonald SM, Nelson MI, Turner PE, Patton JT. Reassortment in segmented RNA viruses: mechanisms and outcomes. Nat Rev Microbiol. 2016;14: 448–460. doi:10.1038/nrmicro.2016.46

51. Kapuscinski ML, Bergren NA, Russell BJ, Lee JS, Borland EM, Hartman DA, et al. Genomic characterization of 99 viruses from the bunyavirus families Nairoviridae, Peribunyaviridae, and Phenuiviridae, including 35 previously unsequenced viruses. PLOS Pathogens. 2021;17: e1009315. doi:10.1371/journal.ppat.1009315

52. Gerrard SR, Li L, Barrett AD, Nichol ST. Ngari virus is a Bunyamwera virus reassortant that can be associated with large outbreaks of hemorrhagic fever in Africa. J Virol. 2004;78: 8922–8926. doi:10.1128/JVI.78.16.8922-8926.2004

53. Bowen MD, Trappier SG, Sanchez AJ, Meyer RF, Goldsmith CS, Zaki SR, et al. A reassortant bunyavirus isolated from acute hemorrhagic fever cases in Kenya and Somalia. Virology. 2001;291: 185–190. doi:10.1006/viro.2001.1201

54. Cheng LL, Rodas JD, Schultz KT, Christensen BM, Yuill TM, Israel BA. Potential for evolution of California serogroup bunyaviruses by genome reassortment in Aedes albopictus. The American Journal of Tropical Medicine and Hygiene. 1999;60: 430–438. doi:10.4269/ajtmh.1999.60.430

55. Aguilar PV, Barrett AD, Saeed MF, Watts DM, Russell K, Guevara C, et al. Iquitos Virus: A Novel Reassortant Orthobunyavirus Associated with Human Illness in Peru. PLoS Negl Trop Dis. 2011;5. doi:10.1371/journal.pntd.0001315

56. Klempa B. Reassortment events in the evolution of hantaviruses. Virus Genes. 2018;54: 638–646. doi:10.1007/s11262-018-1590-z

57. Sall AA, Zanotto PM de A, Sene OK, Zeller HG, Digoutte JP, Thiongane Y, et al. Genetic Reassortment of Rift Valley Fever Virus in Nature. Journal of Virology. 1999;73: 8196–8200.

58. Negredo A, Sánchez-Arroyo R, Díez-Fuertes F, de Ory F, Budiño MA, Vázquez A, et al. Fatal Case of Crimean-Congo Hemorrhagic Fever Caused by Reassortant Virus, Spain, 2018. Emerg Infect Dis. 2021;27: 1211–1215. doi:10.3201/eid2704.203462

59. Reese SM, Blitvich BJ, Blair CD, Geske D, Beaty BJ, Black WC. Potential for La Crosse virus segment reassortment in nature. Virol J. 2008;5: 164. doi:10.1186/1743-422X-5-164

60. Wernike K, Brocchi E, Beer M. Effective interference between Simbu serogroup orthobunyaviruses in mammalian cells. Vet Microbiol. 2016;196: 23–26. doi:10.1016/j.vetmic.2016.10.007

61. Bebber DP, Marriott FHC, Gaston KJ, Harris SA, Scotland RW. Predicting unknown species numbers using discovery curves. Proc Biol Sci. 2007;274: 1651–1658. doi:10.1098/rspb.2007.0464

62. Ecological Origins of Novel Human Pathogens: Critical Reviews in Microbiology: Vol 33, No 4. [cited 18 May 2023]. Available: https://www.tandfonline.com/doi/abs/10.1080/10408410701647560?journalCode=imby20

63. Woolhouse MEJ, Howey R, Gaunt E, Reilly L, Chase-Topping M, Savill N. Temporal trends in the discovery of human viruses. Proc Biol Sci. 2008;275: 2111–2115. doi:10.1098/rspb.2008.0294

64. Wanyoike F, Mtimet N, Bett B. Willingness to pay for a Rift valley fever (RVF) vaccine among Kenyan cattle producers. Prev Vet Med. 2019;171: 104763. doi:10.1016/j.prevetmed.2019.104763

65. Maes P, Adkins S, Alkhovsky SV, Avšič-Županc T, Ballinger MJ, Bente DA, et al. Taxonomy of the order Bunyavirales: second update 2018. Arch Virol. 2019;164: 927–941. doi:10.1007/s00705-018-04127-3

66. Yu X-J, Liang M-F, Zhang S-Y, Liu Y, Li J-D, Sun Y-L, et al. Fever with Thrombocytopenia Associated with a Novel Bunyavirus in China. N Engl J Med. 2011;364: 1523–1532. doi:10.1056/NEJMoa1010095

67. Hoffmann B, Scheuch M, Höper D, Jungblut R, Holsteg M, Schirrmeier H, et al. Novel Orthobunyavirus in Cattle, Europe, 2011. Emerg Infect Dis. 2012;18: 469–472. doi:10.3201/eid1803.111905

68. Lanciotti RS, Kosoy OI, Bosco-Lauth AM, Pohl J, Stuchlik O, Reed M, et al. Isolation of a novel orthobunyavirus (Brazoran virus) with a 1.7kb S segment that encodes a unique nucleocapsid protein possessing two putative functional domains. Virology. 2013;444: 55–63. doi:10.1016/j.virol.2013.05.031

69. Hontz RD, Guevara C, Halsey ES, Silvas J, Santiago FW, Widen SG, et al. Itaya virus, a Novel Orthobunyavirus Associated with Human Febrile Illness, Peru. Emerg Infect Dis. 2015;21: 781–788. doi:10.3201/eid2105.141368

70. Hughes HR, Adkins S, Alkhovskiy S, Beer M, Blair C, Calisher CH, et al. ICTV Virus Taxonomy Profile: Peribunyaviridae. J Gen Virol. 2020;101: 1–2. doi:10.1099/jgv.0.001365

71. Tatineni S, McMechan AJ, Wosula EN, Wegulo SN, Graybosch RA, French R, et al. An eriophyid mite-transmitted plant virus contains eight genomic RNA segments with unusual heterogeneity in the nucleocapsid protein. J Virol. 2014;88: 11834–11845. doi:10.1128/JVI.01901-14

72. Liu J, Sun Y, Shi W, Tan S, Pan Y, Cui S, et al. The first imported case of Rift Valley fever in China reveals a genetic reassortment of different viral lineages. Emerg Microbes Infect. 2017;6: e4–e4. doi:10.1038/emi.2016.136

73. Ding N-Z, Luo Z-F, Niu D-D, Ji W, Kang X-H, Cai S-S, et al. Identification of two severe fever with thrombocytopenia syndrome virus strains originating from reassortment. Virus Res. 2013;178: 543–546. doi:10.1016/j.virusres.2013.09.017

74. Ladner JT, Beitzel B, Chain PSG, Davenport MG, Donaldson EF, Frieman M, et al. Standards for sequencing viral genomes in the era of high-throughput sequencing. MBio. 2014;5: e01360-01314. doi:10.1128/mBio.01360-14

75. Calisher CH, Gutierrez VE, Bruce Francy D, Aracely Alava A, Muth DJ, Lazuick JS. Identification of hitherto unrecognized arboviruses from Ecuador: Members of serogroups B, C, Bunyamwera, Patois, and Minatitlan. Am J Trip Med Hyg. 1983;32: 877–885.

76. Simpósio sobre a Biota Amazônica Belém, Lent H. Atas do simpósio sobre a biota amazônica Belém, Pará, Brasil, Junho 6-11, 1966. Rio de Janeiro Conselho Nacional de Pesquisas (CNPQ); 1967. Available: https://www.biodiversitylibrary.org/item/194233

77. Taylor RM, American Committee on Arthropod-borne Viruses. Subcommittee on Information Exchange; National Institute of Allergy and Infectious Diseases (U.S.). Catalogue of arthropod-borne viruses of the world; a collection of data on registered arthropod-borne animal viruses. Washington, Public Health Service; for sale by the Supt. of Docs., U.S. Govt. Print. Off.; 1967.

78. Takahashi K, Oya A, Okazda T, Matsuo R, Kuma M. Aino virus, a new a new member of simbu group of arbovirus from mosquitoes in Japan. Jpn J Med Sci Biol. 1968;21: 95–101.

79. Calisher CH, Coimbra TL, Lopez O de S, Muth DJ, Sacchetta L de A, Francy DB, et al. Identification of new Guama and Group C serogroup bunyaviruses and an ungrouped virus from Southern Brazil. Am J Trop Med Hyg. 1983;32: 424–431.

80. Roca-Garcia M. The Isolation of Three Neurotropic Viruses from Forest Mosquitoes in Eastern Colombia. The Journal of Infectious Diseases. 1944;75: 160–169.

81. Calisher CH, Monath TP, Mitchell CJ, Sabattini MS, Cropp CB, Kerschner J, et al. Arbovirus investigations in Argentina, 1977-1980. III. Identification and characterization of viruses isolated, including new subtypes of western and Venezuelan equine encephalitis viruses and four new bunyaviruses (Las Maloyas, Resistencia, Barranqueras, and Antequera). Am J Trop Med Hyg. 1985;34: 956–965.

82. Mitchell CJ, Monath TP, Sabattini MS, Cropp CB, Daffner JF, Calisher CH, et al. Arbovirus investigations in Argentina, 1977-1980. II. Arthropod collections and virus isolations from Argentine mosquitoes. Am J Trop Med Hyg. 1985;34: 945–955.

83. Karabatsos N, Buckley SM. Susceptibility of the baby-hamster kidney-cell line (BHK-21) to infection with arboviruses. Am J Trop Med Hyg. 1967;16: 99–105. doi:10.4269/ajtmh.1967.16.99

84. Digoutte JP, Robin Y, Cagnard VJ. [Bangui virus (HB 70-754), a new virus isolated from a case of acute exanthemata]. Ann Microbiol (Paris). 1973;124: 147–153.

85. El Mekki AA, Nieuwenhuysen P, van der Groen G, Pattyn SR. Characterization of some ungrouped viruses. Trans R Soc Trop Med Hyg. 1981;75: 799–806. doi:10.1016/0035-9203(81)90416-8

86. Digoutte JP. Rapport Annuel de l'Institut Pasteur de Bangui. 1970.

87. Zeller HG, Karabatsos N, Calisher CH, Digoutte JP, Cropp CB, Murphy FA, et al. Electron microscopic and antigenic studies of uncharacterized viruses. II. Evidence suggesting the placement of viruses in the family Bunyaviridae. Arch Virol. 1989;108: 211–227. doi:10.1007/bf01310935

88. Calisher CH, Shope RE. Bunyaviridae: The Bunyaviruses. Laboratory Diagnosis of Infectious Diseases Principles and Practice. New York, NY: Springer New York; 1988. pp. 626–646. doi:10.1007/978-1-4612-3900-0_32

89. Stim TB. Arbovirus Plaquing in Two Simian Kidney Cell Lines. Journal of General Virology. 1969;5: 329–338. doi:10.1099/0022-1317-5-3-329

90. DE Souza Lopes O, DE Abreu Sacchetta L, Fonseca IE, Lacerda JP. Bertioga (Guama group) and Anhembi (Bunyamwera group), two new arboviruses isolated in São Paulo, Brazil. Am J Trop Med Hyg. 1975;24: 131–134. doi:10.4269/ajtmh.1975.24.131

91. Hunt AR, Calisher CH. Relationships of bunyamwera group viruses by neutralization. Am J Trop Med Hyg. 1979;28: 740–749.

92. Lopes O de S, Forattini OP, Fonseca IE, Lacerda JP, Sacchetta LA, Rabello EX. Boracéia virus. A new virus related to anopheles B virus. Proc Soc Exp Biol Med. 1966;123: 502–504. doi:10.3181/00379727-123-31526

93. Lopes O de S, Forattini OP, Fonseca IE, Lacerda JP, Sacchetta LA, Rabello EX. Boracéia virus. A new virus related to anopheles B virus. Proc Soc Exp Biol Med. 1966;123: 502–504. doi:10.3181/00379727-123-31526

94. Saluzzo J-F, Germain M, Huard M, Robin Y, Gonzalez J-P, Herve J-P, et al. Le virus bozo (ArB 7343): Un nouvel arbovirus du groupe bunyamwera isolé en république centrafricaine; sa transmission expérimentale par Aedes aegypti. Annales de l'Institut Pasteur / Virologie. 1983;134: 221–232. doi:10.1016/S0769-2617(83)80061-6

95. Smithburn KC, Haddow AJ, Mahaffy AF. A Neurotropic Virus Isolated from Aedes Mosquitoes Caught in the Semliki Forest. The American Journal of Tropical Medicine and Hygiene. 1946;s1-26: 189–208. doi:10.4269/ajtmh.1946.s1-26.189

96. Spence L, Anderson CR, Aitken TH, Downs WG. Bushbush, Ieri and Lukuni viruses, three unrelated new agents isolated from Trinidadian forest mosquitoes. Proc Soc Exp Biol Med. 1967;125: 45–50. doi:10.3181/00379727-125-32009

97. Reeves WC, Scrivani RP, Hardy JL, Roberts DR, Nelson RL. Buttonwillow virus, a new Arbovirus isolated from mammals and Culicoides midges in Kern County, California. Am J Trop Med Hyg. 1970;19: 544–551. doi:10.4269/ajtmh.1970.19.544

98. Hardy JL, Scrivani RP, Lyness RN, Nelson RL, Roberts DR. Ecologic studies of Buttonwillow virus in Kern County, California, 1961-1968. Am J Trop Med Hyg. 1970;19: 552–563. doi:10.4269/ajtmh.1970.19.552

99. Tesh RB, Chaniotis BN, Peralta PH, Johnson KM. Ecology of Viruses Isolated from Panamanian Phlebotomine Sandflies. The American Journal of Tropical Medicine and Hygiene. 1974;23: 258–269. doi:10.4269/ajtmh.1974.23.258

100. Tesh RB, Boshell J, Young DG, Morales A, Corredor A, Modi GB, et al. Biology of Arboledas virus, a new phlebotomus fever serogroup virus (Bunyaviridae: Phlebovirus) isolated from sand flies in Colombia. Am J Trop Med Hyg. 1986;35: 1310–1316. doi:10.4269/ajtmh.1986.35.1310

101. Henderson JR, Taylor RM. Propagation of certain arthropod-borne viruses in avian and primate cell cultures. J Immunol. 1960;84: 590–598.

102. Mangiafico JA, Sanchez JL, Figueiredo LT, LeDuc JW, Peters CJ. Isolation of a newly recognized Bunyamwera serogroup virus from a febrile human in Panama. Am J Trop Med Hyg. 1988;39: 593–596. doi:10.4269/ajtmh.1988.39.593

103. Catalogue of arthropod-borne viruses of the world. The Subcommittee on Information Exchange. The American Committee on Arthropod-borne Viruses. Am J Trop Med Hyg. 1970;19: Suppl:1149-50. doi:10.4269/ajtmh.1970.19.1082

104. Calisher CH, Lazuick JS, Justines G, Francy DB, Monath TP, V EG, et al. Viruses Isolated from Aedeomyia Squamipennis Mosquitoes Collected in Panama, Ecuador, and Argentina: Establishment of the Gamboa Serogroup. The American Journal of Tropical Medicine and Hygiene. 1981;30: 219–223. doi:10.4269/ajtmh.1981.30.219

105. Henderson BE, Calisher CH, Coleman PH, Fields BN, Work TH. Gumbo Limbo, a new group C arbovirus from the Florida everglades. Am J Epidemiol. 1969;89: 227–231. doi:10.1093/oxfordjournals.aje.a120933

106. Shope RE, Causey CE, Causey OR. Itaqui Virus, a New Member of Arthropod-Borne Group C*. The American Journal of Tropical Medicine and Hygiene. 1961;10: 264–265. doi:10.4269/ajtmh.1961.10.264

107. Buckley SM, Shope RE. Comparative Assay of Arthropod-Borne Group C Virus Antibodies by Tissue Culture Neutralization and Hemagglutination-Inhibition Tests. The American Journal of Tropical Medicine and Hygiene. 1961;10: 53–61. doi:10.4269/ajtmh.1961.10.53

108. Rodrigues FM, Singh PB, Dandawate CN, Soman RS, Bhatt PN. Kaikalur virus--a new arthropod-borne virus belonging to the Simbu group isolated in India from Culex tritaeniorhynchus (Giles). Indian J Med Res. 1977;66: 719–725.

109. Anderson CR, Aitken TH, Spence LP, Downs WG. Kairi virus, a new virus from Trinidadian forest mosquitoes. Am J Trop Med Hyg. 1960;9: 70–72. doi:10.4269/ajtmh.1960.9.70

110. Casals J, Whitman L. A New Antigenic Group of Arthropod-Borne Viruses. The American Journal of Tropical Medicine and Hygiene. 1960;9: 73–77. doi:10.4269/ajtmh.1960.9.73

111. Málková D. Yaba 1 virus in Czechoslovakia. I. Some physical and chemical properties of yaba 1 (Lednice 110) virus. Acta Virol. 1972;16: 264–266.

112. Main OM, Hardy JL, Reeves WC. Growth of Arboviruses and Other Viruses in a Continuous Line of Culex Tarsalis Cells. J Med Entomol. 1977;14: 107–112. doi:10.1093/jmedent/14.1.107

113. Causey OR, Causey CE, Maroja OM, Macedo DG. The isolation of arthropod-borne viruses, including members of two hitherto undescribed serological groups, in the Amazon region of Brazil. Am J Trop Med Hyg. 1961;10: 227–249. doi:10.4269/ajtmh.1961.10.227

114. Derodaniche E, Paesdeandrade A, Galindo P. Isolation of Two Antigenically Distinct Arthropod-Borne Viruses of Group C in Panama. Am J Trop Med Hyg. 1964;13: 839–843.

115. Porterfield JS, Casals J, Chumakov MP, Gaidamovich SY, Hannoun C, Holmes IH, et al. Bunyaviruses and Bunyaviridae. Intervirology. 1975;6: 13–24. doi:10.1159/000149449

116. Mellor PS, Boorman J, Loke R. The multiplication of Main Drain Virus in two species of Culicoides (Diptera, Ceratopogonidae). Archiv f Virusforschung. 1974;46: 105–110. doi:10.1007/BF01240210

117. Sunaga H, Taylor RM, Henderson JR. Comparative Sensitivity of Viruses to Treatment with Diethyl Ether and Sodium Desoxycholate. The American Journal of Tropical Medicine and Hygiene. 1960;9: 419–424. doi:10.4269/ajtmh.1960.9.419

118. Buckley SM. Applicability of the Hela (Gey) Strain of Human Malignant Epithelial Cells to the Propagation of Arboviruses. Proc Soc Exp Biol Med. 1964;116: 354–358. doi:10.3181/00379727-116-29246

119. Jonkers AH, Spence L, Downs WG, Aitken THG, Tikasingh ES. Arbovirus Studies in Bush Bush Forest, Trinidad, W. I., September 1959–December 1964. The American Journal of Tropical Medicine and Hygiene. 1968;17: 276–284. doi:10.4269/ajtmh.1968.17.276

120. Henderson BE. East African Virus Research Institute Report. 1969;No. 18:31-33.

121. Shope RE, Whitman L. Nepuyo virus, a new group C agent isolated in Trinidad and Brazil. II. Serological studies. Am J Trop Med Hyg. 1966;15: 772–774. doi:10.4269/ajtmh.1966.15.772

122. Spence L, Anderson CR, Aitken TH, Downs WG. Nepuyo virus, a new group C agent isolated in Trinidad and Brazil. I. Isolation and properties of the Trinidadian strain. Am J Trop Med Hyg. 1966;15: 71–74. doi:10.4269/ajtmh.1966.15.71

123. Calisher CH, Lindsey HS, Ritter DG, Sommerman KM. Northway virus: a new Bunyamwera group arbovirus from Alaska. Can J Microbiol. 1974;20: 219–223. doi:10.1139/m74-034

124. Akashi H, Kaku Y, Kong X, Pang H. Antigenic and genetic comparisons of Japanese and Australian Simbu serogroup viruses: evidence for the recovery of natural virus reassortants. Virus Res. 1997;50: 205–213.

125. Fields BN, Henderson BE, Coleman PH, Work TH. Pahayokee and Shark River, two new arboviruses related to Patois and Zegla from the Florida everglades. Am J Epidemiol. 1969;89: 222–226. doi:10.1093/oxfordjournals.aje.a120932

126. Srihongse S, Galindo P, Grayson MA. Isolation of group C arboviruses in Panama including two new members, Patois and Zegla. Am J Trop Med Hyg. 1966;15: 379–384. doi:10.4269/ajtmh.1966.15.379

127. Galindo P, Srihongse S, Rodaniche ED, Grayson MA. An Ecological Survey for Arboviruses in Almirante, Panama, 1959–1962*. The American Journal of Tropical Medicine and Hygiene. 1966;15: 385–400. doi:10.4269/ajtmh.1966.15.385

128. St George TD, Standfast HA, Cybinski DH, Filippich C, Carley JG. Peaton virus: a new Simbu group arbovirus isolated from cattle and Culicoides brevitarsis in Australia. Aust J Biol Sci. 1980;33: 235–243.

129. Francy DB, Karabatsos N, Wesson DM, Moore CG, Lazuick JS, Niebylski ML, et al. A new arbovirus from Aedes albopictus, an Asian mosquito established in the United States. Science. 1990;250: 1738–1740. doi:10.1126/science.2270489

130. Jonkers AH, Metselaar D, de Andrade AH, Tikasingh ES. Restan virus, a new group C arbovirus from Trinidad and Surinam. Am J Trop Med Hyg. 1967;16: 74–78. doi:10.4269/ajtmh.1967.16.74

131. Hubálek Z, Juricová Z, Halouzka J, Butenko AM, Kondrasina NG, Guscina EA, et al. Isolation and characterization of Sedlec virus, a new bunyavirus from birds. Acta Virol. 1990;34: 339–345.

132. Bishop DHL, Shope RE. Comprehensive Virology. N.Y.: Plenum Press; 1979. pp. 1–156.

133. Cornet M, Robin Y, Chateau R, Heme G, Adam C, Valade M, et al. Isolation of arboviruses from mosquitoes in eastern Senegal Notes on epidemiology of aedes--borne viruses especially yellow fever virus. Cahiers ORSTOM Serie entomologie medicale et parasitologie. 1979;17: 149–163.

134. Woodall JP, Williams MC. Tanga virus: a hitherto undescribed virus from Anopheles mosquitoes from Tanzania. East African Medical Journal. 1967;44: 83–6.

135. Ardoin PM, Simpson DI. Artificial infection of Aedes (Stegomyia) aegypti (Linnaeus) with five African arboviruses. J Med Entomol. 1967;4: 189–191. doi:10.1093/jmedent/4.2.189

136. Brès P, Williams M, Chambon L. Isolement au Sénégal d'un nouveau prototype d'arbovirus, la souche "Tataguine" (IPD/A 252). Ann Inst Pasteur. 1966;11: 585–591.

137. Murphy FA, Harrison AK, Tzianabos T. Electron microscopic observations of mouse brain infected with Bunyamwera group arboviruses. J Virol. 1968;2: 1315–1325.

138. Marshall ID, Woodroofe GM, Gard GP. Arboviruses of Coastal South-Eastern Australia. Australian Journal of Experimental Biology and Medical Science. 1980;58: 91–102. doi:10.1038/icb.1980.9

139. Carey DE, Reuben R, George S, Shope RE, Myers RM. Kammavanpettai, Kannamangalam, Sembalam and Thimiri viruses: four unrelated new agents isolated from birds in India. Indian J Med Res. 1971;59: 1708–1711.

140. Carvalho VL, Nunes MRT, Medeiros DBA, da Silva SP, Lima CPS, Inada DT, et al. New Virus Genome Sequences of the Guama Serogroup (Genus Orthobunyavirus, Family Bunyaviridae), Isolated in the Brazilian Amazon Region. Genome Announc. 2017;5. doi:10.1128/genomeA.01750-16

141. St George TD, Cybinski DH, Filippich C, Carley JG. The isolation of three Simbu group viruses new to Australia. Aust J Exp Biol Med Sci. 1979;57: 581–582. doi:10.1038/icb.1979.60

142. Scherer WF, Campillo-Sainz C, Dickerman RW, Diaz-Najera A, Madalengoitia J. Isolation of Tlacotalpan virus, a new Bunyamwera-group virus from Mexican mosquitoes. Am J Trop Med Hyg. 1967;16: 79–91. doi:10.4269/ajtmh.1967.16.79

143. Lennette EH, Ota MI, Fujimoto FY, Wiener A, Loomis EC. Turlock virus: a presumably new arthropod-borne virus; isolation and identification. Am J Trop Med Hyg. 1957;6: 1024–1035. doi:10.4269/ajtmh.1957.6.1024

144. Lennette EH, Ota MI, Hoffman MN. Turlock virus: a description of some of its properties. Am J Trop Med Hyg. 1957;6: 1036–1046. doi:10.4269/ajtmh.1957.6.1036

145. Calisher CH, McLean RG, Zeller HG, Francy DB, Karabatsos N, Bowen RA. Isolation of Tete serogroup bunyaviruses from Ceratopogonidae collected in Colorado. Am J Trop Med Hyg. 1990;43: 314–318. doi:10.4269/ajtmh.1990.43.314

146. Doherty RL, Carley JG, Mackerras MJ, Marks EN. Studies of Arthropod-Borne Virus Infections in Queensland. Australian Journal of Experimental Biology and Medical Science. 1963;41: 17–39. doi:10.1038/icb.1963.2

147. Casals J. New developments in the classification of arthropod-borne viruses. Anais de Microbiolgia. 1963; 13–34.

148. Causey OR, Kemp GE, Causey CE, Lee VH. Isolations of Simbu-group viruses in Ibadan, Nigeria 1964-69, including the new types Sango, Shamonda, Sabo and Shuni. Ann Trop Med Parasitol. 1972;66: 357–362. doi:10.1080/00034983.1972.11686835

149. Bhatt PN, Kulkarni KG, Boshell J, Rajagopalan PK, Patil AP, Goverdhan MK, et al. Kaisodi virus, a new agent isolated from Haemaphysalis spinigera in Mysore State, South India. I. Isolation of strains. Am J Trop Med Hyg. 1966;15: 958–960. doi:10.4269/ajtmh.1966.15.958

150. Pavri KM, Casals J. Kaisodi virus, a new agent isolated from Haemaphysalis spinigera in Mysore state, South India. Am J Trop Med Hyg. 1966;15: 961–963. doi:10.4269/ajtmh.1966.15.961

151. Filipe AR, Alves MJ, Karabatsos N, Matos APA de, Núncio MS, Bacellar F. Palma Virus, a New Bunyaviridae Isolated from Ticks in Portugal. Intervirology. 1994;37: 348–351. doi:10.1159/000150399

152. Murphy FA, Harrison AK, Whitfield SG. Bunyaviridae: Morphologic and Morphogenetic Similarities of Bunyamwera Serologic Supergroup Viruses and Several Other Arthropod-Borne Viruses. Intervirology. 1973; 297–316. doi:10.1159/000148858

153. Yunker CE, Clifford CM, Thomas LA, Keirans JE, Casals J, George JE, et al. Sunday Canyon virus, a new ungrouped agent from the tick Argas (A.) cooleyi in Texas. Acta Virol. 1977;21: 36–44.

154. Lvov DK, Timopheeva AA, Gromashevski VL, Gostinshchikova GV, Veselovskaya OV, Chervonski VI, et al. “Zaliv Terpeniya” virus, a new Uukuniemi group arbovirus isolated from Ixodes (Ceratixodes) putus Pick.-Camb. 1878 on Tyuleniy Island (Sakhalin region) and Commodore Islands (Kamchatsk region). Arch Gesamte Virusforsch. 1973;41: 165–169. doi:10.1007/bf01252761

155. Málková D, Holubová J, Cerný V, Daniel M, Fernández A, de la Cruz J, et al. Estero real virus: a new virus isolated from argasid ticks Ornithodoros tadaridae in Cuba. Acta Virol. 1985;29: 247–250.

156. Philip CB. Hughes Virus, A New Arboviral Agent from Marine Bird Ticks. J Parasitol. 1965;51: 252.

157. Yunker CE, Clifford CM, Thomas LA, Cory J, George JE. Isolation of viruses from swallowticks, Argas cooleyi, in the southwestern United States. Acta Virol. 1972;16: 415–421.

158. Shchetinin A, Lvov D, Deriabin P, Botikov A, Gitelman A, Kuhn J, et al. Genetic and Phylogenetic Characterization of Tataguine and Witwatersrand Viruses and Other Orthobunyaviruses of the Anopheles A, Capim, Guamá, Koongol, Mapputta, Tete, and Turlock Serogroups. Viruses. 2015;7: 5987–6008. doi:10.3390/v7112918

159. Huang B, Firth C, Watterson D, Allcock R, Colmant AMG, Hobson-Peters J, et al. Genetic Characterization of Archived Bunyaviruses and their Potential for Emergence in Australia. Emerg Infect Dis. 2016;22: 833–840. doi:10.3201/eid2205.151566

160. Gauci PJ, McAllister J, Mitchell IR, Boyle DB, Bulach DM, Weir RP, et al. Genomic characterisation of three Mapputta group viruses, a serogroup of Australian and Papua New Guinean bunyaviruses associated with human disease. PLoS ONE. 2015;10: e0116561. doi:10.1371/journal.pone.0116561

161. Hughes H, Lambert A. ICTV Taxonomy Proposal. Move one species from the phenuivirid genus Phlebovirus to the peribunyavirid genus Pacuvirus, and create one novel pacuvirus species. 2019022M. 2019.

162. Groseth A, Vine V, Weisend C, Guevara C, Watts D, Russell B, et al. Maguari Virus Associated with Human Disease. Emerg Infect Dis. 2017;23: 1325–1331. doi:10.3201/eid2308.161254

163. Tangudu CS, Charles J, Blitvich BJ. Evidence that Lokern virus (family Peribunyaviridae) is a reassortant that acquired its small and large genome segments from Main Drain virus and its medium genome segment from an undiscovered virus. Virol J. 2018;15. doi:10.1186/s12985-018-1031-6

164. Nunes MRT, Travassos da Rosa APA, Weaver SC, Tesh RB, Vasconcelos PFC. Molecular epidemiology of group C viruses (Bunyaviridae, Orthobunyavirus) isolated in the Americas. J Virol. 2005;79: 10561–10570. doi:10.1128/JVI.79.16.10561-10570.2005

165. Castillo Oré RM, Caceda RE, Huaman AA, Williams M, Hang J, Juarez DE, et al. Molecular and antigenic characterization of group C orthobunyaviruses isolated in Peru. PLoS ONE. 2018;13: e0200576. doi:10.1371/journal.pone.0200576

166. Aguilar PV. Genetic Characterization of the Patois Serogroup (Genus Orthobunyavirus; Family Peribunyaviridae) and Evidence That Estero Real Virus is a Member of the Genus Orthonairovirus. Am J Trip Med Hyg. 2018;99(2): 451–457. doi:10.4269/ajtmh.18-0201

167. de Souza WM, Acrani GO, Romeiro MF, Reis O, Tolardo AL, da Silva SP, et al. Molecular characterization of Capim and Enseada orthobunyaviruses. Infection, Genetics and Evolution. 2016;40: 47–53. doi:10.1016/j.meegid.2016.02.024

168. Briese T, Bird B, Kapoor V, Nichol ST, Lipkin WI. Batai and Ngari viruses: M segment reassortment and association with severe febrile disease outbreaks in East Africa. J Virol. 2006;80: 5627–5630. doi:10.1128/JVI.02448-05

169. Yanase T, Aizawa M, Kato T, Yamakawa M, Shirafuji H, Tsuda T. Genetic characterization of Aino and Peaton virus field isolates reveals a genetic reassortment between these viruses in nature. Virus Res. 2010;153: 1–7. doi:10.1016/j.virusres.2010.06.020

170. Yanase T, Kato T, Aizawa M, Shuto Y, Shirafuji H, Yamakawa M, et al. Genetic reassortment between Sathuperi and Shamonda viruses of the genus Orthobunyavirus in nature: implications for their genetic relationship to Schmallenberg virus. Arch Virol. 2012;157: 1611–1616. doi:10.1007/s00705-012-1341-8

171. Calisher CH, Francy DB, Smith GC, Muth DJ, Lazuick JS, Karabatsos N, et al. Distribution of Bunyamwera serogroup viruses in North America, 1956-1984. Am J Trop Med Hyg. 1986;35: 429–443.

172. Adams MJ, Lefkowitz EJ, King AMQ, Harrach B, Harrison RL, Knowles NJ, et al. Changes to taxonomy and the International Code of Virus Classification and Nomenclature ratified by the International Committee on Taxonomy of Viruses (2017). Archives of Virology. 2017;162: 2505–2538. doi:10.1007/s00705-017-3358-5

173. Marklewitz M, Palacios G, Ebihara H, Kuhn J, Junglen S. Create six new genera, create eight-five new species, rename/move ten species and abolish two species in the family Phenuiviridae, order Bunyavirales. ICTV [International Committee for Taxonomy of Viruses]. 2019;Proposal (Taxoprop) No. 2019.026M.

174. Blitvich BJ, Beaty BJ, Blair CD, Brault AC, Dobler G, Drebot MA, et al. Bunyavirus Taxonomy: Limitations and Misconceptions Associated with the Current ICTV Criteria Used for Species Demarcation. Am J Trop Med Hyg. 2018;99: 11–16. doi:10.4269/ajtmh.18-0038

175. Arbovirus Catalog - CDC Division of Vector-Borne Diseases (DVBD). [cited 9 Apr 2019]. Available: https://wwwn.cdc.gov/arbocat/

176. Babraham Bioinformatics - FastQC A Quality Control tool for High Throughput Sequence Data. Available: https://www.bioinformatics.babraham.ac.uk/projects/fastqc/

177. Martin M. Cutadapt removes adapter sequences from high-throughput sequencing reads. EMBnet.journal. 2011;17: 10–12. doi:10.14806/ej.17.1.200

178. Li W, Godzik A. Cd-hit: a fast program for clustering and comparing large sets of protein or nucleotide sequences. Bioinformatics. 2006;22: 1658–1659. doi:10.1093/bioinformatics/btl158

179. Li W, Jaroszewski L, Godzik A. Clustering of highly homologous sequences to reduce the size of large protein databases. Bioinformatics. 2001;17: 282–283.

180. Langmead B, Salzberg SL. Fast gapped-read alignment with Bowtie 2. Nat Methods. 2012;9: 357–359. doi:10.1038/nmeth.1923

181. Bankevich A, Nurk S, Antipov D, Gurevich AA, Dvorkin M, Kulikov AS, et al. SPAdes: a new genome assembly algorithm and its applications to single-cell sequencing. J Comput Biol. 2012;19: 455–477. doi:10.1089/cmb.2012.0021

182. Altschul SF, Gish W, Miller W, Myers EW, Lipman DJ. Basic local alignment search tool. J Mol Biol. 1990;215: 403–410. doi:10.1016/S0022-2836(05)80360-2

183. Camacho C, Coulouris G, Avagyan V, Ma N, Papadopoulos J, Bealer K, et al. BLAST+: architecture and applications. BMC Bioinformatics. 2009;10: 421. doi:10.1186/1471-2105-10-421

184. Buchfink B, Xie C, Huson DH. Fast and sensitive protein alignment using DIAMOND. Nat Methods. 2015;12: 59–60. doi:10.1038/nmeth.3176

185. Kearse M, Moir R, Wilson A, Stones-Havas S, Cheung M, Sturrock S, et al. Geneious Basic: An integrated and extendable desktop software platform for the organization and analysis of sequence data. Bioinformatics. 2012;28: 1647–1649. doi:10.1093/bioinformatics/bts199

186. Lambert AJ, Lanciotti RS. Consensus amplification and novel multiplex sequencing method for S segment species identification of 47 viruses of the Orthobunyavirus, Phlebovirus, and Nairovirus genera of the family Bunyaviridae. J Clin Microbiol. 2009;47: 2398–2404. doi:10.1128/JCM.00182-09

187. Kono Y, Yusnita Y, Mohd Ali AR, Maizan M, Sharifah SH, Fauzia O, et al. Characterization and identification of Oya virus, a Simbu serogroup virus of the genus Bunyavirus, isolated from a pig suspected of Nipah virus infection. Arch Virol. 2002;147: 1623–1630. doi:10.1007/s00705-002-0838-y

188. Edgar RC. MUSCLE: multiple sequence alignment with high accuracy and high throughput. Nucleic Acids Res. 2004;32: 1792–1797. doi:10.1093/nar/gkh340

189. Galtier N, Gouy M, Gautier C. SEAVIEW and PHYLO_WIN: two graphic tools for sequence alignment and molecular phylogeny. Comput Appl Biosci. 1996;12: 543–548.

190. Castresana J. Selection of conserved blocks from multiple alignments for their use in phylogenetic analysis. Mol Biol Evol. 2000;17: 540–552. doi:10.1093/oxfordjournals.molbev.a026334

191. Huelsenbeck JP, Ronquist F. MRBAYES: Bayesian inference of phylogenetic trees. Bioinformatics. 2001;17: 754–755. doi:10.1093/bioinformatics/17.8.754

192. Ronquist F, Huelsenbeck JP. MrBayes 3: Bayesian phylogenetic inference under mixed models. Bioinformatics. 2003;19: 1572–1574. doi:10.1093/bioinformatics/btg180

193. Posada D, Crandall KA. MODELTEST: testing the model of DNA substitution. Bioinformatics. 1998;14: 817–818. doi:10.1093/bioinformatics/14.9.817

194. Miller MA, Pfeiffer W, Schwartz T. Creating the CIPRES Science Gateway for inference of large phylogenetic trees. 2010 Gateway Computing Environments Workshop (GCE). New Orleans, LA, USA: IEEE; 2010. pp. 1–8. doi:10.1109/GCE.2010.5676129

195. Stöver BC, Müller KF. TreeGraph 2: Combining and visualizing evidence from different phylogenetic analyses. BMC Bioinformatics. 2010;11: 7. doi:10.1186/1471-2105-11-7

196. Katoh K, Standley DM. MAFFT multiple sequence alignment software version 7: improvements in performance and usability. Mol Biol Evol. 2013;30: 772–780. doi:10.1093/molbev/mst010

197. Price MN, Dehal PS, Arkin AP. FastTree 2--approximately maximum-likelihood trees for large alignments. PLoS One. 2010;5: e9490. doi:10.1371/journal.pone.0009490

198. Edridge AWD, van der Hoek L. Emerging orthobunyaviruses associated with CNS disease. PLoS Negl Trop Dis. 2020;14: e0008856. doi:10.1371/journal.pntd.0008856

199. Dias HG, Dos Santos FB, Pauvolid-Corrêa A. An Overview of Neglected Orthobunyaviruses in Brazil. Viruses. 2022;14. doi:10.3390/v14050987

200. Beaty BJ, Bishop DH. Bunyavirus-vector interactions. Virus Res. 1988;10: 289–301.

201. Iroegbu CU, Pringle CR. Genetic Interactions Among Viruses of the Bunyamwera Complex. J VIROL. 1981;37: 12.

202. Briese T, Rambaut A, Lipkin WI. Analysis of the medium (M) segment sequence of Guaroa virus and its comparison to other orthobunyaviruses. J Gen Virol. 2004;85: 3071–3077. doi:10.1099/vir.0.80122-0

203. Whitman L, Shope RE. The California Complex of Arthropod-Borne Viruses and Its Relationship to the Bunyamwera Group Through Guaroa Virus. The American Journal of Tropical Medicine and Hygiene. 1962;11: 691–696. doi:10.4269/ajtmh.1962.11.691

204. Dunn EF, Pritlove DC, Elliott RM. The S RNA genome segments of Batai, Cache Valley, Guaroa, Kairi, Lumbo, Main Drain and Northway bunyaviruses: sequence determination and analysis. J Gen Virol. 1994;75 (Pt 3): 597–608. doi:10.1099/0022-1317-75-3-597

205. Kobayashi T, Yanase T, Yamakawa M, Kato T, Yoshida K, Tsuda T. Genetic diversity and reassortments among Akabane virus field isolates. Virus Res. 2007;130: 162–171. doi:10.1016/j.virusres.2007.06.007

206. Elliott RM. Orthobunyaviruses: recent genetic and structural insights. Nat Rev Microbiol. 2014;12: 673–685. doi:10.1038/nrmicro3332

207. Dunn EF, Pritlove DC, Jin H, Elliott RM. Transcription of a recombinant bunyavirus RNA template by transiently expressed bunyavirus proteins. Virology. 1995;211: 133–143. doi:10.1006/viro.1995.1386

208. Flick R, Pettersson RF. Reverse Genetics System for Uukuniemi Virus (Bunyaviridae): RNA Polymerase I-Catalyzed Expression of Chimeric Viral RNAs. Journal of Virology. 2001;75: 1643–1655. doi:10.1128/JVI.75.4.1643-1655.2001

209. Osborne JC, Elliott RM. RNA Binding Properties of Bunyamwera Virus Nucleocapsid Protein and Selective Binding to an Element in the 5′ Terminus of the Negative-Sense S Segment. J Virol. 2000;74: 9946–9952.

210. Weber F, Dunn EF, Bridgen A, Elliott RM. The Bunyamwera Virus Nonstructural Protein NSs Inhibits Viral RNA Synthesis in a Minireplicon System. Virology. 2001;281: 67–74. doi:10.1006/viro.2000.0774

211. Blakqori G, van Knippenberg I, Elliott RM. Bunyamwera orthobunyavirus S-segment untranslated regions mediate poly(A) tail-independent translation. J Virol. 2009;83: 3637–3646. doi:10.1128/JVI.02201-08

212. Barr JN, Elliott RM, Dunn EF, Wertz GW. Segment-specific terminal sequences of Bunyamwera bunyavirus regulate genome replication. Virology. 2003;311: 326–338. doi:10.1016/S0042-6822(03)00130-2

213. Kohl A. Complementarity, sequence and structural elements within the 3′ and 5′ non-coding regions of the Bunyamwera orthobunyavirus S segment determine promoter strength. Journal of General Virology. 2004;85: 3269–3278. doi:10.1099/vir.0.80407-0

214. Plaskon NE, Adelman ZN, Myles KM. Accurate Strand-Specific Quantification of Viral RNA. PLoS One. 2009;4. doi:10.1371/journal.pone.0007468

215. Tilston-Lunel NL, Shi X, Elliott RM, Acrani GO. The Potential for Reassortment between Oropouche and Schmallenberg Orthobunyaviruses. Viruses. 2017;9. doi:10.3390/v9080220

216. Dunlop JI, Szemiel AM, Navarro A, Wilkie GS, Tong L, Modha S, et al. Development of reverse genetics systems and investigation of host response antagonism and reassortment potential for Cache Valley and Kairi viruses, two emerging orthobunyaviruses of the Americas. Ebel GD, editor. PLoS Negl Trop Dis. 2018;12: e0006884. doi:10.1371/journal.pntd.0006884

217. Barr JN, Wertz GW. Role of the conserved nucleotide mismatch within 3′- and 5′-terminal regions of Bunyamwera virus in signaling transcription. J Virol. 2005;79: 3586–3594. doi:10.1128/JVI.79.6.3586-3594.2005

218. Hoon-Hanks LL, Layton ML, Ossiboff RJ, Parker JSL, Dubovi EJ, Stenglein MD. Respiratory disease in ball pythons (Python regius) experimentally infected with ball python nidovirus. Virology. 2018;517: 77–87. doi:10.1016/j.virol.2017.12.008

219. Vasilakis N, Tesh RB, Popov VL, Widen SG, Wood TG, Forrester NL, et al. Exploiting the Legacy of the Arbovirus Hunters. Viruses. 2019;11: 471. doi:10.3390/v11050471